

Sediment Deposition on a Tidal Salt Marsh

Trine Christiansen

Aarhus, Denmark

B.S.C.E., The Engineering Academy of Denmark, 1990

M.S.C.E., University of Washington, 1993

A Dissertation presented to the Graduate Faculty of the University of Virginia in Candidacy for the
Degree of Doctor of Philosophy

Department of Environmental Sciences

University of Virginia

August 1998

Abstract

The physical processes that control mineral sediment deposition on a mesotidal salt marsh surface on the Atlantic Coast of Virginia have been characterized through a series of measurements of sediment concentration, flow velocity, water surface elevation and local rates of deposition on the marsh surface. Flow and sediment transport have been characterized both temporally and spatially as a function of distance from the bordering tidal creek. Measurements were made at tidal conditions ranging from tides barely flooding the marsh surface to spring tides and storm surges.

Flow velocities on the marsh surface are extremely low (< 1 cm/s) during all tidal conditions measured. Flow direction on the marsh surface is perpendicular to the flow in the main tidal channel, flowing onto the marsh surface on the rising tide and off the marsh surface on the falling tide. The marsh surface vegetation, *Spartina alterniflora*, has a significant dampening effect on the turbulence of the flow, promoting deposition of suspended particles. Shear stresses within the *Spartina alterniflora* canopy are insufficient to mobilize sediment from the marsh surface.

Sediment concentrations at the marsh edge are higher on the rising tide than on the falling tide, and combined with a flow directed from the tidal creek towards the marsh interior or during a tidal cycle, this pattern indicates sediment deposition on the rising tide. Sediment concentrations at the edge of the marsh increase with increased tidal amplitude, whereas in the marsh interior sediment concentration remained low regardless of tidal amplitude. The concentration gradient between creek bank and marsh interior indicates that more sediment is deposited on the creek bank as tidal amplitude increases. Correlation of high sediment transport events with meteorological conditions indicate that all high transport events are associated with strong northeasterly winds. Based on these measurements, it is estimated that 27 % sediment deposited on the marsh surface is contributed by storms; the rest is deposited during normal high spring tides.

Acknowledgments

My experience at the University of Virginia has been an extremely positive one, both academically and personally. I credit my advisor Dr. Patricia Wiberg with creating a work environment that made such an experience possible. It has been a true privilege to work with Dr. Wiberg. Her clear and thoughtful guidance is reflected throughout this document. I also thank her for recommending me for the Maury Research Award.

The input from my committee: Dr. Peter Berg, Dr. Linda Blum, Dr. Alan Howard and Dr. Wu-Sen Lung has contributed to the interdisciplinary nature of this work. I have appreciated the academic and moral support I have received from them throughout this process. In particular, Dr. Blum was extremely helpful and encouraging during field work at the LTER-site and Dr. Berg helped me make the most realistic estimates of time required to complete this work.

Through the VCR-LTER, Dr. John Porter made VCR-LTER data available almost as quickly as it was measured. David Richardson helped with surveying the study site and generated the GIS maps used in this study. Jimmy Spitler went beyond the call of duty in helping with heavy field equipment and taking me to the study site many times, sometimes during the most extreme of weather conditions (snow included). Through the LTER, I have also received help and encouragement from Dr. Iris Anderson, Randy Carlson, Dr. Mike Erwin, Dr. Bruce Hayden and Bo Lusk. My peer student group at the LTER: Craig Layman, Kindra Loomis, Brian Silliman, Christy Tyler and John Walsh have provided a lot of good laughs during field work times at the Eastern Shore. Two undergraduate students at UVA, Katharine Favret and Ryan Heitz have been good sports helping me in the field while also doing their own senior thesis research. In Redbank, I appreciated the hospitality of Rowland, Mary and Seth Rux.

In the field component of this study, I used a number of electronic measuring devices that did not always cooperate as intended. Many of these equipment related problems were solved by the Physical Oceanography Laboratory at Virginia Institute of Marine Science. Contact to the lab was provided through Dr. Carl Friedrichs and my electronic problems were solved by Frank Farmer and Todd Nelson.

In the early part of the study I had productive discussions about how to best design field equipment with Anne Halpin, Dr. Patrick Halpin and Dr. Aaron Mills. In the latter part of the study, Dr. John Albertson and Dr. Gaby Katul advised me on theoretical aspects of turbulence. Throughout this study, I have benefited a lot from many discussions of theoretical and practical aspects of

sediment transport with Courtney Harris.

I have made many friends within my peer student group at UVA. In particular, Beth Boyer, Ishi Buffam, Lisa Chang, Claire Cosgrove, Bob Craddock, Scott Eaton, Shalini Gauba, Courtney Harris, Erik and Alison Hobbie, Mark Mitch, Joan Pope, David Richardson, Katie Ross and Mary Ellen Tuccillo have provided a great balance of moral support, encouragement and fun that anyone needs to get through a Ph.D.

I wish to thank my parents and their families, my brothers and their families and Eva Olsen for standing by me through this very long process. Most of all I want to thank Karl for putting up with the challenge of living our lives apart and never losing faith that it would work out in the end.

Contents

1	Introduction and Background	1
1.1	Introduction	1
1.2	Study site	4
1.2.1	Other Coastal Wetlands	6
1.3	Transport of Cohesive Sediment in a Tidal Environment	8
1.4	Flow and Sediment Transport in Tidal Creeks	9
1.5	Flow and Sediment Transport on Salt Marsh Surfaces	11
1.6	Deposition	12
1.7	Mechanisms of Deposition	14
1.8	Mathematical Modeling Efforts	16
1.9	Fair Weather Versus Storm Influence on Sediment Transport	17
1.10	Objectives	19
2	Methods	21
2.1	Experimental Setup	21
2.2	Marsh surface survey	23
2.3	Water Levels	23
2.4	Velocity measurements	27
2.5	Turbulence Characteristics	30
2.6	Turbidity Measurements	32
2.7	Calculated Sediment Deposition	33
2.8	Sediment Deposition Measurements	34
2.8.1	Mass accumulation	34

2.8.2	Marker Horizon	35
2.9	Grain size analysis of deposited sediments	36
2.10	Particle settling	37
2.11	Sediment Settling Properties	37
2.11.1	Sediment adhesion to plants	39
3	Flow and Sediment Transport on a Tidal Salt Marsh	40
3.1	Marsh surface topography and inundation frequencies	40
3.2	Estimate of flow velocities on the marsh surface	41
3.3	Velocity measurements	44
3.3.1	Circulation	49
3.3.2	The effect of marsh vegetation on the flow.	51
3.3.3	Vertical structure of velocity	54
3.4	Suspended sediment concentration measurements	54
3.4.1	Temporal and spatial variation	58
3.4.2	Variation among tidal cycles	58
3.5	Grain size distributions	63
3.6	Settling properties of the sediment	65
3.7	Controls on mean flow velocity and direction	66
3.8	Turbulence and sediment transport	67
4	Sediment Deposition on a Marsh Surface	73
4.1	Sediment deposition measured on sediment traps	73
4.2	Sediment deposition calculated from measurements	76
4.3	Sediment accumulation on stems	80
4.4	A model for sediment deposition	82
5	Sediment Transport Events	87
5.1	Relationship between water level and meteorological forcing	87
5.2	Sediment Transport	88
5.3	Correlation between water level and meteorological forcing	91
5.3.1	Results	98
5.4	Frequency of sediment transport events	102

6	Conclusions	105
6.1	Annual deposition rates on the marsh surface	105
6.2	Summary of results	106

List of Figures

1.1	Location of study site on the Atlantic Coast of Virginia	3
1.2	Location of study site in Phillips Creek marsh.	4
2.1	Map of marsh surface.	22
2.2	Relative position of stations along sampling transect.	23
2.3	Distribution of tidal amplitudes.	25
2.4	Comparison of water level during peaks and troughs at Wachapreague and Redbank.	26
2.5	Tides measured on marsh surface in May, 1995 compared to tides measured at the LTER tide gauge in Redbank.	27
2.6	Velocity profile and mean velocity	29
2.7	Turbulent flow example.	31
2.8	Calibration of optical backscatter sensors.	33
2.9	Example of concentration change with time during settling.	39
3.1	Inundation frequencies of the marsh surface.	41
3.2	Infilling of marsh surface with rising tide.	42
3.3	Determining area and length of contour intervals.	43
3.4	Comparison of measurements made at a range of tidal amplitudes at stations 1 and 5.	45
3.5	Maximum flow velocities measured on the rising and on the falling tides.	46
3.6	Variation in depth and flow velocity over three tidal cycles.	48
3.7	Circulation on marsh surface.	50
3.8	Turbulence spectra at the five sampling stations and in the creek.	52
3.9	Turbulent energy variation with time and location.	53
3.10	Variation in shear velocity with time at stations 1 and 5.	55

3.11	Velocity and stress variation with depth.	56
3.12	Change in sediment concentration with time and with distance from tidal creek. . .	59
3.13	Sediment concentration as a function of time at station 1 and station 5.	60
3.14	Grain size distributions of fully disaggregated sediment	64
3.15	Grain size distributions inferred from clearing rates.	65
3.16	Comparison between temporal variation in concentration and turbulent energy. . .	68
3.17	Simultaneous concentration measurements in the creek, at station 1 and at station 2	70
3.18	Concentration as a function of tidal amplitude on the creek bank and in the interior.	71
3.19	Sediment transport on the marsh surface.	72
4.1	Sediment deposition on marsh surface.	75
4.2	Example of time series used in flux calculation	77
4.3	Correlation between tidal amplitude and sediment flux at station 1	79
4.4	Calculated deposition on marsh surface during two different events using 100 μm particles	85
4.5	Calculated deposition on marsh surface during two different events using a distribu- tion of particles	86
5.1	Water level at Wachapreague, sediment concentrations in Phillips Creek and wind and atmospheric pressure Measured at NDBC buoy 44014 during May and June, 1997. Days in May are negative.	89
5.2	Correlation between sediment concentration, tidal amplitude, wind direction and wind speed.	90
5.3	Location of Wachapreague tide gauge, NDBC buoy 44014 and Study site.	91
5.4	Distribution of measured and predicted tidal amplitudes.	92
5.5	Cross correlation between residual water level and subordinate and dominant wind directions.	94
5.6	Selection of parameters associated with two events during a storm in March, 1993.	95
5.7	Distribution of wind directions during events.	97
5.8	Correlation between water level and wind speed and water level and event duration	100
5.9	Correlation between water level and wind direction and water level and pressure . .	101
5.10	Distribution of tidal peaks at Redbank in the period between 1990 - 1997.	102

5.11 Relative proportion of northeasterly winds. 104

List of Tables

1.1	Accretion rates compared to rates of relative sea level rise.	7
2.1	Comparison of mean tidal amplitudes among years.	24
2.2	Principal tidal constituents of the tide at Wachapreague.	27
3.1	Summary of velocity measurements.	47
3.2	Vegetation densities and stem thickness at each sampling location	51
3.3	Summary of measured concentration time series.	57
3.4	Summary of concentration variability among tides, part I.	61
3.5	Summary of concentration variability among tides, part II.	62
3.6	Estimate of particle sizes maintained in suspension.	69
4.1	Comparison of measured and calculated deposition for three sampling periods in May and June, 1997. Measured deposition is the average value of measured sedi- ment deposition at station 1 and station 2.	79
4.2	Sediment accumulation on <i>Spartina Alterniflora</i>	80
4.3	Comparison of mean sediment accumulation on stems.	81
5.1	Regression coefficients and test statistics for events (full model).	98
5.2	Regression coefficients and test statistics for reduced model.	99
5.3	Calculated annual deposition rate.	103
6.1	Annual deposition rates	106

Chapter 1

Introduction and Background

1.1 Introduction

Coastal salt marshes are located at the boundary between ocean and land. The organisms in this environment have adapted to intertidal conditions, but it has been shown that the ecological stability of these systems is sensitive to the marsh surface elevation relative to mean sea level. Relative sea level rise, organic matter accumulation and mineral sediment input affect the vertical position of the marsh surface. Long term assessments of the fate of marshes that are primarily accreting mineral sediment depend on accurate understanding of the physical processes that control mineral sediment deposition on a marsh surface. Measurements of deposition rates alone do not provide insight into the processes that control sediment transport onto and off the marsh surface or whether sediment redistribution occurs after the initial deposition. It is further necessary to identify the most important depositional events. In coastal sedimentary environments, sediment is primarily redistributed during extreme events. Although extreme events are infrequent they may exert a dominant control on a depositional environment. In a tidal salt marsh, sediment deposition occurs during tidal inundation at high tide. The tides that contribute sediment to the marsh surface range from tides high enough to inundate the entire marsh surface, to storm surges where depths on the marsh surface can reach up to 1-2 meters above the marsh surface.

This work is a study of the processes that control sediment deposition on a mainland fringing tidal salt marsh on the Eastern Shore of Virginia. In this area, the rate of relative sea level rise

is approximately 2 mm/year (Holdahl and Morrison (1974)), and long term deposition rates of 1-2 mm per year have been quantified using ^{210}Pb dating techniques (Kastler and Wiberg (1996)), indicating that marshes in this area are accreting at a rate comparable to the rate of sea level rise. Due to concern over long term effects of relative sea level rise in many coastal areas, long term sediment deposition rates have been determined in many coastal wetlands, but the physical processes that govern sediment deposition on these vegetated surfaces, and their relative importance have not previously been extensively studied. In this study, I have determined the physical processes that control mineral sediment deposition on the marsh surface through a series of measurements that describe the hydrodynamic environment and the sediment transport paths. Flow and sediment transport have been characterized both temporally and spatially as a function of distance from the bordering tidal creek. Tidal amplitudes in this area range 200 cm, from 10 cm to 210 cm above MSL during extreme storm surges. Only tides with amplitudes greater than 80 cm are high enough to overtop the creek banks separating the marsh from the adjacent tidal creek. I have characterized the variability in transport for a range of tides of different amplitudes, and used this information to determine the relative contribution of sediment deposited during tidal flooding and during storms.

Marsh sediment dynamics were investigated experimentally by measuring sediment concentration, flow velocity, water surface elevation and local rates of deposition. The measurements were made at five stations along a transect oriented parallel with the flow direction on the marsh surface on the rising tide. The measurements allowed calculation of sediment flux at each station, and the change in sediment flux between locations provided a measurement of mean sediment deposition. It was found that the marsh surface vegetation had a significant dampening effect on the flow, promoting deposition of suspended particles, and that shear stresses within the vegetation canopy were insufficient to mobilize sediment from the marsh surface. Measurements were made at tidal conditions ranging from high tides barely flooding the marsh surface, to spring tides and storm surges which allowed assessment of the relative contribution of sediment to the marsh during these events.

We have, for the study, selected a mainland fringing salt marsh in the Phillips Creek area near Brownsville, located on the Atlantic side of the Delmarva Peninsula on the Eastern Shore of Virginia (Figure 1.1). It was found practical to focus the work on the low salt marsh environment, because tidal flooding here occurs on a regular basis and the vegetation (short or tall form of *Spartina alterniflora*) is uniform. The tidal range in this area is generally 1.5-2 meters. Daily flooding provides the opportunity to conduct repeated measurements and allows for a reasonable spatial resolution

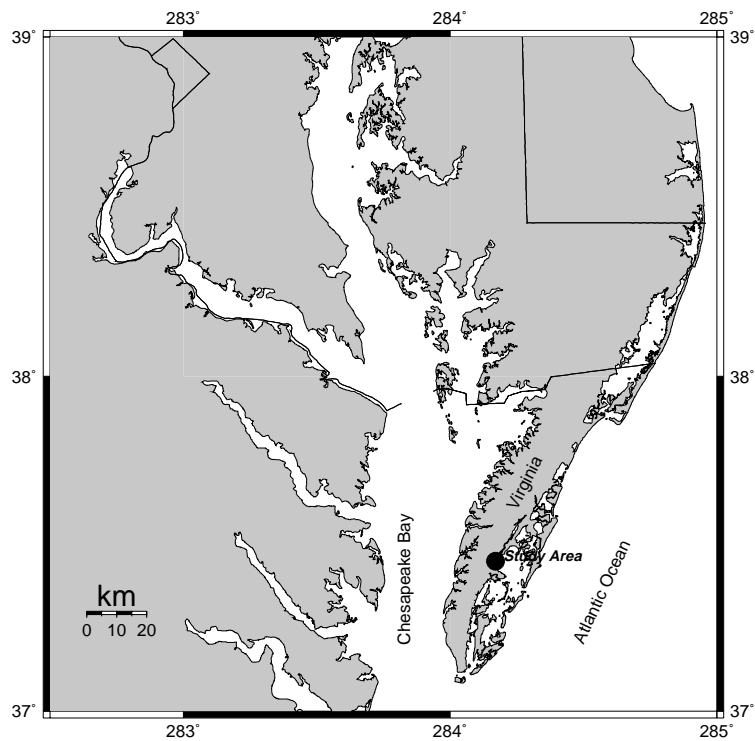


Figure 1.1: Location of study site on the Atlantic Coast of Virginia

with one set of instruments to measure currents and suspended sediments. This particular location was chosen because the site could be accessed both from land and by boat, which was an important part of being able to collect many repeated measurements. Further, annual accumulation rates and particle size distributions had already been determined at this location by Kastler and Wiberg (1996). Access to the study site was provided by the Nature Conservancy.

This report has been divided into six chapters. Chapter one is a review of other work relevant to this study. The review is structured in sections describing processes that are relevant to marsh surface deposition, and leads into the objectives formulated for this work. The second chapter describes the methods used in the field sampling program and in analyzing measurements. Chapter three describes the flow and sediment transport processes on the Phillips creek marsh. Chapter four describes deposition on the marsh surface. Chapter five describes sediment transport events in the Phillips Creek area, and in this section the relative contribution of sediment deposition during the regular tidal cycle and during storms are estimated. Finally, in chapter six the results are summarized and conclusions are made.



Figure 1.2: Location of study site in Phillips Creek marsh. The study site is located at Cr of the word Creek of Phillips Creek.

1.2 Study site

The Delmarva Peninsula forms the eastern margin of the Chesapeake Bay. On the Eastern Shore of Virginia, along the Atlantic side of the Delmarva Peninsula, a 100 km long chain of barrier islands protects the bay waters between the peninsula mainland and the barrier islands. The bay between the mainland and barrier islands consists of shoals and marshes dissected by a few very deep channels that provide a very efficient exchange of water in the bay (Figure 1.1). The tidal range on the mainland is similar to the tidal range in the ocean; 1.5-2 meters. The marshes in the bay are entirely vegetated with *Spartina alterniflora*, and the shoals are unvegetated. The marsh surface is fully inundated on the highest part of the highest tides, but the vegetation is not. The shoals are exposed during low tide on the lowest tides.

The barrier lagoon has developed as a consequence of sea level rise. Continuous sediment supply from the continental shelf has caused marshes and tidal flats to develop on the former terrestrial

landscape within the last 1000-2000 years (Oertel et al. (1992)). Fringing marshes have developed along the mainland side of all of the Delmarva Peninsula. The mainland marshes are the youngest marshes in this system because the terrestrial landscape here was most recently inundated. The mainland marshes are currently expanding landwards (encroaching on upland), in response to sea level rise (Kastler and Wiberg (1996)).

The area around Chesapeake Bay is responding to subsidence related to post glacial effects and possibly to removal of groundwater from aquifers in the region (Nerem et al. (1998)). Subsidence rates for the Chesapeake Bay area have been estimated from models ((Peltier and Jiang 1996)). Calculated subsidence around the Chesapeake Bay ranges 0.8-1.2 mm/year, and on the Delmarva Peninsula, the rate of subsidence is 1.1 mm/year (Kiptopeke, Virginia) and 1.2 mm/year (Wachapreague, Virginia). Using 13 tide gauges around Chesapeake Bay, Nerem et al. (1998) calculate a mean relative sea level rise (eustatic sea level rise + subsidence) in Chesapeake Bay of 3.5 mm/year. The tide gauge network includes two tide gauges on the Delmarva Peninsula; at Kiptopeke, Virginia and Wachapreague, Virginia. Rates of relative sea level rise for these two locations were measured at 3.2 mm/year and 6.7 mm/year respectively.

In this century major changes have occurred in the lagoon environment that may affect sediment transport rates. In the first half of the 20th century, eelgrass *Zostera marina* colonized a large portion of the bottom of the lagoon, stabilizing the bottom sediments against erosion. The eelgrass died as a consequence of wasting disease in the 1930s and has not recolonized the lagoon (Fonseca (1996)). Further, anecdotal accounts suggest that the oyster *Crassostrea virginica* in the past inhabited much larger portions of the banks of tidal creeks than it currently does. The oyster reef structure provides a natural protection against erosion, and the filter feeding process of the oyster peletizes sediments, making the sediments less susceptible to erosion.

The marsh selected for this study is a mainland fringing marsh located in the Phillips creek area (Figure 1.2). On a human time scale, the Phillips Creek marshes are very stable features. Kastler and Wiberg (1996) compared an aerial photograph taken in 1938 to one taken in 1990 and found that the majority of the change in the area was due to upland areas converting to marsh as a consequence of sea level rise. The tidal channels remained at the same locations during those 52 years.

On the Eastern Shore of Virginia, terrestrial drainage contributes only a small fraction of the total volume of water in the lagoon and there are no major terrestrial sediment sources. Consequently, the sediments found in the lagoon primarily originate from the continental shelf (Robinson (1994)).

Once sediments are within the lagoon, they are continually reworked (Postma (1967)) and sediment suspended in the area of the mainland marshes is eroded locally from the lagoon and tidal creeks, rather than derived directly from the continental shelf.

The marsh surface sediments in the Phillips Creek area are primarily in the silt and clay size range ($D < 4\phi$). Particles coarser than 4ϕ are typically aggregated fecal material. The silt sized sediments are primarily quartz whereas the clay mineralogy is dominated by illite (Kastler (1993) and Robinson (1994)). Robinson (1994) also found that sediments from the mainland tidal creeks have similar clay mineralogy to sediments found on the marsh surface and to suspended sediment, indicating that the tidal channels are the source of sediment deposited on the marsh surface. The mean organic content of the marsh sediment in Phillips Creek low marsh is 6.5 % (Kastler (1993)).

The marsh fiddler crab (*Uca* sp.) is found in abundance in Phillips Creek marsh. These crabs eat marsh surface mud and excrete pellets of mud that may stabilize sediment on the marsh surface. Kraeuter (1976) suggests that the surface sediments in a Georgia salt marsh each year are entirely reworked by a crab population of 205 crabs/m² which are active 12 hours per day for 66 % of the time in a year.

1.2.1 Other Coastal Wetlands

In areas where coastal subsidence is large or the main source of sediment has been reduced as consequence of damming of rivers feeding in to an estuary or river diversion projects, extensive wetland loss occurs. The Mississippi delta, the most widely publicized example of a region undergoing rapid rates of coastal subsidence, is an area where sediment input has been greatly reduced and relative sea level rise exceeds 1.0 cm/yr (Bauman et al. (1984)). A negative feed back loop occurs in marshes that are not receiving sufficient sediment input to maintain their elevation against relative sea level rise. Increased flood frequency and duration causes the vegetation (*Spartina alterniflora* and *Spartina patens*) to reduce its production of both above and below ground biomass, and consequently also to reduce peat production, which decreases the rate of organic matter accumulation in addition to the already reduced rate of mineral matter accumulation. Eventually the vegetation can no longer be sustained and the marsh transforms in to a fully aquatic environment (DeLaune et al. (1994)). Another example of marshes stressed by subsidence in closer proximity to the study site, are marshes in the Chesapeake Bay. In particular, highly organic (organic content of 40-80 %) marshes on the Chesapeake Bay side of the Delmarva peninsula are changing in response to coastal

erosion and marsh subsidence (Stevenson and Kearney (1996)). In the Netherlands, a storm surge barrier has been constructed in the Scheldt estuary that has cut off tidal peaks and reduced flood frequency. These changes have led to decreased accretion rates in the marshes located within the Scheldt estuary (Oenema and DeLaune (1988)).

Source	Location	Method	Accretion rate [mm/yr]	Relative sea level rise [mm/yr]
Mississippi Delta:				
DeLaune et al. (1978)	Barataria Bay, LA	^{137}Cs	7.5	9.2 -13.5
Bauman et al. (1984)	Barataria Bay, LA	m.h.	7-19	9.2
Bauman et al. (1984)	Fourleague Bay, LA	m.h.	3-19	9.2
Gulf of Mexico:				
Leonard et al. (1995)	West-central FLA	s.t.	1.2-7.6	2
Chesapeake Bay:				
Stevenson et al. (1985)	Blackwater, MD	^{210}Pb	1.7-3.6	3.9
Kearney and Ward (1986)	Nanticoke River, MD	^{210}Pb	1.8-2.4	3.9
Kearney et al. (1994)	Monie Bay, MD	^{210}Pb , ^{137}Cs	1.5-6.3	3.9
U.S. Atlantic Coast:				
Harrison and Bloom (1977)	Long Island Sound, CT	m.h.	2-7	2.6
Letzsch and Frey (1980)	Sapelo Island, GA	m.h.	2-6	?
Sharma et al. (1987)	North Inlet, SC	^{210}Pb , ^{137}Cs	1.4-9.5	4.4
Kastler and Wiberg (1996)	Mainland marsh, VA	^{210}Pb	2	2
Kastler and Wiberg (1996)	Lagoon marsh, VA	^{210}Pb	2	2
U.K. marshes:				
French et al. (1995)	Norfolk, UK	m.h.	1-6	2
Reed (1988)	Dengie, UK	pins	5-11	3

Table 1.1: Accretion rates compared to rates of relative sea level rise. Abbreviations: m.h.: marker horizon, s.t.: sediment traps

Based on a review of studies where marsh accretion had been estimated from measurements of flux into and out of marsh systems, Stevenson et al. (1988) concluded that marshes on the Atlantic coast of the United States in general were eroding and that sea level rise would eventually lead to large areal losses of coastal salt marshes. Other studies (Table 1.1), suggest that marshes along the Atlantic coast are maintaining their elevation against sea level rise. Examples of other marsh systems that are maintaining themselves against sea-level rise include the Hut marsh (French and Spencer (1993)) and Bridge Creek Marsh (Reed (1988)) on the east coast of England. Deposition rates along with local relative rate of sea level rise have been listed for a number of studies in Table 1.1.

Marshes on the Atlantic side of the Delmarva Peninsula do not exhibit the traits of marshes in areas where coastal subsidence is greater or sediment input has been reduced. There are no signs of interior ponding which is an early indication of a deteriorating marsh (DeLaune et al. (1994)). Kastler and Wiberg (1996) found that both Chimney Pole marsh, a marsh island in Hog Island Bay, and Phillips Creek marsh were accreting at rates comparable to relative sea level rise at that location. The high mineral content of these low marshes (approximately 95 %) further suggests that they do not depend strongly on organic matter accumulation to maintain themselves against sea level rise and the negative feedback loop described by DeLaune et al. (1994) is less likely to be the dominant control in this system.

1.3 Transport of Cohesive Sediment in a Tidal Environment

Mineral sediment is brought onto marshes when currents and waves are sufficiently strong to put sediment into suspension. The fetch across Hog Island Bay is sufficient to develop small waves (height < 1 m) in response to strong winds. In the main tidal channels, waves are small relative to the channel depth (5-10 m), but currents are strong, and may mobilize sediment from the channel bottom and sides. Across the shoals, the water is shallow (depth < 1 m), and wave action may contribute to erosion of these surfaces. The critical stress for erosion by waves has been shown to be 10 times less than the critical stress of erosion by currents alone for the same clay material (Mehta (1988)). Small waves may erode sediment over the shoals that is advected with the flow in the main tidal channels. It is likely that shoals are the primary source of suspended sediment when winds are strong and produce waves on the bay waters.

In Phillips Creek, sediment is primarily moving as suspended load. The channels are in a protected location where waves do not tend to develop, and sediment is suspended by the boundary shear stress produced by current alone. The banks of Phillips Creek are comprised of loosely consolidated mud, and the surface layer of the banks contributes sediment to the suspended sediment load of Phillips Creek.

Erosion of sediment particles occurs when boundary shear stress, τ_b , exceeds a critical value τ_e :

$$E = M \left(\frac{\tau_b}{\tau_e} - 1 \right) \quad \text{for } \tau_b \geq \tau_e \quad (1.1)$$

where E is sediment erosion rate and M is an empirical coefficient related to the erodability of the mud considered. The critical shear stress for erosion of the bed, τ_e , is related to sediment composition and degree of bed consolidation (Mehta (1988)), but the precise relationship needs to be determined empirically for different locations. Typically, the critical shear stress is determined empirically in flume experiments using mud from a specific location ((Odd 1988)). Flume and *in situ* flume measurements were compared by Widdows et al. (1998), who used an *in situ* annular flume to determine the critical erosion stress, τ_e , of estuarine muds in the Humber Estuary, UK. The critical erosion stress determined *in situ* was 3 times greater than the one determined in the lab.

Deposition occurs when the boundary shear stress is less than the critical value for deposition τ_d . The rate of deposition, D , is calculated as a downward flux of sediment in to the bed, Cw_s , times the probability of deposition $(1 - \frac{\tau_b}{\tau_d})$ (Mehta (1988)):

$$D = Cw_s(1 - \frac{\tau_b}{\tau_d}) \quad \text{for } \tau_b < \tau_e \quad (1.2)$$

The limiting stress for deposition ranges between 0.6 and 1 dy/cm^2 (Odd (1988)).

Equations 1.1 and 1.2 provide the conceptual framework for calculating sediment erosion and deposition rates in a cohesive sedimentary environment. Determining accurate values of the parameters, E and D as well as the magnitude of boundary shear stress as it changes with time are, however, endeavors in their own right. Due to the impracticality of applying Equations 1.1 or 1.2, it has not been attempted to calculate sediment transport rates in Phillips Creek.

1.4 Flow and Sediment Transport in Tidal Creeks

Sediment transport in an estuary such as Hog Island Bay occurs when sediment is suspended during the regular tidal cycle as well as during storms. Small particles may be advected as much as 3-4 km with the flow in the tidal channels, and consequently, marsh evolution is closely connected to the fluctuating tidal flows in adjacent tidal creeks. The rate of mineral sediment accretion on a marsh is related to the concentration of suspended sediment in the water flooding the marsh surface. Suspended sediment concentrations in tidal creeks depend on the magnitude of the boundary shear stress exerted on the banks and bed by the tidal currents; the magnitude of currents depends on water elevation and tidal phase.

A large number of studies have been made documenting the relationship between tidal elevation and flow velocity in tidal creeks in macrotidal marshes in Norfolk, U.K. (Bayliss-Smith et al. (1979), Healey et al. (1981) and French and Stoddart (1992)). The measurements documented in these studies clearly indicate that mean velocity in a tidal creek is higher on tides that exceed bankfull level, and that the velocity maximum occurs at the same time as the bankfull level is reached. The higher a tide was above bankfull, the higher the observed maximum velocity was. Conversely, Leonard et al. (1995) measured tidal creek velocities in a microtidal environment, and did not observe increases in mean flow velocity during overbank flow. French and Stoddart (1992) observed elevated sediment concentrations in the tidal creek on over bank tides when the velocity in the tidal creeks was intensified. On below marsh tides, velocities were consistently lower and little sediment was in suspension.

French et al. (1993) made high frequency measurements of velocity for the duration of a neap tide and a spring tide in a tidal creek. From these measurements, they were able to calculate the shear stress based on the downstream and vertical velocity fluctuations (but only at one level). They found that stresses were much higher during spring tides than during neap tides. During a spring tide they also made regular measurements of suspended sediment concentration and they correlated temporal variation in shear stress to the temporal variation in suspended sediment concentration. They found surprisingly little correlation between times of high shear stress and times of high concentration, suggesting that suspended sediment is advected to the point of measurement from an exterior source. For example, shear stress was highest on the falling tide, whereas concentration was highest on the rising tide. They attributed the lower concentrations on the falling tide to sediment retention on the marsh surface during marsh surface flooding. They also found that the temporal variation in concentrations in the tidal creek matched the temporal variation in concentrations on the marsh surface, suggesting that marsh surface concentrations are responding to conditions in the tidal creek.

Both advection and diffusion have small components perpendicular to the main direction of flow that could transfer sediment to the marsh surface, but these are processes that are not well understood and it is not possible to relate deposition on a marsh surface directly to sediment concentrations in the tidal creek. Tsujimoto and Shimizu (1994) made detailed high frequency velocity measurements of flow in a compound laboratory flume with an artificially vegetated flood plain. Their measurements demonstrate that flood plain vegetation is extremely effective at reducing the flow velocity on the flood plain relative to that in the main channel. Model calculations based on

these observations, indicate strong circulation perpendicular to the main flow direction in the channel. If such a circulation exists between a tidal creek and a marsh surface, it could contribute to advection of sediment from the main channel onto the flood plain.

1.5 Flow and Sediment Transport on Salt Marsh Surfaces

Flow speed and direction on a marsh surface is controlled by local differences in water surface elevation. The velocity and direction of flow continues to change throughout the the period of inundation. Burke and Stoltzenbach (1983) measured flow speed on a salt marsh surface by timing the movement of dye injected into the flow on a New England salt marsh. Most flow speeds on that marsh were less than 5 cm/sec. Leonard and Luther (1995) measured flow speeds ranging from 1-10 cm/sec over a tidal cycle within the vegetation canopy of a West-central Florida marsh in a microtidal environment. Velocity profile measurements made on marsh surfaces (Burke and Stoltzenbach (1983) and Leonard and Luther (1995)) indicate that velocity increases towards the surface, but the structure is not logarithmic. Leonard and Luther (1995) found that the structure of the velocity profile corresponded to the morphology of marsh vegetation; where the leaves were closer together and less flexible, the velocities were lower.

Marsh surface vegetation adds drag to the flow. Kadlec (1990) established that existing measurements of flow through vegetation indicate that flow is in the transitional regime between laminar and turbulent flow. Tsujimoto et al. (1991), made a series of measurements of turbulence characteristics of flow over a bed covered with cylinders. When the cylinders protruded through the surface of the flow, the turbulence intensity was reduced to zero throughout the depth of flow and the velocity distribution was uniform in the vertical. Spectra of the turbulence structure within a *Spartina alterniflora* canopy have been determined (Leonard and Luther (1995)). Within the canopy, turbulence structure is modified by breaking down larger turbulent eddies that transfer the majority of the momentum in the flow. Leonard and Luther (1995) measured flow speeds as a function of distance from the tidal creek and within canopies of different densities and found that vegetation density was a stronger control on flow speeds than proximity of tidal creek.

Suspended sediment moves with the flow on the marsh surface. Time series of suspended sediment concentrations have been measured on a marsh surface to determine which part of the flooding tide is more important. Wang et al. (1993) and French et al. (1993) independently observed that

the concentration of sediment in the water running off the marsh on the falling tide is lower than the concentration of sediment in the water flooding the marsh on the rising tide, indicating either resuspension of sediments from the marsh surface on the rising tide upstream of the measurements site or sediment advected on to the marsh from an exterior source such as a tidal creek and deposited on the marsh surface. These two sets of measurements were made in two very different marsh systems. One was made on the Mississippi Delta in a microtidal environment and the other was made in a Norfolk marsh on the coast of England in a macrotidal environment.

1.6 Deposition

Phillips Creek marsh is depositional at present. Kastler and Wiberg (1996) measured sediment accumulation rates using ^{210}Pb dating of sediment cores. They also measured deposition on sediment traps during regular tidal cycles and found that the mass of sediment material collected on the traps significantly exceeded the annual ^{210}Pb deposition rate, suggesting that redistribution of material on the marsh surface occurs. They attributed some of the accumulation to sediment mobilization on the marsh surface.

Spatial variations in depositional patterns on a marsh surface have been observed using sand markers (French and Spencer (1993)). Vertical accretion in the Hut Marsh, England, was found to vary between 8 mm/year in low areas of the marsh to 1 mm/year in higher inland areas. Deposition was primarily related to frequency of flooding and proximity of tidal creeks. On a local scale (within 25 meters of the creek), deposition was found to vary as much as on the marsh scale. Deposition was observed on the creek banks but tapered off within 50 meters of the creek. Other studies have also described the existence of a concentration gradient across the marsh surface, with high suspended sediment concentrations near the banks of a tidal channel and low suspended sediment concentrations in the interior of the marsh (Leonard et al. (1995), Stumpf (1983) and Wang et al. (1993)). At the study site in the Phillips Creek Marsh, well developed levees exist along the creek bank suggesting that a similar pattern of deposition may be found in that area.

Leonard et al. (1995) used a combination of concentration and velocity measurements on the marsh surface to calculate rates of deposition, and found that they were able to calculate deposition rates of similar magnitude to the measured amount of sediment deposited on the marsh surface in a West-central Florida marsh over two tidal cycles. In this marsh the difference between creek bank

and interior deposition was $0.00175 \text{ g/cm}^2/\text{day}$ versus $0.00067 \text{ g/cm}^2/\text{day}$. Leonard et al. (1995) also observed seasonal variation in deposition rates, with higher rates of deposition in summer months than in the winter. Kastler (1993) observed the opposite trend on the Phillips Creek marsh. She observed the lowest depositional rates in the summer and the highest in the winter.

Vertical elevation change of the marsh surface occurs both with sediment deposition on the marsh surface and through compaction of the marsh soils (Cahoon et al. (1995)). In particular in marshes with high organic content, compaction may account for a greater portion of the vertical change than surface deposition. For example, Cahoon et al. (1995), measured both surface deposition and compaction in two Louisiana marshes, a Florida marsh and a North Carolina marsh, and found that only in one of these marshes, Old Oyster Bayou, Louisiana was vertical accretion represented by deposition on the marsh surface. In the other three marshes, subsidence was a more dominant control on accretion.

The relative importance of surface compaction and sediment deposition on the marsh surface depends on the organic content of the marsh soils. Knott et al. (1987) determined a relationship between organic content of the soil and a compressibility coefficient α_v :

$$\alpha_v = 2.05710^{0.0179(\%org.)-6} \quad (1.3)$$

The unit of α_v is $\text{cm s}^2/\text{g}$. Using Equation 1.3, the compressibility of a marsh with high organic content (60 %) is 9 times greater than the compressibility of Phillips Creek marsh with organic content of 6.5 %. The low organic content of the soils in the Phillips Creek marsh suggests that in this marsh vertical elevation change is mostly due to deposition on the marsh surface. Deposition includes new or reworked material deposited on the marsh surface, whereas vertical elevation change includes both sediment deposited on the marsh surface, organic matter accumulation of plant roots and long term compaction (Allen (1990)). In a deteriorating Louisiana marsh, the organic matter accumulation was approximately 20 % of the total accumulation (Cahoon and Reed (1995)).

Allen (1990) shows that stratigraphy of a marsh in the Severn Estuary indicates that the rate of vertical accretion of a marsh surface is related to flood frequency of the marsh surface; the lower the marsh, the more often it is flooded and the more rapidly it increases in elevation. While Allen (1990) recognizes variability in deposition rate among tides, he does not specifically quantify this variability. Cahoon and Reed (1995) show that the amount of sediment deposited on a Louisiana

marsh is proportional with increased inundation time of the marsh surface, and French and Stoddart (1992) observed large increases in suspended load on tides of higher elevation. Allen (1990) hypothesizes that a relationship exists among marsh elevation, relative tidal elevation and rate of organic matter accumulation. In the extreme case of the marsh having accreted to an elevation where it is no longer flooded, 100 % of the accretion is due to organic matter accumulation. Allen (1990) does not account for the possibility of organic matter deposition from exterior sources, suggested by Cahoon and Reed (1995) to be an important contribution to organic matter accumulation on the marsh.

1.7 Mechanisms of Deposition

Mechanisms of sediment deposition on a tidal salt marsh described in other studies include pelletization by filter feeders, enhanced settling rates due to flocculation of sediment and interception by plants (Stumpf (1983) and French and Spencer (1993)).

In Phillips Creek Marsh there are few filter feeders, and although local mounds of sediments were observed around small colonies of ribbed mussels *Geukensia demissa*, their abundance was very limited and pelletization by filter feeders was not considered an important mechanism of deposition in Phillips Creek marsh. Stumpf (1983) determined that sediment retention by *Spartina alterniflora* could account for up to 50 % of the material lost from suspension in a Delaware marsh whereas French and Spencer (1993) found that plant retention could only account for 2-5 % of the total deposition in the Hut Marsh. Leonard et al. (1995) found that retention by stems of *Juncus roemerianus* could account for 9% of the material deposited on the marsh surface of a west-central Florida marsh.

The likelihood of flocculation being an important mechanism for enhancing sediment deposition increases with increased sediment concentration. Pejrup (1991) found a strong increase in settling velocity during times of elevated sediment concentrations. The concentration levels (app. 100 mg/liter) at which he observed flocculation are comparable to those observed on the Phillips Creek marsh during spring tides. On the other hand, van Leussen and Cornelisse (1993) observed unique relationships between settling velocity and concentration, but the relationship varied among locations. Consequently parallels cannot be drawn between floc formation and settling rates at different locations without further investigation.

Grain size distributions of fully disaggregated sediment samples from a range of different environments were analyzed by Kranck et al. (1996). Among other locations, they analyzed sediments from a tidal flat in Nova Scotia and bottom sediment from Severn Estuary, U.K., and found that in both cases, sediment size distributions represented “one-round” distributions, i.e. sediment deposited from suspension with no subsequent reworking. Further, the size spectrum of these distributions had an extended tail in the fine end of the distribution, with particles in the fine end represented in equal amounts. This flat, fine tail is an indication that sediment was deposited from a flocculated source.

Sediment observed in suspension during the flooding of a tidal salt marsh is very fine grained (in the silt or clay range). Individual particles of these size classes have very low settling velocities (10^{-4} - 10^{-3} cm/sec). Sediment in this size range may flocculate into larger low density particles comprised of many small individual particles. Kranck et al. (1993) compared floc size, using size distributions obtained with a plankton camera, and found very little variation in the distribution of aggregate sizes between Amazon shelf sediments, Nith River sediments, San Francisco Bay sediments and Skagitt River sediments, suggesting common processes control aggregate formation.

Aggregates have a lower settling velocity (due to lower density) than individual particles of the same size, but a higher settling velocity than individual constituent particles. The aggregates are fragile and tend to break with handling (Eisma et al. (1991)). Consequently, it is extremely difficult to obtain an accurate measure of their size. Several methods have been or are being developed to determine *in situ* settling velocity of flocs. These include sampling with settling tubes, *in situ* settling tubes and *in situ* observations with video camera. Dyer et al. (1996) compared settling rates measured using four different types of settling tubes to those found using two types of direct measurements, *in situ* video camera and *in situ* settling velocity instrument. They found that the settling velocities derived from settling tube experiments tended to have a mean settling velocity an order of magnitude lower than settling velocities determined using the direct measurements. The discrepancy between the two methods was attributed either to flocs breaking with sampling in the settling tubes or because the video system does not resolve floc sizes less than $100 \mu\text{m}$ in diameter. It is thought by some researchers that floc sizes of $100 \mu\text{m}$ represents a lower floc size limit. For example, Sternberg et al. (in press) show that only 1 % of the sediment sampled using the *in situ* video camera was in the size class $130\mu\text{m} < D < 180\mu\text{m}$. Sizes inferred from an *in situ* settling velocity instrument indicated floc sizes with $20 \mu\text{m} < D < 100 \mu\text{m}$ (Fennesey et al. (1994)), but in the

case of the measurements by Dyer et al. (1996) where the same instrument was used, the smaller grains only represented a small portion of the total grain size distribution.

Sternberg et al. (in press) use the settling velocity measured with their video camera in conjunction with the measurements of particle size to derive a relationship between settling velocity w_s and grain size D for flocs on the northern California continental shelf:

$$w_s = 0.0002D_{\mu m}^{1.54} \quad (1.4)$$

The particle diameter is measured in μm and the unit of settling velocity is mm/sec .

1.8 Mathematical Modeling Efforts

The vertical structure of velocity for flow through a *Spartina alterniflora* canopy was modeled by Burke and Stoltzenbach (1983) using a $k - \epsilon$ model. They obtained good agreement with measured velocity structure, but in their model they did not account properly for the effect of vegetation on turbulent kinetic energy and dissipation. Burke and Stoltzenbach (1983) used a closure scheme that used a drag-related source term that resulted in an overestimate of the turbulent kinetic energy. Instead, Raupauch and Shaw (1982) propose using a closure scheme that properly averages the pressure and viscous terms in the Navier-Stokes equation for flow in plant canopies. The scheme presented by Raupauch and Shaw (1982) has been used to model vertical structure of flow and transport in a vegetation canopy by Katul and Albertson (in press).

Very few studies have been published that describe modeling approaches in coastal tidal wetlands. Hu et al. (1996) used a finite element model to evaluate different approaches to restoration of a tidal salt marsh in San Francisco Bay. A finite element model does well in handling changing bathymetry with changing water levels. The model simulation indicated that it was necessary to enhance sediment transport to the restored marsh by establishing tidal channels in the restored area. They also found that in a five year period, marsh surface elevations would reach a level where vegetation would establish itself. The model calculations did not include differences in retention ability between a vegetated and an unvegetated surface.

Woolnough et al. (1995) present an exploratory model for marsh surface buildup. This model assumes that sediment suspended in the nearby tidal creek is advected with the flow on the marsh

surface while particles also settle to the bottom. The model solution is based on method of characteristics. Flow velocity on the marsh surface is assumed to vary with time and distance from creek:

$$u = (L - x)\omega \cot(\omega t) \quad (1.5)$$

where L is width of the marsh and x is a coordinate that varies from 0 on the creek bank to L at the edge of the marsh. Equation 1.5 implies that the wider the marsh, the greater the velocity at the creek edge of the marsh, and that the effect of vegetation drag is proportional to distance from the creek. The model results indicate that the width of the levee depends on marsh elevation above MSL; the higher the marsh the narrower the levee.

1.9 Fair Weather Versus Storm Influence on Sediment Transport

It has been a subject of debate in the literature whether marsh deposition is primarily dependent on regular tidal forcing or if major storm events produce significant but infrequent depositional events (Stumpf (1983), Stevenson et al. (1988), and French and Spencer (1993)). Within the lunar cycle tidal height varies, but other climatic forcing factors such as storm surges often alter the tidal variation substantially from the predicted astronomical levels, so that high tides may occur at times other than during spring tides. In the tidal creeks, boundary shear stresses may be further enhanced by wind shear during storm events which is expected to produce higher levels of suspended sediment concentrations, but no measurements exist that support this hypothesis (French and Stoddart (1992)). French and Spencer (1993) observed that normal tidal conditions could account for the maintenance of marsh elevation in lower marshes, whereas on the high marsh, storm events accounted for a significant portion of the long-term sedimentation. Cahoon et al. (1996) show that in the Tijuana estuary, deposition only occurs during storm-induced river flows. Allen (1990) notes that storm surges introduce abnormally thick increments of sediment onto salt marshes in the Severn Estuary and several researchers have observed one to two order of magnitude increases in tidal creek sediment concentration during strong wind events (Leonard et al. (1995) and Stevenson et al. (1985)).

On the Atlantic coast of the United States the storm climate is determined by two types of storm systems, northeasters and hurricanes. The northeasters occur more frequently, but hurricanes

are locally more destructive. Northeasters are low-pressure systems that develop as a response to large depressions in the jet stream that occur more commonly in winter months than in summer months. Davis and Dolan (1993) devised a classification system for these storms. They specified five categories of storms and found that storm classes I-III (the least destructive) were most common from December through April whereas the most destructive storms (classes IV and V) were most prevalent in the months of October, January and March. The fetch of northeasterly storms is very long and, in combination with the shallow water on the Atlantic continental shelf, optimal conditions are provided for storm surges to develop.

The exact magnitude of a storm surge is a result of the combination of wind direction, wind speed, atmospheric pressure and storm duration. Storm surges occur when strong onshore winds push water against the coast and generate a wind-driven set-up of water level. Water level height may further be enhanced if low pressure is associated with the storm system. The “inverted barometer effect” indicates that water level increases 1 cm for each 1 hPa drop in atmospheric pressure (Bowden (1983)). Storm surges are forecast by combining the forecast pressure and wind fields over the ocean with a hydrodynamical model (Bowden (1983)).

In the coastal environment, storms are usually associated with major sediment transporting events. The combination of large waves and strong currents act to enhance sediment transport during these times. This is particularly true in the open ocean where large waves can develop. In a barrier island lagoon such as Hog Island Bay, the fetch available to generate waves within the lagoon is quite small, and the water in the lagoon is very shallow, so large waves do not develop. Currents in the main tidal channels within the lagoon are quite strong, however, but no measurements exist that describe their magnitude.

The Eastern shore of Virginia was last struck by hurricanes in 1933, 1935 and 1936. Anecdotal evidence collected by the VCR/LTER suggests that the 1933 storm was a major sediment transporting event, but no measurements were made. A hurricane passing within close proximity of Hog Island Bay is likely to cause a depositional event in excess of depositional events caused by northeasters. The marsh substrate is, however, very resistant to erosion, and anecdotal reports did not recount major changes in the location of tidal channels or marsh islands. The infrequent occurrence of hurricanes in Virginia and lack of data from other similar locations prevents assessment of the effect of such storms on sediment deposition on tidal salt marshes.

1.10 Objectives

It has been documented in previous studies that suspended sediment is moving in tidal creeks, predominantly on tides that reach amplitudes that are sufficiently high to flood the marsh surface. Some of the sediment suspended in the creek is advected with the flow on to the marsh surface where it is deposited. The details of the depositional process on the marsh surface are, however, not well understood. Most studies have focused on determining deposition rates, but not on describing the physical processes that control mineral sediment deposition within a vegetation canopy. It has also been documented that variability in concentration between tides exists, but this variability has not been related to sediment deposition or to frequency of occurrence of different types of depositional events. In other studies it was noted that storms provided more sediment input than to the marsh surface, but the relative importance of infrequent storm deposition and regular tidal deposition has not previously been quantified. To address these issues, the following objectives were developed for this study:

1. Identification of sediment transport processes on a low marsh surface.
 - a. Determine the influence of flocculation, settling, interception by plants and decreased turbulence levels on sediment deposition.
 - b. Identify the relationship between concentration levels on the marsh surface and sediment deposition.
 - c. Identify variability in sediment input as a function of tidal amplitude and as a function of location on the marsh surface.
2. Determine whether all sediment deposited on the marsh surface is derived from an exterior source or if resuspension occurs on the marsh.
 - a. Identify during which part of the tidal cycle suspended sediment concentrations increase.
 - b. Determine whether boundary shear stresses are sufficiently high to erode sediment from the marsh surface during any time in the flooding cycle or at any location.

3. Determine the relationship between sediment transport on the marsh and circulation of water on the marsh.
 - a. Identify variability in flow speed and direction on the marsh surface as a function of tidal amplitude and as a function of location on the marsh surface.
 - b. Determine the effect of vegetation on the turbulent properties of the flow.
 - c. Calculate sediment deposition rates by determining changes in flux between locations.

4. Determine whether storms produce significant sediment deposition and if they do, what conditions define a storm.
 - a. Identify the atmospheric conditions that produce increased water levels relative to the astronomical tides.
 - b. Identify relationship between concentration levels in creek and maximum tidal elevation.

Chapter 2

Methods

2.1 Experimental Setup

A transect with 5 stations was set up perpendicular to the adjacent tidal creek (Figures 2.1 and 2.2). The transect extended 50 meters from the bank of the tidal creek to the marsh interior. Three stations were established within close proximity of one another on the creek bank because the largest gradients in sediment deposition were expected in this area. The remaining two stations were set up in the marsh interior, away from the creek bank. At each station, I measured time series of turbidity and of flow speed and direction during inundation events. In addition to these measurements, sediment deposition during the time of each experiment (one or two tidal cycles) was measured. A limited number of instruments were available so measurements could only be made at one station at a time. I took advantage of the regular tidal flooding by assuming that measurements made at the same location during similar tidal conditions, but during different tidal cycles can be directly compared. Sediment deposition was measured using three methods: measuring sediment accumulated on sediment traps during 1-4 tidal cycles, measuring sediment accumulation on sediment traps over a two week period and by using marker horizons as a baseline for deposition. The topography of the marsh surface was surveyed at high resolution, with a surveyed point approximately every 2 square meters. Water level was monitored on the marsh surface and at a nearby tide gauge in Redbank. The tidal elevations measured at this tide gauge were related to the elevation of the marsh surface by relating the tide gauge readings to the same datum as the marsh surface topography. Meteorological

conditions characterized by wind speed, wind direction and barometric pressure at the water surface have been obtained from buoy station 44014 and CMAN station CHLV2 maintained by NOAA. The buoy and the CMAN stations are located approximately 100 km south of the study site, off shore from the mouth of the Chesapeake Bay. Details of the methods used to obtain and analyze data describing sediment transport and deposition processes on the marsh surface are described in this chapter.

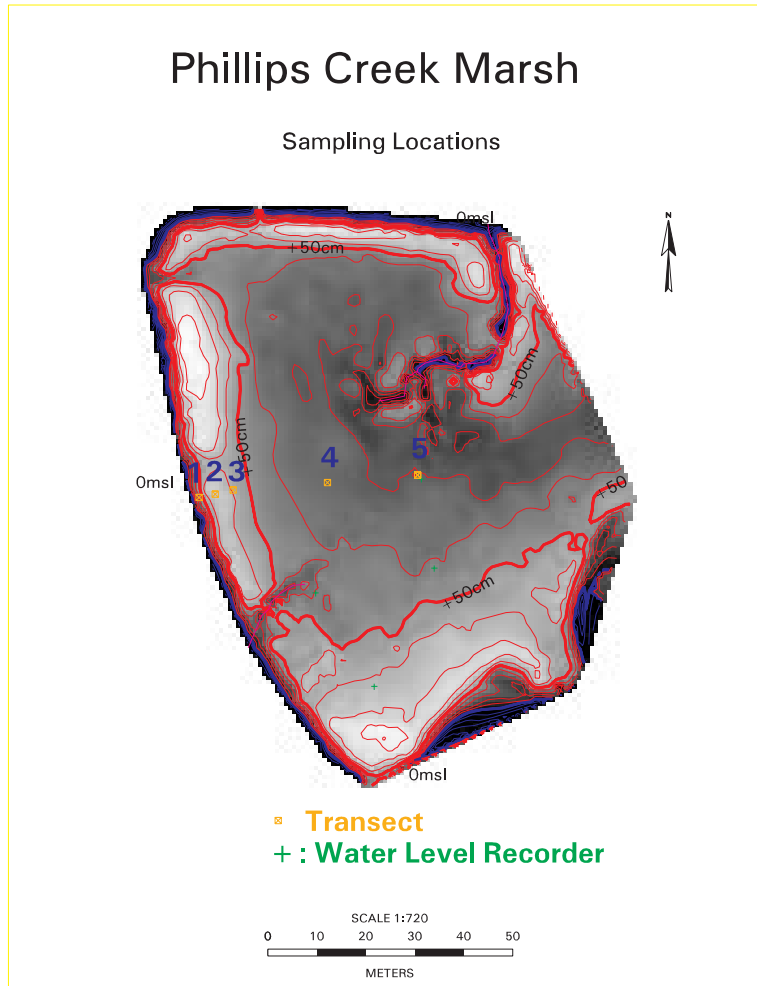


Figure 2.1: Map of marsh surface. The map indicates sampling positions along the transect.

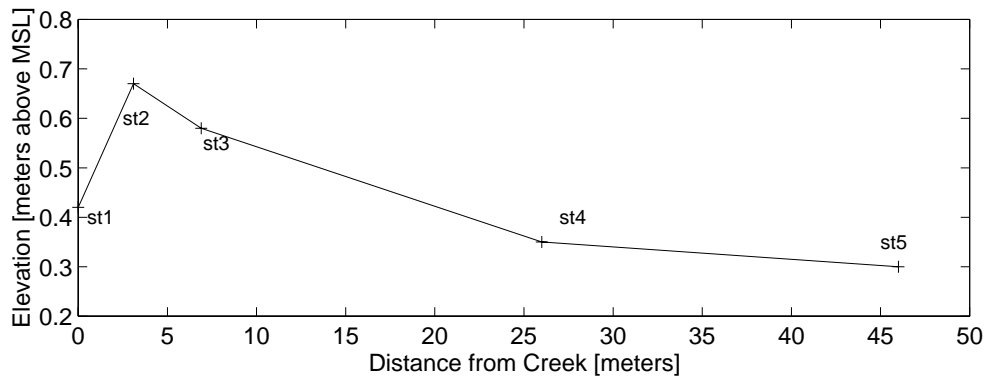


Figure 2.2: Relative position of stations along sampling transect.

2.2 Marsh surface survey

The marsh surface was surveyed using a laser theodolite. A point was surveyed every 2 square meters, and the vertical elevations were tied into the benchmark PHIL in the Brownsville area. The benchmark PHIL is part of the LTER network of benchmarks and has the coordinates: 37° 27' 13.333404 latitude, 75° 50' 1.745792 longitude, height = 1.5905 meters above MSL. The tide gauge in Redbank was also surveyed and related to this datum. The benchmark VCR1, at the LTER research lab has been fixed by the National Geodetic Survey, and all other benchmarks established by the VCR-LTER, including PHIL, have been related to this point, but without geoid correction. The elevation of VCR1 is related to mean sea-level, and consequently the elevation of PHIL, the marsh surface survey and water level in Redbank are also related to mean sea-level, but without geoid correction. The geoid correction accounts for curvature of earth's surface, and not including geoid correction means that the survey is not related to a datum established by the National Geodetic Survey, but all elevations surveyed in this study are referenced to the same datum.

2.3 Water Levels

The tides are semi-diurnal and slightly unequal. Wind conditions can significantly distort the pattern of daily and spring-neap tidal variations, but not in a predictable manner. The LTER maintains a tide gauge in Redbank, one mile from the site; water level is measured every 12 minutes. The tidal record from Redbank covers parts of 1993, 94, 95, 96 and 1997. Unfortunately, the tide gauge has been mounted in a way that prevents measurements of the lowest water levels; the limit of the

sensor range is -82 cm below MSL. Further, the datum of the tide gauge has not remained constant throughout the 5 years the gauge has been in operation. When comparing the distribution of tidal amplitudes for each of the five years (Figure 2.3, top panel), it was observed that the mean tidal amplitude varied between years, although it is reasonable to assume that the mean tidal amplitude for each year has remained the same. The calibration of the tide gauge measurements to the PHIL benchmark was made in the summer of 1995, and water levels measured in 1993, 1996 and 1997 have been adjusted to the 1995 level. To determine whether an adjustment was necessary for a particular year, I tested whether the mean tidal amplitude for each year is the same as the mean amplitude in 1995 (Figure 2.3 and Table 2.1). The null hypothesis tested is $\mu_{year} = \mu_{95}$ (Devore (1991)). The normal distribution of tidal amplitudes as well as large sample size warranted using a z-test to compare the means. The null hypothesis was rejected for 1993, 1996 and 1997. For the three years where the means were not the same, the difference between μ_{95} and μ_{year} was determined and it was assumed that the difference in means represented the difference in datum between two years. Measurements from 1993, 1996 and 1997 were adjusted by this difference

Year:	1993	1994	1995	1996	1997
Mean peak elevation, μ_{year} [cm]:	82.8	76.4	78.1	86.4	86.2
Standard deviation [cm]:	23.4	22.9	21.4	22.4	20.8
Number of values:	603	591	331	453	579
Comparison before adjustment:	-4.29	1.13	-	-5.26	-5.54
z-value ($\alpha = 0.01$)	-2.58	2.58	-	-2.58	-2.58
Rejection of H_0 :	yes	no	-	yes	yes
Adjustment of mean [cm]:	-5	0	0	-8	-8
Comparison after adjustment:	-0.45	-	-	0.19	0.06
Rejection of H_0 :	no	no	-	no	no

Table 2.1: Comparison of mean tidal amplitudes among years. The null hypothesis tested is whether $\mu_{year} = \mu_{95}$. Prior to adjusting the measured water levels, only $\mu_{94} = \mu_{95}$. After adjusting the water levels measured in 1993 by -5 cm and the water levels measured in 1996 and 1997 by -8 cm, the means of these years are equivalent to the mean of 1995.

The Redbank tide gauge consists of a staff and a pressure sensor. Simultaneous readings of water level according to the staff and according to the pressure sensor were used to relate pressure readings to the staff datum (MSL of the PHIL benchmark). After the adjustments indicated in table 2.1 have been made, the water level measurements made at the Redbank tide gauge can be related

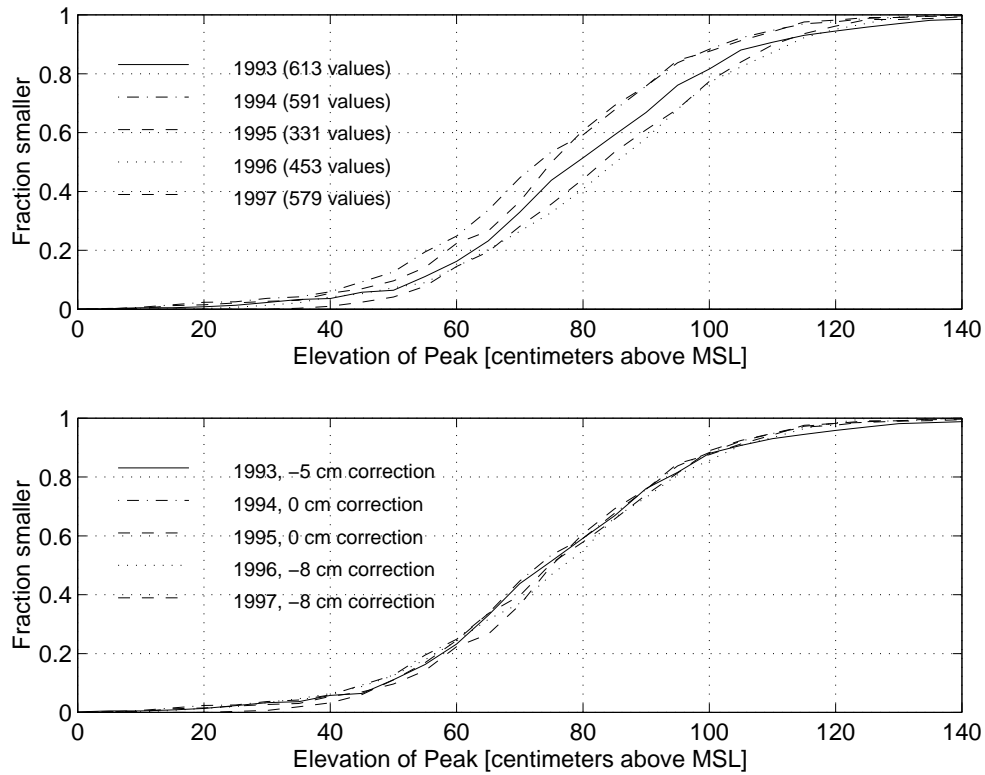


Figure 2.3: Distribution of tidal amplitudes. The distributions have been categorized according to year of measurement; 1993, 1994, 1994, 1996 and 1997. The top panel shows distributions without adjustment, and the bottom panel shows distributions after the adjustmenst indicated in Table 2.1.

to mean sea-level of the PHIL benchmark through the conversion in equation 2.1:

$$wl = wl_{meas} * 108 - 199; \quad (2.1)$$

where wl is water level in centimeters above MSL, and wl_{meas} is water level measured at the Redbank tide gauge.

In addition, NOAA maintains a tide gauge in Wachapreague, 20 km north of the study site which has been in operation for 20 years. At Wachapreague, the tidal range is smaller (1.75 meters) than at Redbank (2.25 meters), and the time of high tide is off-set by one 1 hour (high tide occurs 1 hour earlier in Wachapreague than in Redbank), but a strong correlation exists between water level at the two stations (Figure 2.4).

Water level was also measured at the study site. The measurements were made using Hobo

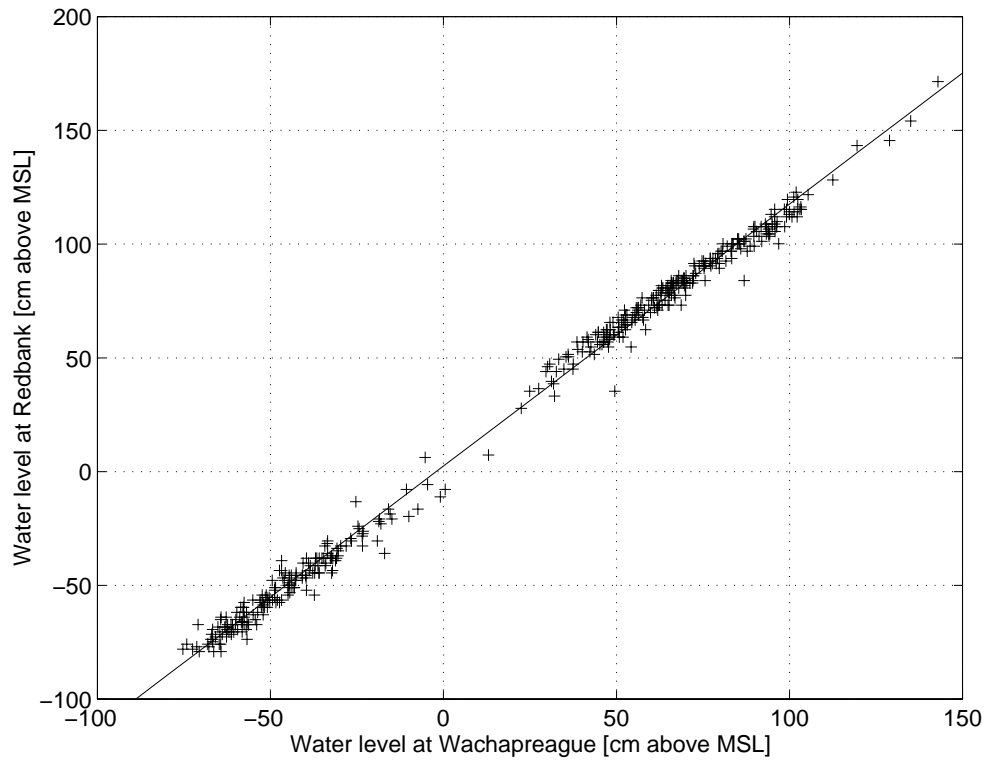


Figure 2.4: Comparison of water level during peaks and troughs at Wachapreague and Redbank. The relationship between the two stations is given by $wl_{Rb} = wl_{Wa} * 1.1521 - 5.56$, with a one hour time lag (high tide occurs 1 hour earlier in Wachapreague than in Redbank). $R^2=0.9954$.

pressure transducers with a 1 meter range. Three pressure transducers were installed on the marsh for one year starting in January 1995 and their response was related to the long term water level record measured in Redbank (Figure 2.3). It is seen that the water level measured in Redbank is a close approximation to the water level measured on the marsh; the mean elevation difference is 4 cm and the time lag between maximum high tide is 15 minutes (high tide is 15 minutes later on the marsh).

A continuous two year segment of hourly water level measurements (16384 measurements) made at Wachapreague was used to derive the tidal constants for that station. The program used to derive tidal constants was developed by Franco (1988), and was made available through the VCR-LTER. The 35 constants derived are diurnal, semidiurnal and terdiurnal components. No long period constituents could be derived. The principal tidal constituents are listed in Table 2.2. Although the record at Redbank covers most of the past 5 years, the record does not have any continuous segments longer than 9 months and combined with the cut-off of the lowest water levels, the record proved

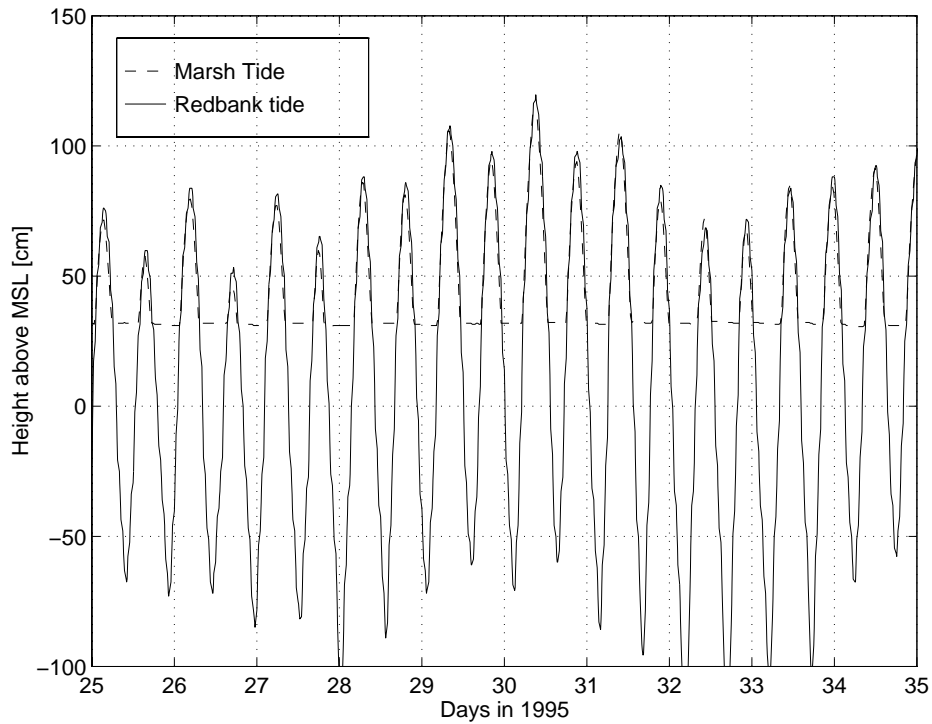


Figure 2.5: Tides measured on marsh surface in May, 1995 compared to tides measured at the LTER tide gauge in Redbank.

insufficient to derive accurate tidal constants for the Redbank location.

Constituent	Height [cm]	Period [solar hours]
Principal Lunar, M_2	55.58	12.42
Principal Solar, S_2	9.62	12.00
Luni Solar diurnal, K_1	6.75	23.93
Principal Lunar diurnal, O_1	8.21	25.82
Principal Solar diurnal, P_1	2.46	24.07
Principal Lunar ter-diurnal, M_3 ,	0.5	7.06

Table 2.2: Principal tidal constituents of the tide at Wachapreague.

2.4 Velocity measurements

Velocity measurements have been made using a SonTek Acoustic Doppler Velocimeter (ADV). This instrument accurately measures high frequency velocity variations, mean flow velocity and flow direction in two horizontal directions, and in the vertical.

The ADV transmits pulses of high frequency sound into the water. The pulse is reflected off particles suspended in the water. If the particles are moving toward the instrument the reflected sound pulse will have a higher frequency than the originally transmitted pulse. Conversely, if the particles are moving away from the instrument the reflected pulse will have a lower frequency (Doppler shift), which is used to determine flow velocity along the beam path. It is assumed that the suspended particles are moving at the same velocity as the water they are suspended in. The signal return is proportional to particle concentration, so the ADV provides a second measure of turbidity, but it is difficult to calibrate the signal response to actual concentration levels.

The ADV was programmed to sample at 10 Hz, in 15 or 20 minute bursts for 5 hours during each tidal cycle. I used a frequency of 10 Hz because this provided the best resolution of the turbulence structure without strong aliasing of the data. The measurements were stored in a tattletale 6F data logger, equipped with a hard drive. The hard drive had a 540 MB storage capacity. For each sampling interval time and velocity in x -, y -, and z -directions were recorded. The orientation of the coordinate system used is such that the x and y coordinates describe the horizontal flow velocities (\vec{u} and \vec{v}) and the z -direction describes the vertical flow velocity (\vec{w}); positive vertical flow velocity is upwards, negative is downwards. A PVC frame was constructed to hold the current meter. PVC was chosen because it is light weight and enabled me to move the current meter around to different locations on the marsh. Initially there was some concern as to whether the instrument frame would be sufficiently stable, but due to the very low flow velocities present on the marsh, stability was not a problem. To determine an appropriate sampling elevation, velocity was initially measured at a number of different elevations. It was found that it was more important to capture velocity measurements for as large a portion of the tidal cycle as possible than to measure higher in the canopy. In addition, a preliminary measured velocity profile indicated that the velocity 10 cm above the boundary was equivalent to the mean flow velocity (Figure 2.6). Except for the initial measurements made at station 2, the measurements were all made 10 cm above the boundary. To measure 10 cm above the boundary the instrument was mounted 15 cm above the boundary because the actual sampling point is 5 cm below the sensor tip. After the instrument was set up, its orientation was determined using a compass, and vertical orientation was ensured with a level. The current meter was always oriented with the positive x -direction towards west.

Velocity time series covering the duration of tidal flooding on the marsh surface were measured at the five stations along the transect during a range of tidal amplitudes. These measurements are

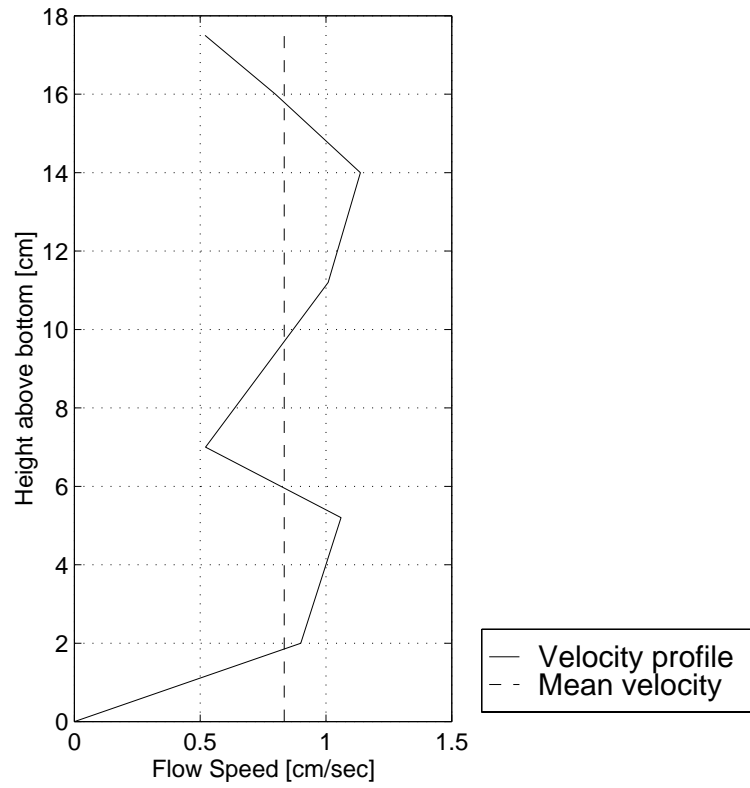


Figure 2.6: Velocity profile and mean velocity.

used to quantify the magnitude and direction of the flow velocity throughout the tidal cycle, and indicates the magnitude and direction of water circulation on the marsh.

2.5 Turbulence Characteristics

The high frequency velocity measurements were used to calculate spectra, turbulent energy and the Reynolds stress tensor. Velocity of a turbulent flow is typically described as the sum of a mean (\bar{u}) and a fluctuating velocity (u') component:

$$u = \bar{u} + u' \quad (2.2)$$

The turbulent properties of the flow are properties determined by the fluctuating velocity components. The turbulent intensity, q , a measure of the kinetic energy in the flow, is calculated as:

$$q = \sqrt{u'^2 + v'^2 + w'^2} \quad (2.3)$$

Each velocity time series was divided into segments of 2048 data points (or 3.4 minute segments). The flow could be considered steady within this time period, and the mean flow velocity in each of the three dimensions was calculated as the mean of the 2048 measurements. The magnitude of the fluctuations was determined by subtracting the mean from the measured velocity (Figure 2.5).

The Reynolds stress tensor has nine components, but because it is symmetric, only six of the components are different:

$$\begin{bmatrix} \tau_{xx} & \tau_{xy} & \tau_{xz} \\ \tau_{yx} & \tau_{yy} & \tau_{yz} \\ \tau_{zx} & \tau_{zy} & \tau_{zz} \end{bmatrix} = \rho \begin{bmatrix} \overline{u'u'} & \overline{u'v'} & \overline{u'w'} \\ \overline{v'u'} & \overline{v'v'} & \overline{v'w'} \\ \overline{w'u'} & \overline{w'v'} & \overline{w'w'} \end{bmatrix} \quad (2.4)$$

The stresses along the diagonal are the normal stresses (pressure) and they do not contribute to the transfer of momentum in the flow. The shear stresses τ_{xz} and τ_{yz} are the stresses that are responsible for vertical transfer of momentum in the flow (Tennekes and Lumley 1972), and at the bottom, these

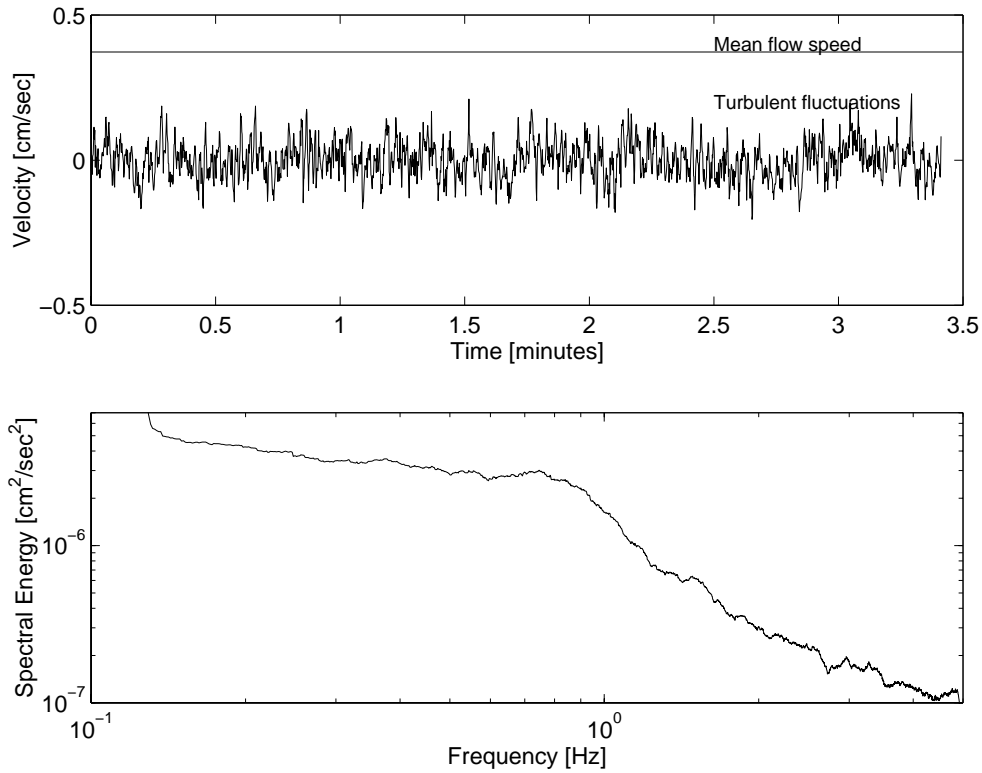


Figure 2.7: Turbulent flow example. The top panel shows the separation of turbulent flow into a mean and a fluctuating component. The bottom panel shows the spectrum of the same data segment.

stresses, if they are sufficiently large, are responsible for entraining sediment into the flow.

The length scales present in the turbulent flow can be characterized by determining the spectrum of the turbulent flow. The spectrum was calculated from data segments of 8192 data points (13.6 minute segments). Prior to calculating the spectrum, the data segment was multiplied by a tapered window, $W(t)$ to avoid leakage. The shape of the window used was one suggested by Stull (1988):

$$W(t) = \begin{cases} \sin^2\left(\frac{5\pi t}{T}\right) & \text{if } 0 \leq t \leq 0.1T \\ 1 & \text{if } 0.1T < t < 0.9T \\ \sin^2\left(\frac{5\pi t}{T}\right) & \text{if } 0.9T \leq t \leq T \end{cases} \quad (2.5)$$

where t is time, and T is the total length of the data segment. The spectrum was calculated by transforming the time series into the frequency domain using the fast Fourier transform. The power

spectral density (the spectrum) is the complex conjugate of the transformed data. The spectrum is scaled such that the area under the spectrum (the integral of the spectrum) is equivalent to the variance of the original time series (Figure 2.5).

The turbulent energy spectrum is a measure of the turbulent time scales present in the flow and how much energy is present at each frequency. Within the inertial subrange ($Re > 10^5$), the spectrum is a power function with an exponent of $-5/3$ (Tennekes and Lumley (1972)). In the inertial subrange, energy is dissipated at the same rate it is produced; energy is cascaded from the larger turbulent eddies to the smaller ones.

2.6 Turbidity Measurements

Time series of sediment concentration were measured at a range of concentrations and water levels. The measurements were made using SEA-TECH optical back scatter (OBS) sensors. The OBS sensors measure turbidity by emitting an infrared light and measuring the backscatter of this light. The back scatter is linearly proportional to concentration of particles in the water. The sensors have two settings, a sensitive range between 0 and 200 mg/l and a broader range between 0-500 mg/l.

The OBS sampling frequency is adjustable, and frequencies of 1 measurement every 2 or 3 seconds have been used. The sampling frequency is primarily constrained by data storage capacity. The measurements are stored in a Tattletale model 5F data logger. It has a memory capacity of 480 KB (RAM), corresponding to approximately 120,000 measurements. At each time step, time and response of two sensors is stored, so the storage capacity corresponds to 40,000 time steps. The sensor response is highly sensitive to grain size (Wiberg et al. (1994)), and consequently the sensor response was calibrated to the sediment found at Phillips Creek Marsh (Figure 2.8). The three sensors used in this study have very similar response which makes comparison of measurements reliable. The sensors were calibrated in a calibration tank at Virginia Institute of Marine Science. The tank has a volume of 80 liters. A bottom propellor stirs the water in the tank and keeps sediment in suspension. Sediment is added to the tank in known increments, and for each increment, the response of the three sensors are recorded.

To determine the variations in concentration with location and with variations in tidal height, sediment concentrations were measured at three locations for a 2 month period. The OBS measurements were made in the creek, and at stations 1 and 2 (only 3 sensors were available). The sensors

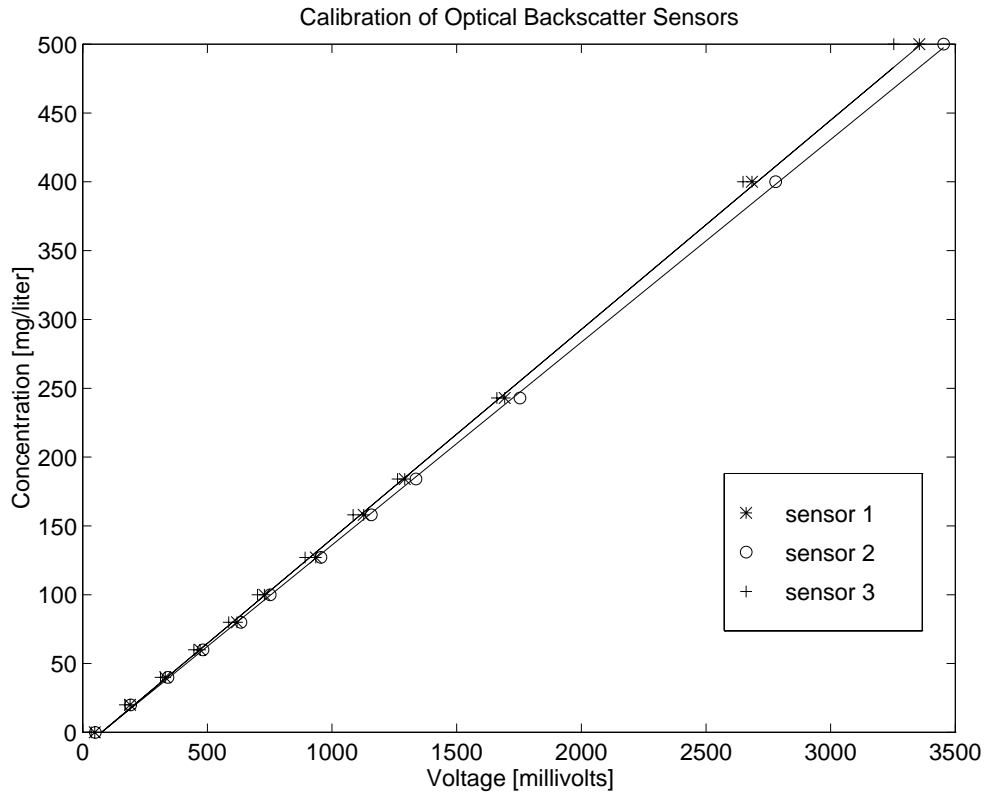


Figure 2.8: Calibration of optical backscatter sensors.

were programmed to sample for a 6 hour period around each high tide. Every two weeks the site was visited to change batteries and to clean the sensors. Fouling of the sensors was, however, not a problem on this time scale.

2.7 Calculated Sediment Deposition

Sediment deposition occurs when more sediment is brought into a control volume than leaves the control volume whereas erosion occurs when more sediment leaves a control volume than enters it. By identifying an appropriate control volume on the marsh and measuring fluxes into and out of this control volume, it can be determined whether deposition occurs within that control volume. Each station was used as a boundary of a control volume, and the measurements of water level, velocity and sediment concentration were combined to calculate sediment flux at each station. The primary assumption for this calculation is that the stations along the transect are located along the same stream line, so all water that passes by the sensors at station 1, pass by the sensors at

station 2 and so on. The stations were intended to be aligned parallel to the flow direction. The flow direction was, however, not the same at all stations, and did not flow along the exact same path on the rising and falling tide; therefore perfect alignment was impossible. The velocity measurements were oriented such that the x-axis was always parallel to the transect, and the suspended sediment flux is determined by using the velocity component parallel to the x-axis. The sediment flux (transport per unit time) is calculated as:

$$Q_s = \int_0^h C_s u_s dz \quad (2.6)$$

Where C_s is sediment concentration, u_s is horizontal velocity and h is depth. It is assumed that sediment concentration is distributed uniformly with depth (concentration is the same at all points in the vertical). This assumption is justified by the low settling velocity of the particles in suspension. The vegetation modifies the velocity structure to one that is more uniform with depth than a logarithmic profile observed in open channel flow. The velocity profile shown in Figure 2.6 indicates that the velocity measured 10 cm above the bottom approximately is equivalent to the mean flow velocity.

2.8 Sediment Deposition Measurements

2.8.1 Mass accumulation

Sediment traps were made using a 232 cm^2 stainless steel plate covered with a removeable nylon net that was placed flush with the marsh surface. After each sampling period, the net was removed and cleaned with deionized water. To determine accumulated mass, the sediment sample was removed from the nylon net and put in trays of known weight and dried at 50 °C for 24 hours or longer and then weighed. To determine organic content the dried sample was ashed at 500 °C for 24 hours and weighed again. The traps were left on the marsh for 1-4 tidal cycles during periods of measurements of velocity and turbidity.

Unfortunately, it was difficult to make mass accumulation measurements in the interior because this part of the marsh was typically submerged during sampling visits. The visits tended to be made in proximity of high tide because it was necessary to access the site by boat, and the lower elevations were frequently flooded upon arrival. Stepping near the site and removing the plates while submerged disturbed the samples making them unreliable. This problem was not encountered when sampling at the higher elevations. During the 1.5 month time series of suspended sediment concen-

tration near the creek bank sediment accumulation was measured during two week periods between site visits at stations 1, 2, 3 and 4. To allow comparison of measurements made over different time scales, mean deposition per tidal cycle has been calculated for each set of measurements.

The sediment traps used in this study were of similar design to those used by Kastler and Wiberg (1996). Sediment accumulation has been determined with sediment traps in other studies (Leonard et al. (1995), Hutchkinson et al. (1995)), although in these studies, precombusted, preweighed filters were used instead of nylon nets. Using filters eliminated the process of cleaning the nets which eliminates the uncertainty of removing all sediment from the nets to get total mass. It is clear that sediment collected on sediment traps represents sediment deposited on the traps. Hutchkinson et al. (1995), however, compared sediment accumulation on traps that were left on the marsh for 6 days to sediment collected on traps where the filters were replaced every day during the same period, and found that more sediment was consistently measured on the one day traps than on the 6 day traps. The difference between the two types of measurements could either be due to reworking of already deposited sediment, or to changing adhesion characteristics of the traps as they become covered with sediment (Hutchkinson et al. (1995)).

2.8.2 Marker Horizon

The effectiveness of using marker horizons to identify layers of deposition depends on the degree of bioturbation in a particular marsh. Marker horizons have been used effectively in northern coastal marshes (Harrison and Bloom (1977), French et al. (1995)). Based on reports from other studies of deposition in southern marshes, (Leonard et al. (1995), Letzsch and Frey (1980)), it seemed likely that bioturbation rates of the marsh surface by *Uca pugnax* were too high to use marker horizons to measure long term deposition rates on Phillips Creek marsh. Marker horizons were, however, successfully used to measure deposition during a large storm event in February, 1998. A 0.25 m² feldspar layer was put out at each station along the transect the day before the storm, and deposition on these marker horizons was measured two weeks later. The measurements were made by cutting through the sediments with a thin spatula, identifying the marker layer, and measuring how much sediment had deposited on top. The sediment deposited on marker horizons was converted to mass by dividing the thickness of the deposited layer by sediment bulk density (0.92 g/cm³), Kastler (1993) and the amount of sediment deposited per tide was obtained by dividing by number of tidal cycles during the storm (11 tidal cycles).

2.9 Grain size analysis of deposited sediments

Grain size distributions of sediment accumulated on the marsh surface were analyzed using techniques developed by Kranck et al. (1996). The samples include both sediment deposited during regular tidal events and sediment deposited during storm events.

Kranck et al. (1996) perform particle size analysis with a TAI Coulter Counter. The grain size analysis is performed on the fully disaggregated inorganic mineral fraction of a sub sample of the unconsolidated bed sediment. The Coulter Counter is an electro-resistance particle size analyzer, and it determines the number and volume of particles held in an electrolytic suspension. For sediments with equivalent diameter less than 100 μm the electrolyte is usually sea water. The sediment sample is resuspended in the electrolyte and a sapphire tipped ultrasonic probe is used to disaggregate the sample. The sample is stirred for 4 minutes prior to counting (Milligan and Kranck (1991)).

In this study, the size analysis was performed using a Sedigraph particle size analyzer. The Sedigraph determines particle size by observing settling velocity of particles whereas the Coulter Counter measures particle size directly, and results from the two methods are not comparable. In future work, particle size distributions of the marsh surface sediments will be obtained using the Coulter Counter to enable comparison with results from other studies.

The Sedigraph analysis provides the frequency distribution of the grain sizes present in the sample. The relative frequency of each grain size is plotted as a function of particle diameter on a log-log scale. The relative frequency is also referred to as concentration, C . The relationship between grain size and settling velocity is determined using Stokes law:

$$w_s = \frac{(\rho_s - \rho_f)gD^2}{18\rho_f\nu} \quad (2.7)$$

where ρ_s is particle density, ρ_f is fluid density, g is gravitational acceleration, D is particle size, and ν is fluid viscosity. For each particle of size D in the grain size distribution, a log-linear relationship exists, that describes the relationship between concentration C and its settling velocity w_s for each size class in the distribution:

$$\log C = X_1 + \log w_s X_2 + -w_s X_3 \quad (2.8)$$

where X_1 , X_2 and X_3 are unknown coefficients. Equation 2.8 is solved to fit a curve to the measured grain size distribution (Kranck et al. (1996)).

2.10 Particle settling

The effectiveness of turbulence in maintaining sediment in suspension can be evaluated from the Rouse number: $P_m = w_s/u_*$, where w_s is particle settling velocity and $u_* = \sqrt{\frac{\tau_b}{\rho}}$ is the shear velocity and τ_b is the stress at the bed. When $P_m > 1$, sediment cannot be maintained in suspension, and when $P_m < 0.3$, sediment is maintained in suspension. Because w_s depends on grain size and u_* which changes with flow conditions, the Rouse number is a function of these as well.

The high frequency velocity measurements have been used to calculate τ_{zx} and τ_{zy} . These stresses are combined to calculate $\tau = \sqrt{\tau_{zx}^2 + \tau_{zy}^2}$, the mean stress 10 cm above the bed (the level of velocity measurements). The shear velocity, u_* , is estimated by assuming that $\tau_b = \tau$. The shear velocity is used with the Rouse number thresholds for suspension to evaluate the limits on settling velocity of particles in suspension.

2.11 Sediment Settling Properties

It is likely that some fraction of the sediment in suspension on the marsh surface is in a flocculated form. Flocs are very fragile aggregates of fine grained sediment with higher settling rates than constituent grains. Particle size distributions for sediment in suspension have been measured using different types of settling tubes (Dyer et al. (1996)). A settling tube is operated by filling the tube with water at the sampling location of interest, rotating it to a vertical position, allowing particles in the water to settle. While the sediment is settling, aliquottes of water and sediment are removed at a particular depth at predetermined time intervals. The amount of sediment present in each aliquotte represents the proportion of particles settling at a particular settling velocity. Many different designs have been tested. It has been found to be critical that sampling from the tube begin immediately after filling and that the sample is disturbed as little as possible in the rotation process to avoid breaking of flocs (Dyer et al. (1996), van Leussen and Cornelisse (1993)). *In situ* measurements of settling velocity have been made using a similar technique except a transmissometer is used to record the change in concentration with time as sediment settles out of suspension (Hill et al. (1994)). In both

cases, particle size distribution is inferred from the changing rate of settling (Hill et al. (1994), Dyer et al. (1996)).

Floc detection requires *in situ* measurement of settling rates. A settling tube was designed to determine *in situ* settling measurements on the marsh. The tube was a 75 cm long clear acrylic cylinder with 15 cm diameter. Two holes were drilled in the sides of the tube 49 cm apart. The OBS sensors were nested inside rubber stoppers and mounted through the side of the tube. The top and bottom 25 cm of the tube were painted black because sun light through the sides of the tube interfered with the optical properties of the OBS sensors. The ends of the tube were sealed with a cap that could be expanded to a snug fit inside the tube. By measuring clearing rates at two different levels a measure of the change in sediment properties between the two levels was obtained. Water samples were taken at the onset of the rising tide when concentration levels were highest. It proved difficult, however, to take a water sample without stirring up a significant amount of sediment. I therefore limited the number of samples taken on the marsh and supplemented the samples with experiments made on the dock where known quantities of sediment were added to salt water in the tube.

The method for determining grain size distribution in the settling tube is similar to the method used in pipette analysis (Krumbein and Pettijohn (1938)). The principle behind the analysis is to relate particle settling velocity to change in concentration. The sensor was positioned 10 cm below the water surface, and it measured clearing rate of particles that settled 10 cm or more. A number of time steps were chosen, and the relative proportion of clearing within each time step was related to settling velocity, $w_s = 10\text{cm}/t_n$. The settling velocities calculated for each time step were related to a grain size using Stokes law (Equation 2.7). The cumulative distribution was determined by making readings of non-dimensional concentration, C/C_{max} (Figure 2.9). OBS readings were made at times 0, 1, 3, 7, 15, 31, 63, 127, 255, 511 and 1023 minutes. Settling velocity corresponding to each time step was calculated, and the cumulative distribution of settling velocities or grain sizes is $1 - C/C_{max}$.

Two experiments were conducted, one in which the maximum concentration in the settling tube was 350 mg/l and another in which the maximum concentration was 250 mg/l. Both initial concentrations are higher than the highest concentrations generally observed on the marsh. Approximately 50-60 % of the clearing occurred within the first hour of the experiment; after that, clearing occurred more slowly.

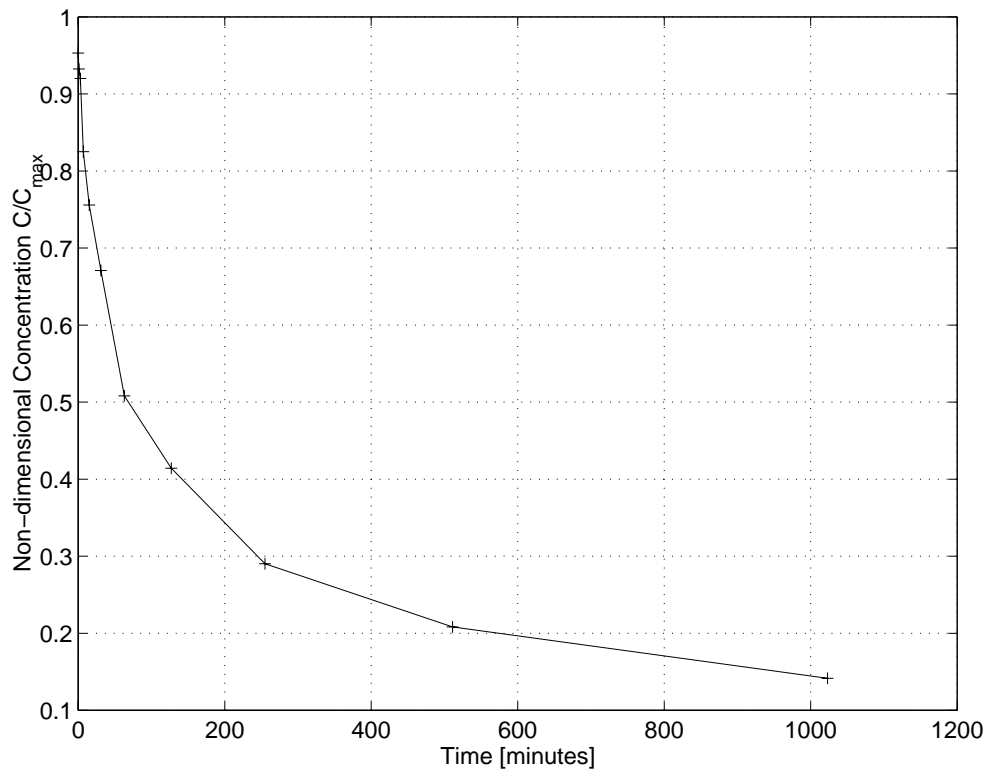


Figure 2.9: Example of concentration change with time during settling.

2.11.1 Sediment adhesion to plants

To determine the amount of sediment accumulated on plants, three 0.25 m^2 plots were identified at each station. All of the plants in each plot were meticulously cleaned with salt water, but the week after the cleaning, the region received very intense rainfall from hurricane Bertha on July 12, 1996. Bertha was much more efficient in cleaning the plants than any person could have been. The plants were cleaned on July 4th-7th, 1996 and harvested on September 25th, 1996. In the lab, sediment was washed off the plants using deionized water. The number of stems from each plot were counted and the plants were dried and weighed. The sediment was put into pre-weighed trays, dried and weighed, and ashed and weighed. By accounting for the plant mass and number of stems, in addition to the sediment mass, a measure of sediment mass relative to size and number of plants was obtained.

Chapter 3

Flow and Sediment Transport on a Tidal Salt Marsh

3.1 Marsh surface topography and inundation frequencies

The survey of the marsh surface has been compiled into a topographic map of the study area (Figure 3.1, right panel). The topographical relief of the marsh surface is only 50 cm, with the highest points on the levee adjacent to the tidal creek 60 to 80 cm above MSL, while the lowest points in the marsh interior are at 30-40 cm above MSL. The topography has been related to the distribution of tidal amplitudes of 591 tidal cycles (Figure 3.1, left panel). The color bar on Figure 3.1 indicates that 91 % of tides flood the marsh at least to contour level 40 cm above MSL. The highest points on the levees (80 cm above MSL) are only flooded with water on 35 % of tidal cycles (Figure 3.1). Although the levees are flooded much less frequently than the marsh interior, their higher elevation is an indication that they are accumulating sediment at a higher rate than the lower interior. A higher sediment accumulation rate at the higher elevations suggests that the tidal cycles with higher amplitudes contribute more sediment to the marsh.

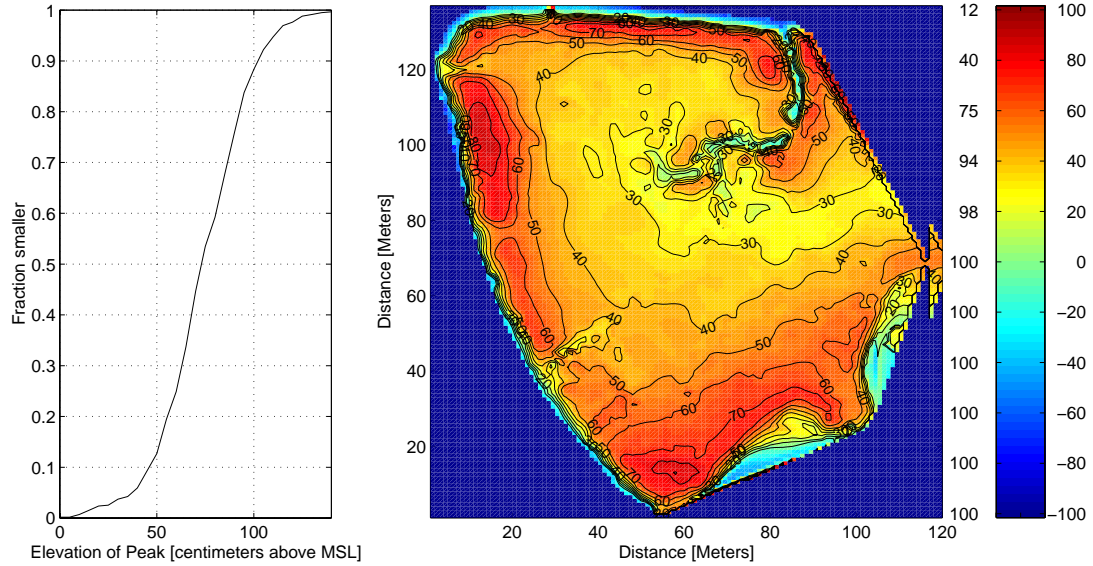


Figure 3.1: Inundation frequencies of the marsh surface. The left panel shows the distribution of tidal amplitudes for 591 tidal cycles. The right panel a contour plot of the marsh surface with contour levels are in cm above mean sea level. The color bar to the right of the contour plot is labeled with contour level on the right and inundation frequency in percent of tidal cycles on the left.

3.2 Estimate of flow velocities on the marsh surface

The topographic map of the site has been used to evaluate the degree of topographic control on flow velocities. A preliminary calculation was made to estimate mean flow velocities on the marsh by combining the length of time it takes for the tide to rise 10 cm (Figure 3.2, fourth panel), with the mean distance the water must travel between two contours that are 10 cm apart (Figure 3.2, top panel). This calculation is only appropriate until the marsh becomes fully inundated.

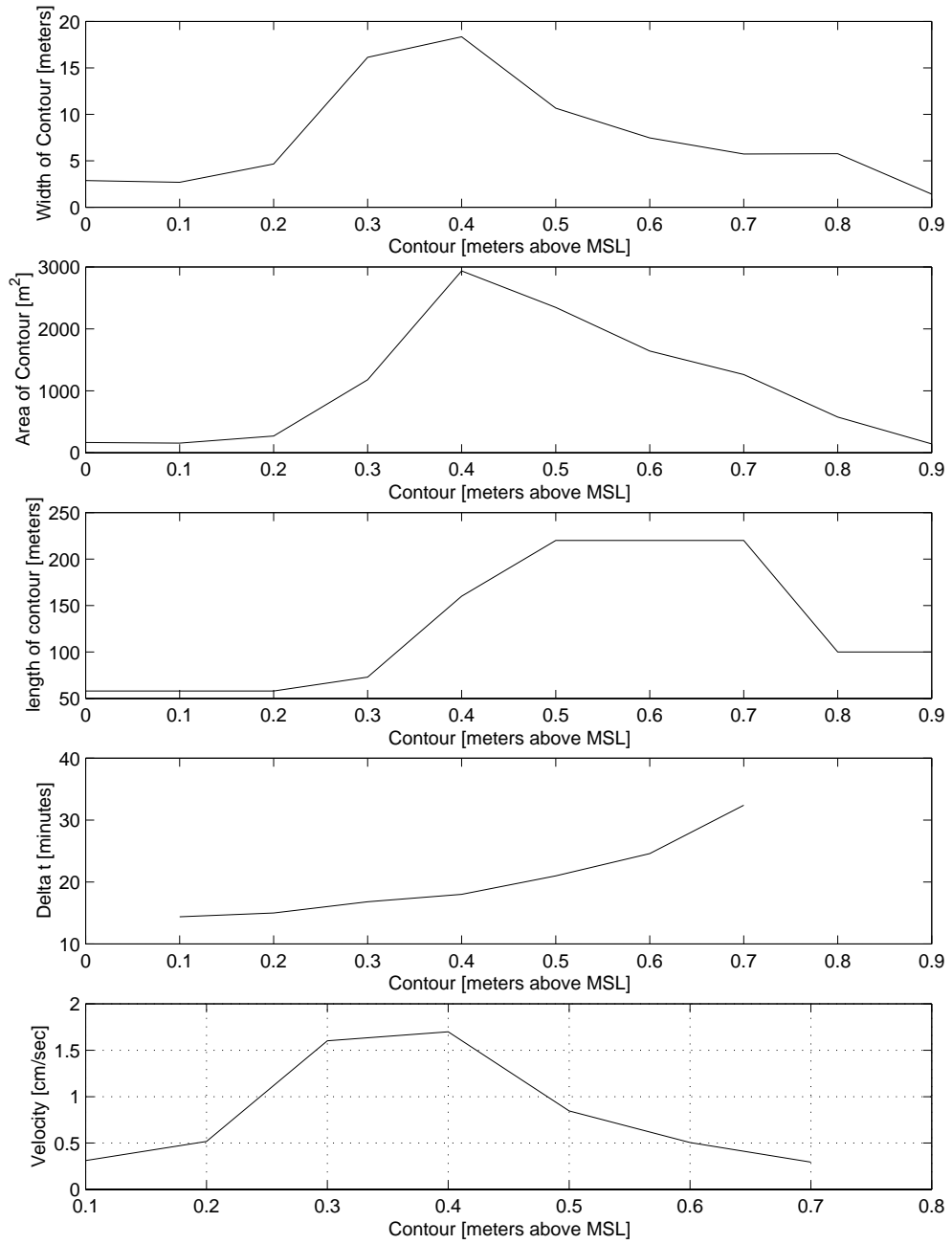


Figure 3.2: Infilling of marsh surface with rising tide.

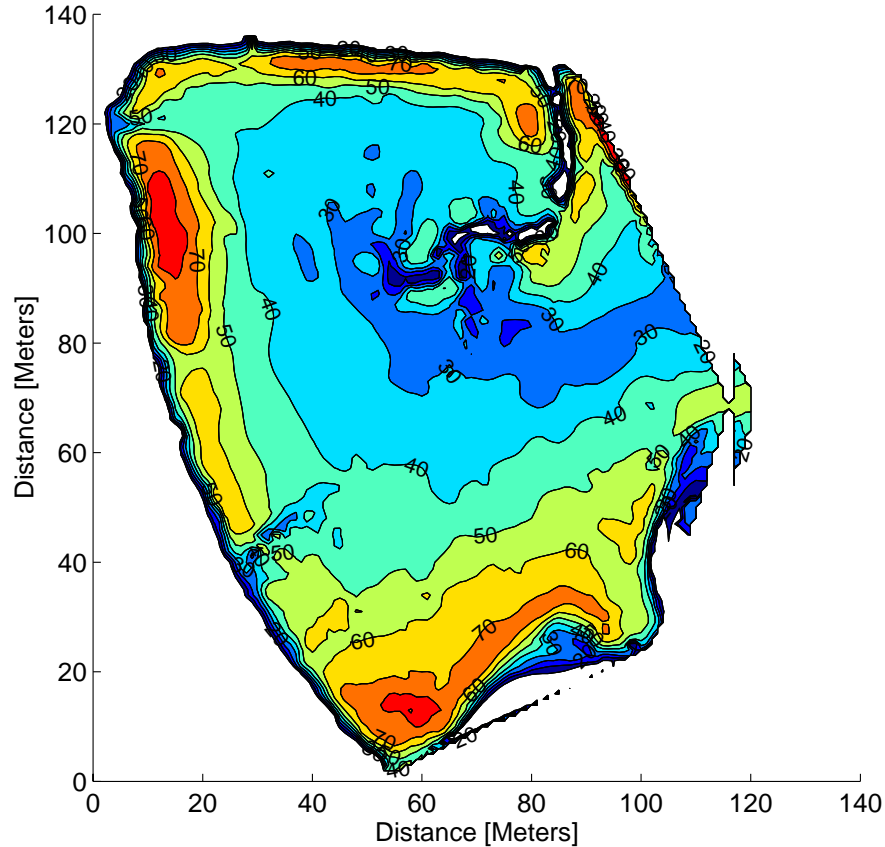


Figure 3.3: Determining area and length of contour intervals.

The mean distance between two contours was estimated by determining the area between two contours, and dividing the area by the length of the contour. The area between two contours is indicated in Figure 3.2, second panel. The length of the contour was estimated by measuring the length between two contours using a map wheel (Figure 3.2, third panel). For example, the area between 30 and 40 cm above MSL contours is indicated by the light blue color on Figure 3.3. A map wheel is used estimate a length by tracing between the 30 and 40 cm contour. The length of time it takes to fill a contour interval depends on the how rapidly the tide rises 10 cm at a particular contour, which in return depends on tidal amplitude of the tidal cycle being considered. Water level increases more rapidly at mid-tide than at high tide. The lower elevations on the marsh are commonly related to mid-tide elevations, and consequently the velocities are higher at these elevations. As the rate of increase in water level becomes smaller, flow velocities decrease. This happens at the higher

contours. Velocities estimated from this calculation range from 1.5 cm/s , 30 cm above MSL to 0.5 cm/s , 60 cm above MSL. The magnitude of the estimated velocities depends on tidal amplitude, with higher amplitudes producing higher velocities. A tide of amplitude 110 cm above mean sea level was used in the example shown in Figure 3.2.

3.3 Velocity measurements

Flow conditions on the marsh surface were measured throughout the duration of tidal flooding at all five stations along the sampling transect during tidal cycles of a range of different tidal amplitudes, to quantify the variability in velocity among tides of different amplitudes. In order to make flow measurements, the sampling location needs to be flooded to a depth of at least 15 cm. This requirement provided the lower bound on tidal amplitudes for which measurements could be made of approximately 80 cm above mean sea-level. The higher tidal amplitudes occur less frequently than those with lower amplitudes so the upper end of tidal amplitudes is controlled by the frequency of their occurrence. The highest tidal amplitude during which velocity was successfully measured was 135 cm above mean sea-level, and this water level on average occurs once every two months.

The velocity measurements made on the marsh surface have been summarized in Table 3.1. Each line in Table 3.1 represents a particular time series. Each time series is described by the maximum velocity during rising and falling tide, its duration, and the amplitude of the tide it was measured on. Also the elevation above the boundary where the velocity measurements were made has been indicated. The measurements made at station 2 were made at a number of different elevations above the bottom to test the influence of the vertical position of the current meter. It was found that it was more important to capture velocity measurements for as large a portion of the tidal cycle as possible than to measure higher in the canopy, and the measurements at the four remaining stations were all made 10 cm above the boundary. It was found that measurements made at station 1 and 2 were characteristic of processes on the creek bank, and measurements made at station 3, 4 and 5 were characteristic of processes in the interior. In this section, velocity measurements made at station 1 have been used to describe processes on the creek bank and velocity measurements made at station 5 have been used to characterize processes in the interior.

There is little variation in flow velocity with tidal amplitude or along the transect (Figures 3.4 and 3.5). The measurements on the creek bank show a more pronounced separation between rising

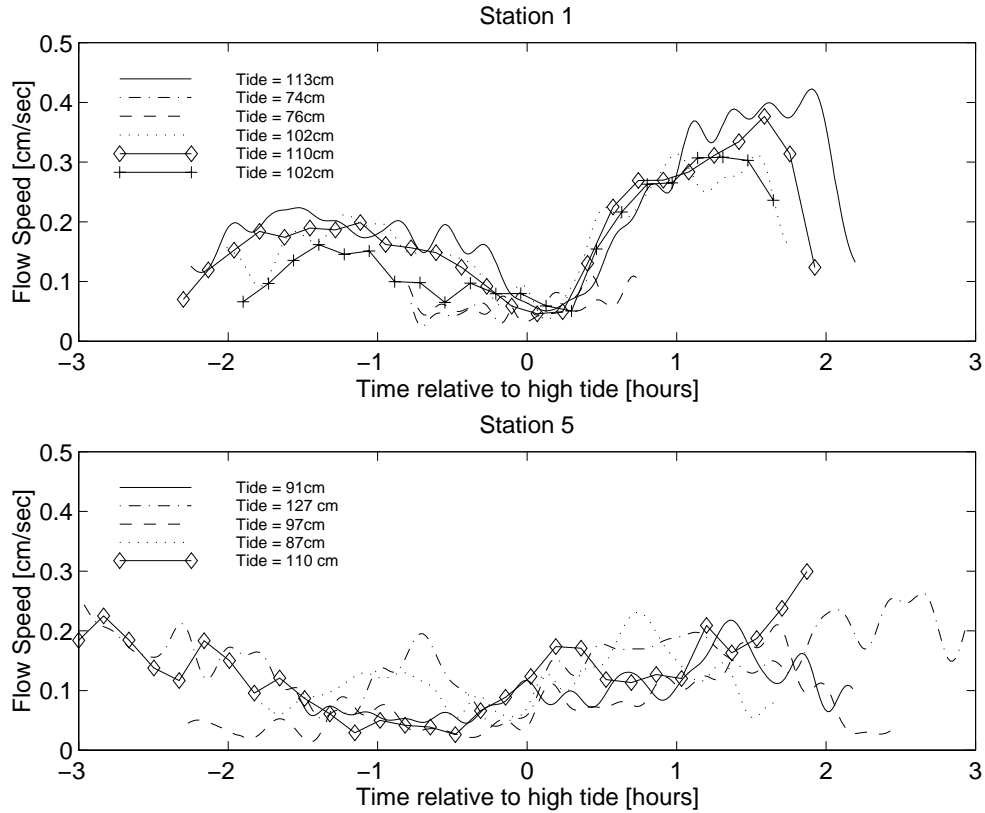


Figure 3.4: Comparison of measurements made at a range of tidal amplitudes at stations 1 and 5.

and falling tide than do the measurements in the marsh interior (Figure 3.4). The highest velocities were measured at station 2, on the highest part of the marsh, but all velocities were less than 1 cm/s, approximately 2 orders of magnitude smaller than the flow velocities in the tidal creek. There is little variation in flow velocity among stations and among tides of different amplitudes relative to flow velocity in the tidal creek.

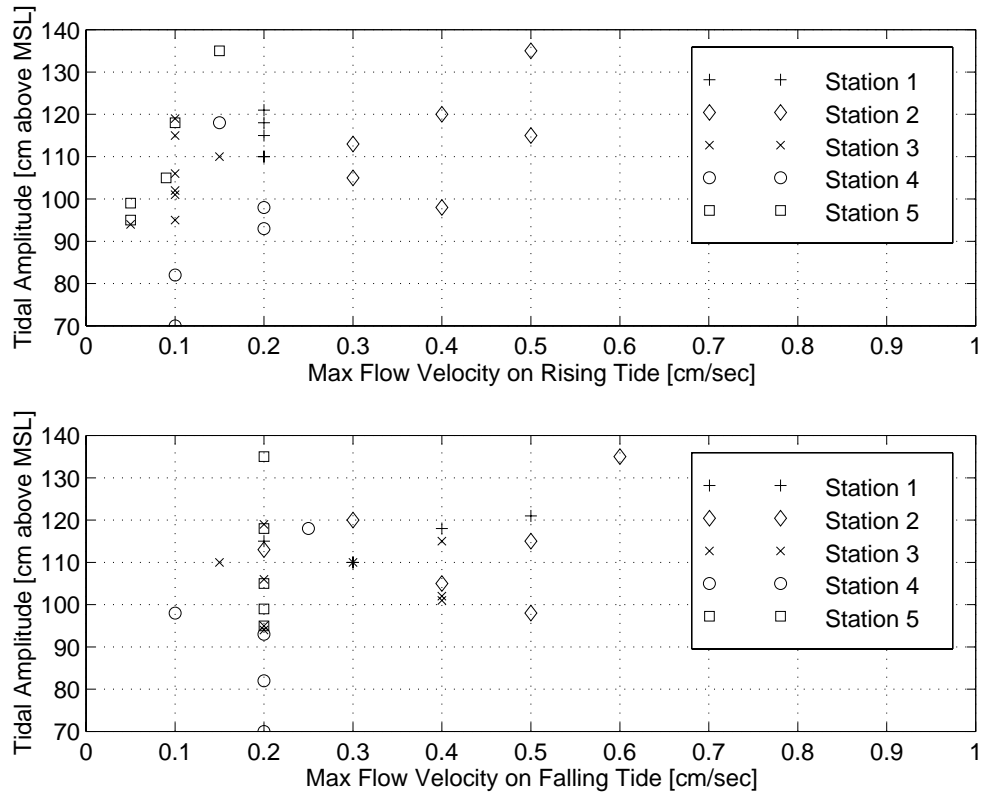


Figure 3.5: Maximum flow velocities measured on the rising and on the falling tides.

Station	Date	Time of high tide	Max velocity rising tide [cm/s]	Max velocity falling tide [cm/s]	Duration [hours]	Amplitude [cm]	Elevation [cm]
1	10 15 96	11:00	-0.2	0.2	4.5	107	10
1	02 21 97	8:36	-0.05	0.1	1.5	74	10
1	02 21 97	20:48	-0.05	0.1	1.5	76	10
1	03 09 97	9:48	-0.2	0.5	4.5	113	10
1	03 10 97	10:12	-0.2	0.3	3.5	102	10
1	03 10 97	22:36	-0.2	0.4	4.5	110	10
1	03 11 97	11:00	-0.2	0.3	3.45	102	10
2	09 23 96	18:24	-0.4	0.3	3	112	5
2	09 24 96	19:00	-0.5	0.6	3.5	127	30
2	09 25 96	7:24	-0.3	0.2	2.5	105	30
2	09 25 96	20:00	-0.3	-	2.5	114	10
2	11 15 96	12:36	-0.7	0.7	4	121	20
2	11 16 96	13:12	-0.5	0.5	3.5	107	20
2	03 11 97	23:24	-0.3	0.4	2.25	97	20
2	03 23 97	21:12	-0.4	0.5	1.5	90	10
3	09 23 96	5:12	-0.05	0.2	2.5	86	10
3	09 22 96	16:48	-0.1	0.2	3.5	98	10
3	09 20 96	14:24	-0.1	0.2	4	102	10
3	09 20 96	1:36	-0.1	0.2	2.5	87	10
3	09 19 96	13:24	-0.15	0.15	3.5	102	10
3	01 09 97	9:36	-0.15	0.3	3.5	102	10
3	04 08 97	22:24	-0.1	0.4	3.5	107	10
3	04 09 97	23:12	-0.1	0.4	3.75	93	10
3	04 11 97	0:00	-0.1	0.4	3	94	10
4	11 12 96	10:00	-0.05	0.05	3.5	90	10
4	10 17 96	0:36	-0.1	0.2	4	76	10
4	10 18 96	13:24	-0.15	0.25	5	110	10
4	10 17 96	12:24	-0.2	0.2	4	85	10
4	11 13 96	10:48	-0.2	0.1	4	90	10
5	12 11 96	22:00	-0.05	0.2	4	91	10
5	12 12 96	10:36	-0.15	0.2	6	127	10
5	12 12 96	23:00	-0.09	0.2	4.5	97	10
5	12 10 96	21:00	-0.05	0.2	3.5	87	10
5	12 11 96	10:00	-0.1	0.2	5	110	10
5	11 21 96	18:24	-0.2	0.2	4	92	10

Table 3.1: Summary of velocity measurements. Each line represents a velocity time series measured over one tidal cycle. The flow on a tidal cycle is characterized by maximum velocity on the rising and falling tide, duration of marsh surface flooding, maximum tidal amplitude in cm above MSL and sampling elevation in cm above the bottom.

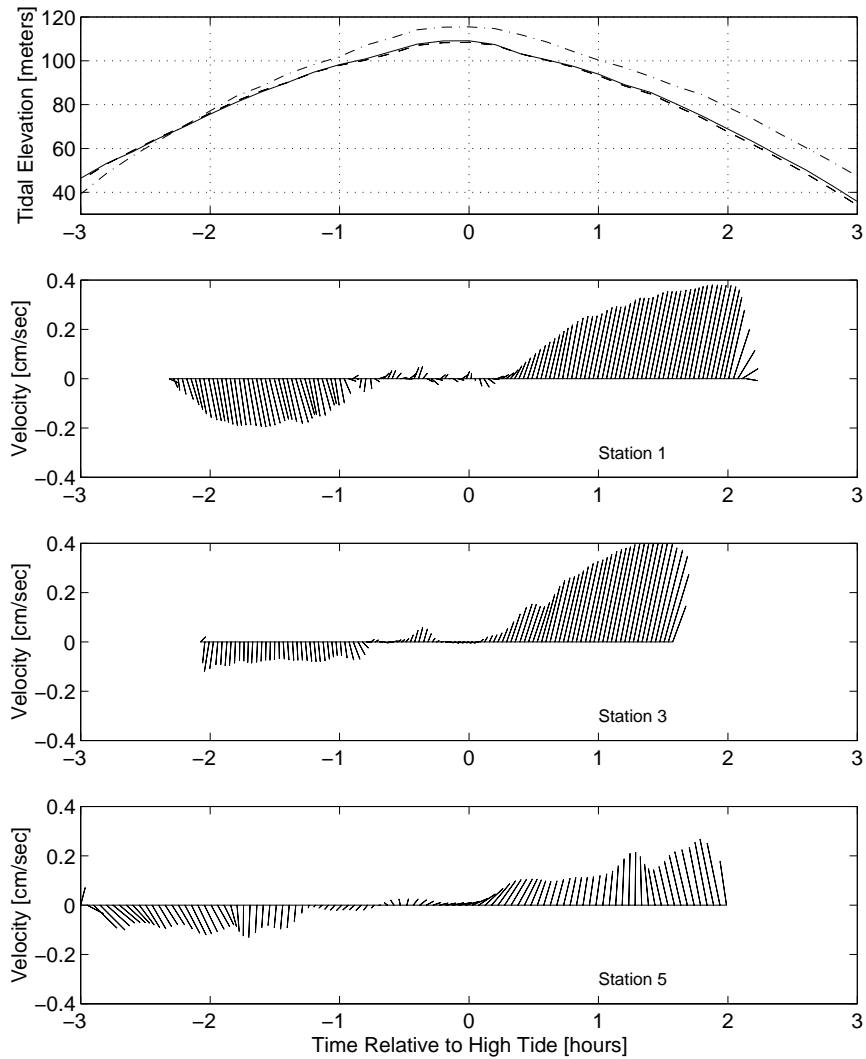


Figure 3.6: Variation in depth and flow velocity over three tidal cycles. In the top panel, water level variation of three different tides of similar amplitude is shown. In the following three panels, vector plots of flow speed and direction at three different stations have been shown. Each vector represents direction and magnitude of the flow as a function of time relative to high tide. The flow direction is from the horizontal axis to the end of the vector. The marsh interior (or east) is at the bottom of each panel, and Phillips creek (or west) is at the top of each panel.

Measurements of flow velocity made using the Acoustic Doppler Velocimeter (ADV) are shown in Figure 3.6 for three different locations, station 1, station 3 and station 5 along the transect. The velocity measurements were made at three different tidal cycles of similar amplitude. The top panel of Figure 3.6 shows the variation in water level during marsh surface flooding, and the three following panels show vector plots of flow speed and direction during marsh surface inundation. High frequency variation was removed from the velocity time series using a low pass filter with a 15 minute cut-off frequency. During measurements, the current meter was oriented with one axis in the east/west direction and another in the north/south direction, which is approximately perpendicular to Phillips Creek (oriented NNW/SSE) and approximately parallel to the flow direction which was east/west. Positive flow directions were towards west. At each of the three stations, the flow velocities on the rising tide were negative, indicating that the flow direction from west to east (from Phillips Creek to the marsh interior). At peak water level, flow velocity decreases to zero, and as water level begins to drop, flow direction reverses. Flow velocities on the falling tide were positive, indicating that the flow direction from east to west (from the marsh interior to Phillips Creek) (Figure 3.6). The flow velocities at all locations along the transect were extremely low. The highest velocities were measured at the onset and at the end of a flooding period, but even the highest velocities were less than 1 cm/s. The largest velocities were observed on the creek bank during the falling tide. In general, velocities on the bank are higher than in the marsh interior. The velocities are lowest when the depth is greatest (slack tide). The velocities are larger during falling tide than during the rising tides.

The three stations shown in Figure 3.6 were at different elevations so depth during measurements varied between stations even though these measurements are made at tides of similar amplitudes. At station 1 the depth range was 0.55 meters, at station 3 the depth range was 0.4 meters and at station 5 the depth range was 0.7 meters. The different ranges in depth meant that each station was flooded for a different period of time. While stations 1 and 3 were flooded for approximately 4 hours, station 5 was flooded for more than 5 hours during tides of similar amplitude.

3.3.1 Circulation

The velocity measurements suggest a pattern of circulation on the marsh surface that changes with time relative to high tide. Each panel in Figure 3.7 represents a one hour step in a series ranging from 3 hours before to 3 hours after high tide. During this 6 hour period, the marsh surface

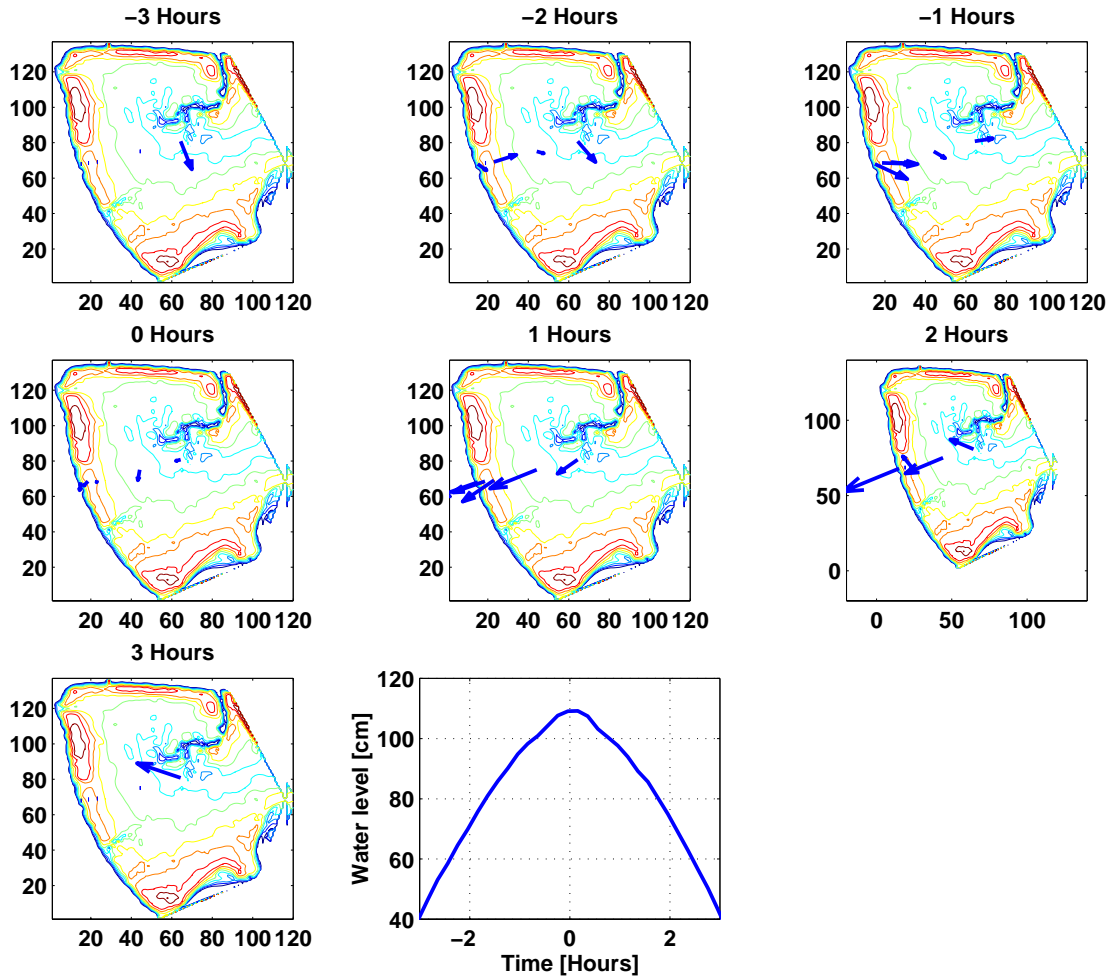


Figure 3.7: Circulation on marsh surface. Each panel represents a one hour time step throughout a 6 hour period of marsh surface flooding. Flow vectors represent velocity and flow direction at each station, and at each time step. The last panel represents water level variation during the inundation period.

	Station 1	Station 2	Station 3	Station 4	Station 5
Stem density [stems/m ²]	124-172	148-204	136-188	88-212	92-148
Stem diameter [cm]	0.9-1.1	0.6-1	0.6-0.8	0.5-0.7	0.6-0.8
Plant height [cm]	85-110	65-75	45-85	50-65	65-86

Table 3.2: Vegetation densities and stem thickness at each sampling location

is completely flooded and completely drained. Each panel shows five flow vectors, one at each of the five stations, representing mean flow velocity and direction during a particular time step. The flooding starts in the lower part of the interior, but once water level reaches elevations greater than the levee, the flow direction is from the tidal creek towards the marsh interior. In the course of the next two hours (the two hours before high tide) the flow direction is from the creek to the marsh interior. At high tide (time 0) flow velocity decreases to zero, and on the falling tide (the two hours after high tide) the flow direction is from interior towards the tidal creek. In the last hour the water level has dropped so low that water level is less than 15 cm at all locations except for at station 5. Once water levels fall below the elevation of the creek bank the remaining water will flow towards the small tidal creek on the north side of the marsh. Tidal asymmetry is apparent with higher velocities on the falling tide than on the rising tide. The tidal asymmetries and the difference in flow direction between rising and falling tides suggests that water does not enter and leave the marsh along the exact same flow path.

3.3.2 The effect of marsh vegetation on the flow.

The marsh surface vegetation provides an important control on flow within the vegetation canopy by modifying both mean velocity and the turbulent properties of the flow. The velocity measurements were made over a period of 8 months, with emphasis on winter months because water levels were higher during this time; vegetation densities were not constant in this period. Vegetation densities along the transect are described in terms of an upper and a lower limit, in terms of estimated stem diameter and in terms of plant height (Table 3.3.2). The plants on the creek bank are thicker and taller, but less dense, than plants in the interior. The magnitude of the effect of the vegetation on the flow was assessed by measuring conditions both within the canopy and in the tidal creek immediately adjacent (upstream on the rising tide, downstream on the falling tide) to the vegetation boundary. These measurements provide a basis for comparing turbulence conditions in the creek with turbulence conditions on the marsh surface.

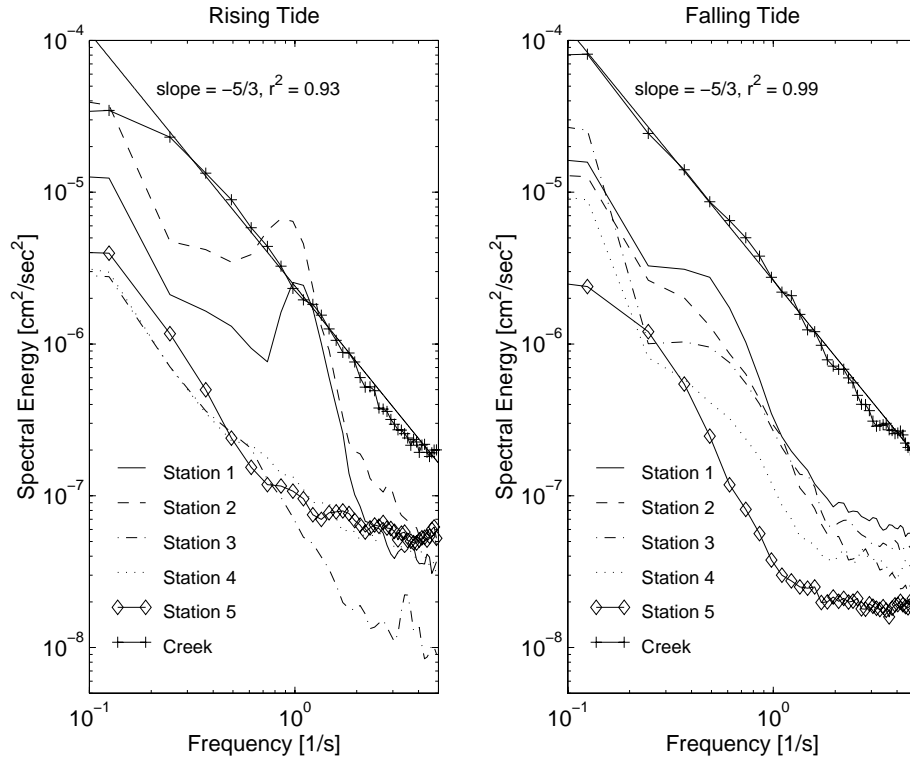


Figure 3.8: Turbulence spectra at the five sampling stations and in the creek. All spectra were calculated for a 819.2 second data segment on the rising tide and on the falling tide. The spectra are scaled such that the area under each spectrum is equivalent to the variance of the turbulent fluctuations.

In the tidal creek, the turbulent energy spectrum has the characteristics of a fully developed turbulent flow in the inertial subrange; the spectrum has the characteristic exponent of $-5/3$ (Figure 3.8). At station 1 which is located within the vegetation canopy, 2 meters from where the creek measurements were made, the energy at the lower frequency is reduced relative to the flow in the tidal creek (Figure 3.8). As the flow propagates further into the canopy the energy in the low frequency end of the spectra is further reduced. The reduction in energy at low frequencies indicates that the vegetation inhibits production of larger turbulent eddies. It is also likely that the vegetation contributes to the break down of larger eddies into smaller ones. While the Reynolds number ranges from 250-500 within the vegetation canopy (indicating laminar flow), the energy in the spectra indicates that the flow is in a transitional regime where there is some production of kinetic energy, but not as much as in a fully turbulent flow.

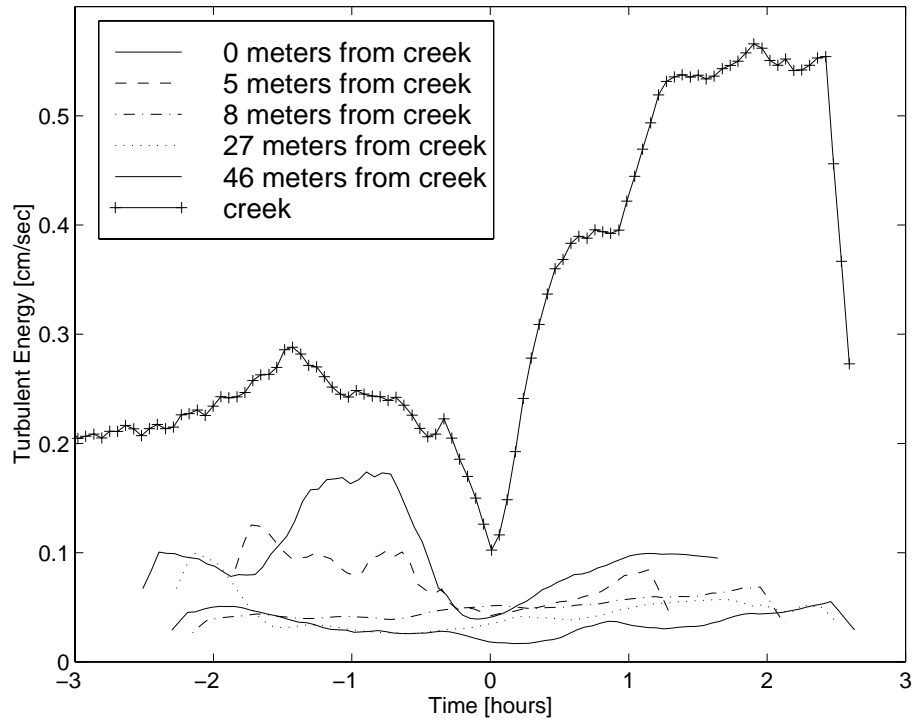


Figure 3.9: Turbulent energy variation with time and location. On the rising tide the tidal creek is upstream from the vegetation canopy, on the falling tide it is down stream from the canopy.

The high frequency velocity measurements were also used to determine the turbulence intensity or turbulent energy of the flow and the Reynolds stress tensor. Of the six different components in the Reynolds stress tensor, the horizontal shear stresses, τ_{xz} and τ_{yz} were combined into a single vector $\tau = \sqrt{\tau_{xz}^2 + \tau_{yz}^2}$ to describe the shear stress in the flow at the level where measurements were made, typically 10 cm above the bottom. In a shear flow such as flow in a channel with no obstructions, a high degree of correlation exists between velocity fluctuations, u' and v' in the the two horizontal directions, particularly in vicinity of the bottom where the shear is strongest (Tennekes and Lumley (1972)). The shear is predominantly transferred by the larger scale turbulent eddies. One of the effects of the vegetation is to break down the larger turbulent eddies and consequently the vertical stress profile is likely to be one that is more uniform than that of an unobstructed shear flow. Using this argument, I approximate the shear stress acting on the boundary, τ_b as the stress measured at 10 cm above the boundary, τ . The boundary shear stress was used to calculate the shear velocity, $u_* = \sqrt{\frac{\tau_b}{\rho}}$, which, among others, is a measure of the ability of the flow to maintain sediment in

suspension.

Turbulent energy decreases with distance across the marsh surface (Figure 3.9). The turbulent energy is highest on the rising tide when the flow direction is from the creek towards the marsh interior. As the flow progresses into the vegetation canopy and the large turbulent eddies are broken down (Figure 3.8), the turbulent energy decreases. Turbulent energy levels at the creek bank stations reflect the conditions in the in the tidal creek; the energy levels are higher and follow the changes seen in the creek. On the falling tide velocities increase but the increase is not matched by production of turbulent energy (Figure 3.9). At this time, the flow is from the marsh interior to the creek, and the turbulent energy reflects conditions within the canopy, characterized by lower turbulent energy levels. There is no correlation with turbulent energy in the tidal creek.

Shear velocities are high (in a relative sense) on the two creek-bank stations on both the rising and the falling tide (Figure 3.10). Higher values of shear velocity correspond to times of higher flow velocity. In the marsh interior (stations 3-5) the shear velocity remains low at all times.

3.3.3 Vertical structure of velocity

In the preliminary phase of this study, changes in velocity and stress with depth were measured (Figure 3.11). These measurements are not precise because only one sensor was available, and water depth changed 5-10 cm between the first and last measurement of the profile. These measurements were also made prior to establishing the sampling transect otherwise used, and were made at a slightly different location, hence the slightly higher velocities. The vertical profile of velocity indicates a characteristic inflection point at 7 cm above the bottom, corresponding to the elevation of the sheath of *Spartina alterniflora* (Leonard and Luther (1995)). The stresses ($\overline{u'w'}$ and $\overline{v'w'}$) have been combined to calculate the vertical distribution of stress in the flow. The stress profile suggests that shear stress increases in proximity of the boundary, and that our approximation of boundary shear stress as the stress at 10 cm above the bottom may be an underestimate of shear stress at the boundary.

3.4 Suspended sediment concentration measurements

Suspended sediment concentrations on the marsh surface were measured throughout the duration of tidal flooding at all five stations along the transect, during tidal cycles of a range of different tidal

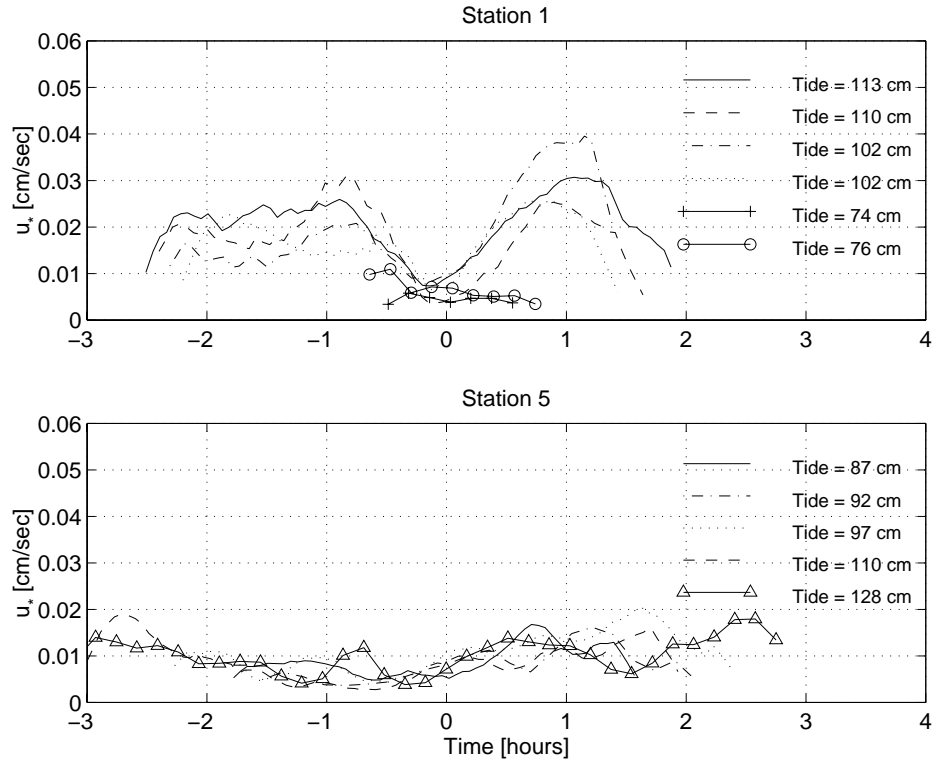


Figure 3.10: Variation in shear velocity with time at stations 1 and 5. The shear velocity at station 1 is representative of conditions on the creek bank and levee, and station 5 is representative of conditions in interior.

amplitudes to quantify the variability in suspended sediment concentrations among tides of different amplitudes. The measurements were made simultaneously with velocity measurements to enable calculation of sediment flux between adjacent stations. In addition to concentration measurements, sediment deposition on sediment traps was measured. The concentration measurements are summarized in Table 3.3. Each line in Table 3.3 represents a time series of concentration measurements made during one tidal cycle.

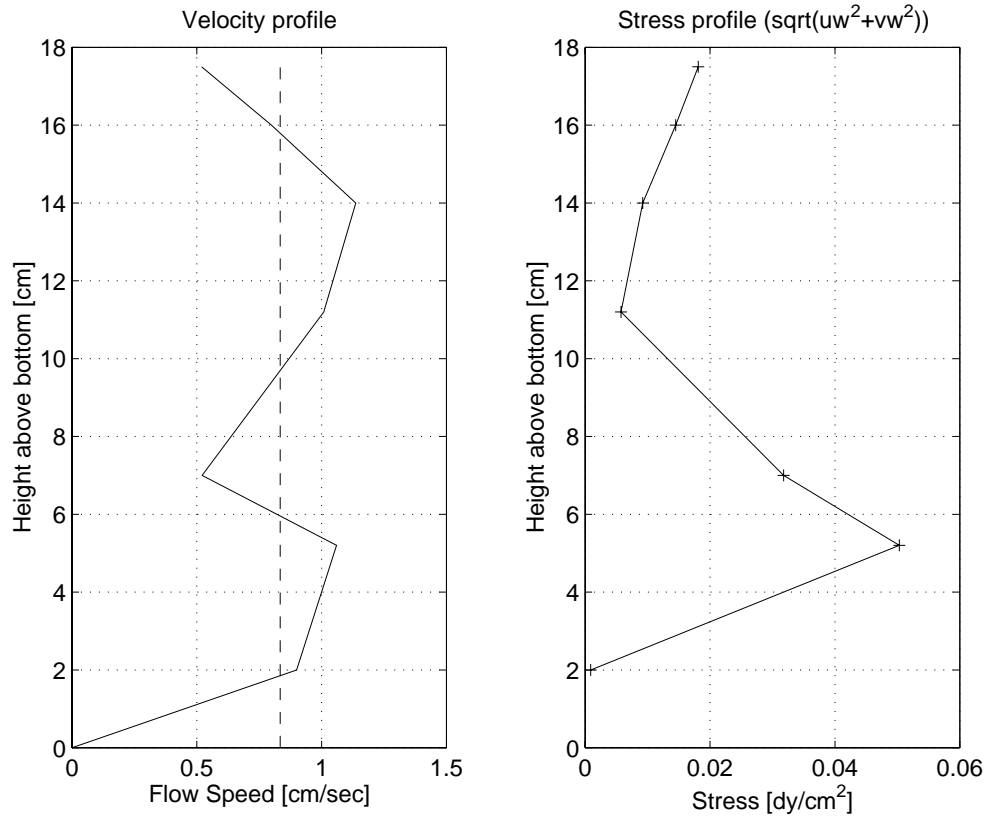


Figure 3.11: Velocity and stress variation with depth.

Station	Date	Time of high tide	Max Conc. rising [mg/l]	Max Conc. falling [mg/l]	Tidal Amplitude [cm above MSL]
1*	03 09 97	10:00	170	75	113
1*	10 15 96	12:18	80	30	110
1*	03 10 97	10:18	110	40	107
1*	03 10 97	22:18	70	20	102
1*	03 11 97	11:18	60	20	102
2*	09 23 96	18:24	150	30	113
2*	09 24 96	19:00	150	30	121
2*	03 23 97	21:12	150	50	128
2*	11 15 96	12:36	40	40	98
2*	03 11 97	23:24	50	20	97
2*	09 25 96	7:24	150	50	105
3*	04 09 97	23:12	70	30	93
3*	04 11 97	0:00	50	30	94
3*	04 08 97	22:24	70	30	106
4*	10 18 96	0:36	20	20	73
4*	11 12 96	22:00	20	20	59
4*	11 13 96	10:48	40	30	88
5	11 20 96	17:48	20	20	97
5*	11 21 96	6:00	20	20	106
5	11 23 96	19:48	20	20	82
5	11 24 96	8:24	20	20	93
5*	12 11 96	21:48	20	15	89
5*	12 12 96	10:24	20	-	125
5*	12 12 96	23:12	25	20	96
5	12 13 96	11:12	20	20	140
5	12 14 96	0:00	40	30	81
5	12 14 96	12:12	40	30	117

Table 3.3: Summary of measured concentration time series. Each line represents a time series of concentration measurements made on one tidal cycle. Each time series is characterized by maximum concentration on rising tide, maximum concentration on falling tide and the amplitude of the tidal cycle. Several of these measurements were made simultaneously with velocity measurements; those measurements are marked by an asterisk.

3.4.1 Temporal and spatial variation

Sediment concentration on the marsh surface varies with time relative to high tide and with distance from the tidal creek (Figure 3.12). On the rising part of the tide, sediment concentrations are higher on the creek bank than in the marsh interior. At stations 1 and 2, sediment concentrations increase on the rising part of the tide. As slack tide is approached, the concentration levels drop, in response to decreased sediment supply from the creek. At station 3, at the transition between creek bank and interior, the concentration levels decrease to half of the levels at station 1 and 2. The flow direction on the rising tide is from the creek towards the marsh interior, and consequently, the decrease in sediment concentration on the rising part of the tide indicates deposition on the creek bank. The concentration measurements do not indicate resuspension of sediment from the marsh surface because sediment concentrations do not increase on the falling tide when velocities and stresses on the marsh surface were greatest. At station 1, on the creek bank, sediment concentrations respond to changing amplitudes, whereas in the marsh interior (station 5) they do not. Although the concentration levels vary among tides at station 1, the temporal pattern is consistent between tides (Figure 3.13). On the tides with lowest amplitude, the difference in concentration between rising and falling tide is negligible.

3.4.2 Variation among tidal cycles

Concentration measurements were also made for a 49 day period divided into 3 two-week periods in May and June, 1997 to obtain a measure of the variability among tides. The measurements were made simultaneously in the tidal creek, at station 1 and at station 2. The data logger was programmed to record concentration for 6 hours on each tide for a two week period. The OBS sensor in the tidal creek was at a lower elevation than the marsh sensors, and occasionally this sensor was flooded for longer than 6 hours. The sensor at station 2 was at the highest elevation, and on the lowest tides to flood the marsh surface, this sensor is only just inundated which results in the sensor measuring a slightly higher concentration than actually present. These measurements are summarized in Tables 3.4 and 3.5. Each line in Table 3.4 and 3.5 represents one tidal cycle. Only the measurements made on tides sufficiently high to flood the marsh surface are listed. Out of 92 measured tidal cycles, 37 had a tidal amplitude high enough to fully inundate the marsh surface. The tidal amplitude during this period ranged from 41 to 158 cm above MSL and tidal creek

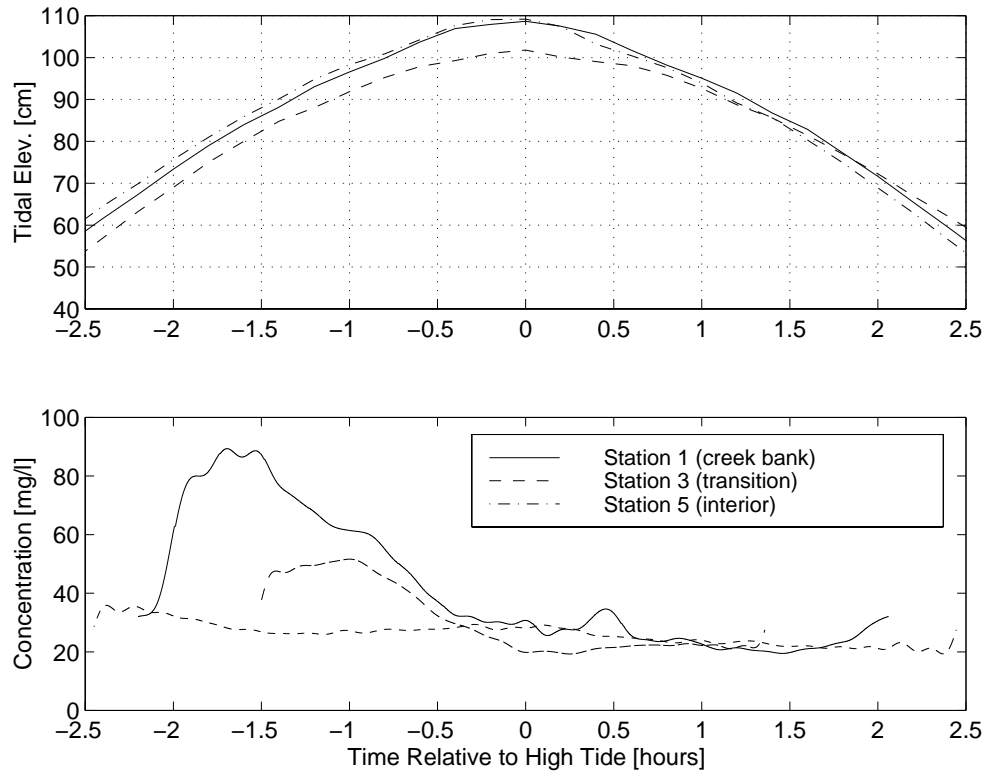


Figure 3.12: Change in sediment concentration with time and with distance from tidal creek.

concentrations on tides inundating the marsh surface ranged from 40 to 550 mg/liter.

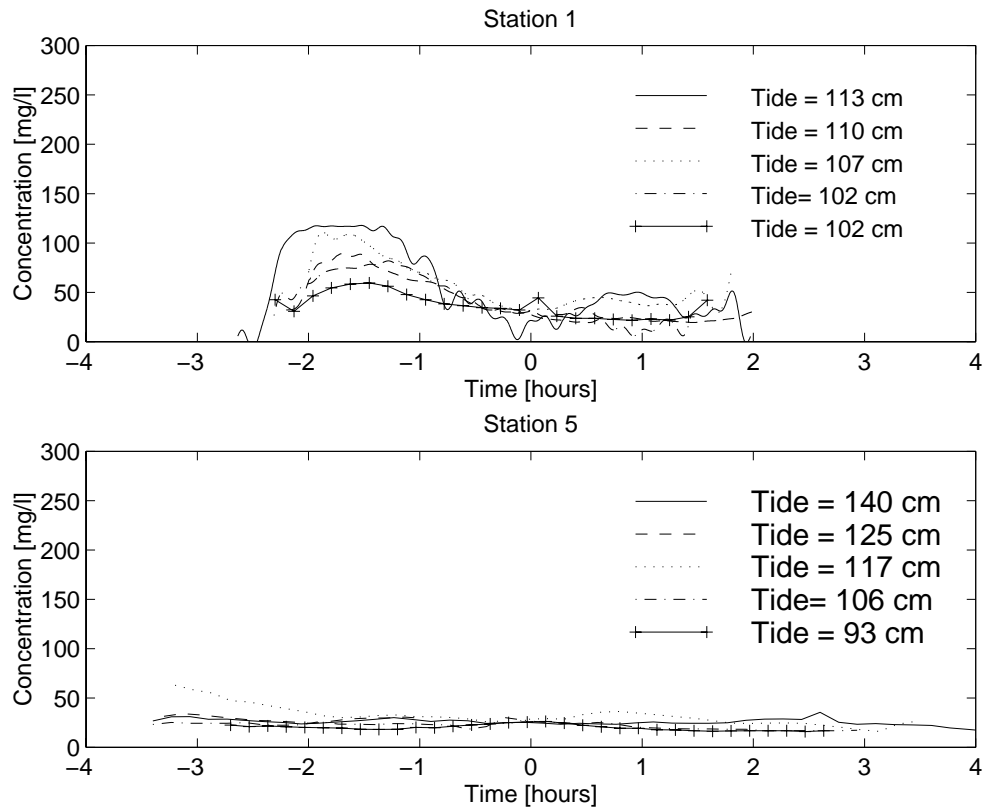


Figure 3.13: Sediment concentration as a function of time at station 1 and station 5. The measurements were made at tides of different amplitude. At station 1, on the creek bank, sediment concentrations respond to changing amplitudes, whereas in the marsh interior, at station 5 they do not. Although the concentration levels vary among tides at station 1, the temporal pattern is consistent between tides.

Date	Time of high tide	Max conc. rising in creek [mg/l]	Max conc. rising Station 1 [mg/l]	Max conc. rising Station 2 [mg/l]	Amplitude [cm]	Predicted tide [cm]	Duration [hours]
05 19 97	19:24	40	40	40	75	97	1
05 24 97	23:00	100	80	60	100	100	1.5
05 26 97	0:00	50	30	80	83	95	0.25
05 26 97	13:00	100	40	60	84	73	0.5
05 27 97	1:00	300	250	170	104	90	1.5
05 27 97	14:00	100	80	-	83	75	0
05 28 97	2:00	550	550	425	111	82	2
05 31 97	5:00	60	40	0	80	78	0
05 31 97	18:00	100	60	40	88	98	0.5
06 01 97	6:00	60	20	0	80	80	0
06 01 97	19:00	80	60	50	99	105	1
06 02 97	7:00	70	30	20	91	78	0.5
06 02 97	20:00	no data	-	-	132	110	
06 03 97	8:00	no data	-	-	122	78	
06 03 97	21:00	550	575	500	158	110	4
06 04 97	9:00	200	200	180	121	80	2.5
06 04 97	21:00	450	450	400	150	108	3
06 05 97	10:00	70	55	45	101	78	1.5
06 05 97	22:00	100	90	70	124	101	2.5
06 06 97	10:00	90	70	40	94	73	1.5
06 06 97	23:00	350	350	250	136	95	2.5
06 07 97	11:00	190	180	100	104	71	1
06 07 97	23:00	250	250	180	126	90	2.25
06 08 97	12:00	45	25	25	86	70	0.25
06 09 97	0:00	50	45	25	108	80	1.5
06 09 97	12:00	35	35	-	70	68	0
06 10 97	1:00	25	15	-	80	75	0

Table 3.4: Summary of concentration variability among tides, part I. Each line represents one tidal cycle. Concentration time series were measured in the creek, at stations 1 and station 2 at the same time. The time series have been summarized by maximum concentration on the rising tide, at each location, the tidal amplitude in cm above MSL and duration of marsh surface inundation.

Date	Time of high tide	Max conc. rising in creek [mg/l]	Max conc. rising Station 1 [mg/l]	Max conc. rising Station 2 [mg/l]	Amplitude [cm]	Predicted tide [cm]	Duration [hours]
06 18 97	20:00	65	55	50	97	105	1
06 19 97	20:48	80	60	50	97	110	1
06 20 97	21:24	80	60	50	106	110	1.5
06 21 97	22:12	65	50	50	102	110	1.5
06 22 97	23:00	75	45	35	96	105	1
06 23 97	23:48	60	40	30	94	94	1
06 25 97	0:48	50	30	25	91	91	1
06 26 97	1:24	35	20	35	87	85	0.5
06 26 97	14:00	50	30	-	85	85	0
06 27 97	2:12	50	30	40	87	78	0.75
06 27 97	14:48	40	30	-	92	92	0
06 28 97	3:12	40	20	-	83	72	0

Table 3.5: Summary of concentration variability among tides, part II. Each line represents one tidal cycle. Concentration time series were measured in the creek, at stations 1 and station 2 at the same time. The time series have been summarized by maximum concentration on the rising tide, at each location, the tidal amplitude in cm above MSL and duration of marsh surface inundation.

3.5 Grain size distributions

Particle size distributions were analyzed according to the methods developed by (?), although estimates of grain size distributions were made using a Sedigraph particle size analyzer rather than a Coulter counter particle size analyzer (Figure 3.14). The Sedigraph particle size analyzer does not resolve the coarse end of the size distribution. In later work, these samples will be analyzed using a Coulter Counter to obtain results comparable to those of (?).

The grain size distributions shown in Figure 3.14 have two parts, a fine tail, and a coarser material component. Each of these two components is indicated by the dashed lines. The fine end of the distributions are characterized by a tail of uniformly distributed sediment that is indicative of sediment derived from flocculated particles. In the coarse end, the steep curve indicates material from an unflocculated source. The limit between particles derived from flocs and individual grains in suspension is marked by the intersection of the two dashed lines (Milligan and Loring (1997)).

The grain size distributions of sediment deposited at station 1, station 2 and station 4 have very similar characteristics. All three distributions have the tail of uniformly distributed sediment characteristic of sediment from a flocculated source. The distributions of sediment deposited on the creek bank indicate that particles coarser than $10 \mu m$ may be moving as individual particles. Approximately 25 % of the material is coarser than $10 \mu m$. The distribution of sediment deposited at station 4, suggests a lower limit, $5 \mu m$ for the material moving as individual particles (35 % of the material is coarser than $5 \mu m$). The distributions at station 4 have a shorter tail in the fine grain end than the distributions measured at station 1 and 2, suggesting that less flocculated material is deposited at this location.

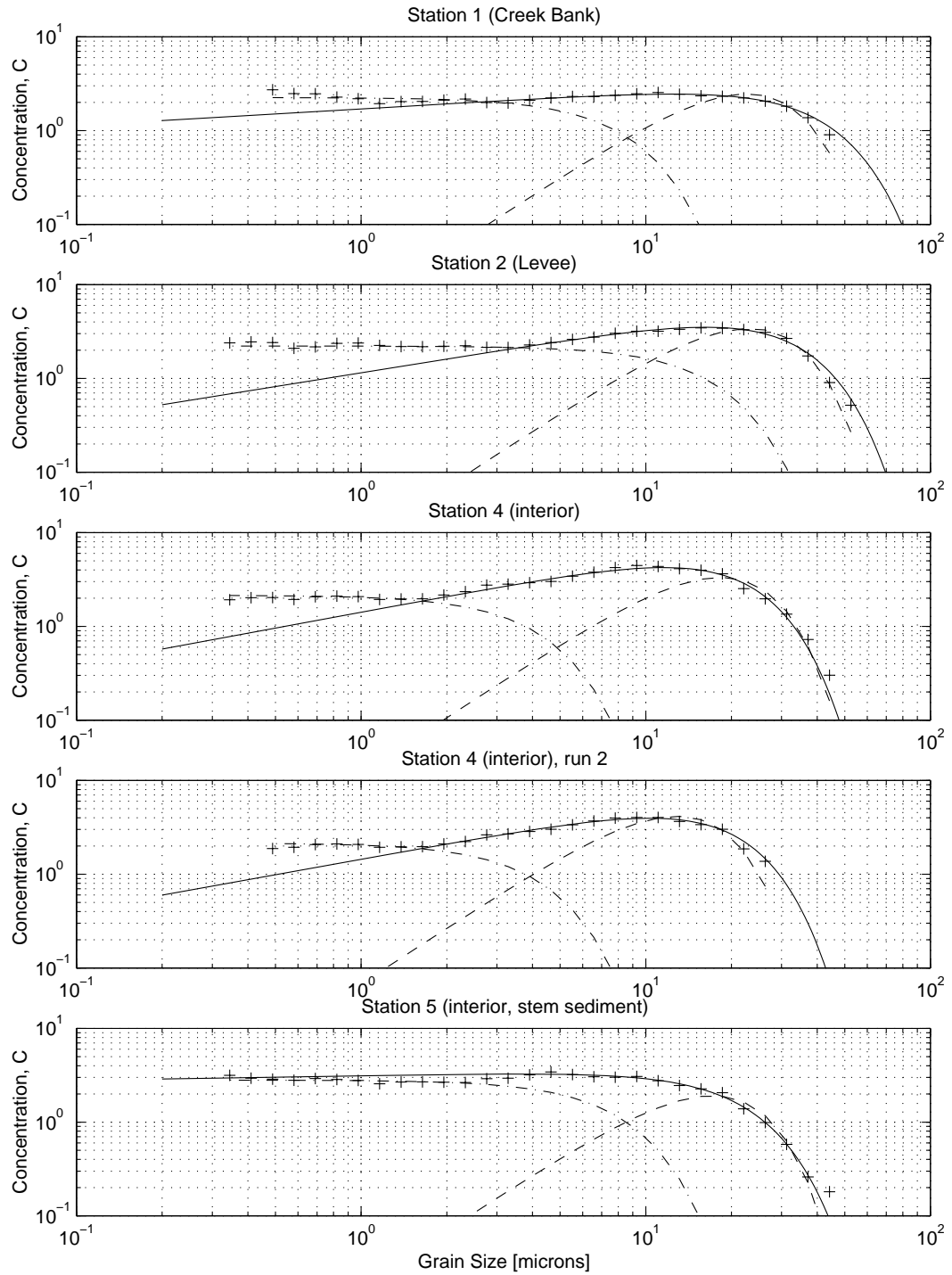


Figure 3.14: Grain size distributions of fully disaggregated sediment. The curves marked by “+” are histograms plotted on a log-log scale. Concentration refers to the fraction of each size class within the entire distribution.

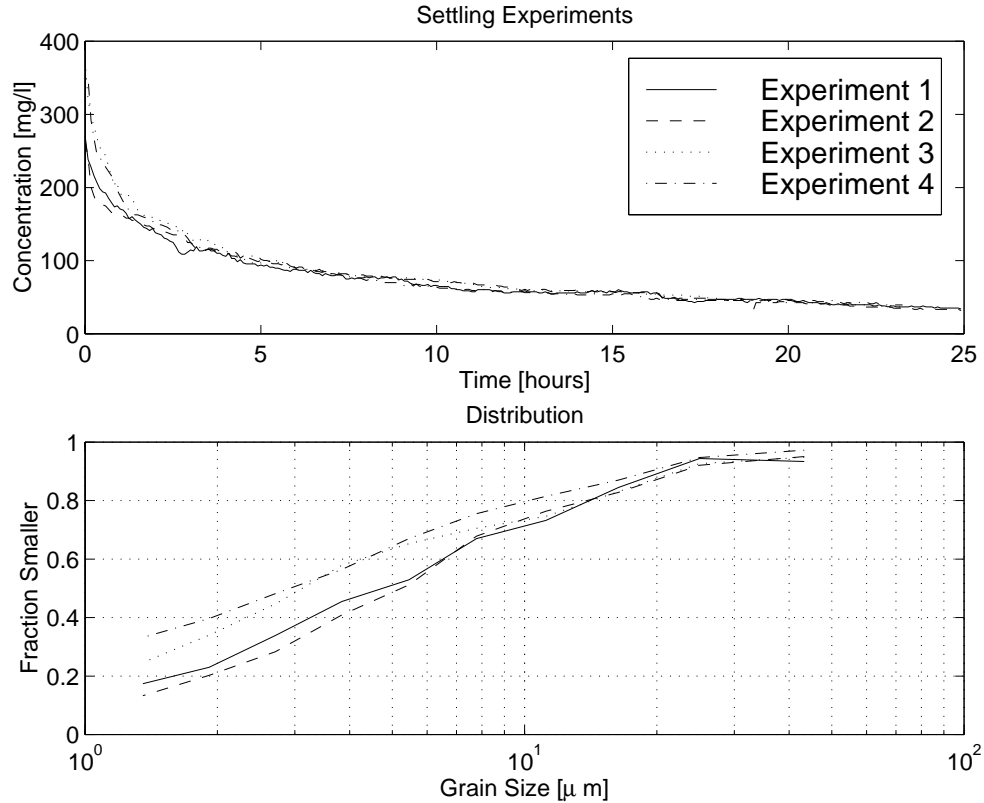


Figure 3.15: Grain size distributions inferred from clearing rates.

3.6 Settling properties of the sediment

A measure of size distribution of sediment in suspension was attempted based on the clearing rate of sediment settling in still water. The results indicated that particle sizes in suspension ranged from $1 \mu\text{m}$ to $40 \mu\text{m}$ in all four experiments (Figure 3.15). The median grain size, D_{50} was $3\text{-}5 \mu\text{m}$. In these calculations, Stokes law (Equation 2.7) has been used to relate settling velocity to grain size. Stokes law was chosen based on the grain sizes in the distribution. The particles are small, and their small size is an indication that they are settling as individual grains. Conversely, during work in the laboratory attempting to determine particles size distributions using other methods, it was observed that the sediment from Phillips Creek marsh had a strong tendency to flocculate, and that flocculation time was very short (within a few seconds). These methods did, however, require higher concentrations than the concentrations present in the settling tube which would enhance the tendency towards flocculation.

3.7 Controls on mean flow velocity and direction

Mean flow speed and direction in Phillips Creek is controlled by tidal forcing with flow in the landward direction on the rising tide and in the seaward direction on the falling tide. Flow speed decreases as the highest water level is approached and increases again on the falling tide. A similar pattern in mean flow direction and speed is observed at station 1, on the creek bank, although flow direction at this location is perpendicular to the flow in the tidal creek. A tidal influence on flow direction was observed at all five stations along the transect, with water flowing from Phillips Creek towards the interior on the rising tide, reversing on the falling tide. A more pronounced difference in flow speed between rising tide, slack water and falling tide was observed on the creek bank than in the marsh interior. In the interior, mean flow appeared more strongly modified by vegetation. All flow speeds measured on the marsh were extremely low ($< 1\text{ cm/s}$). Velocities were lower in the marsh interior than on the creek bank but no measured velocities exceeded 1 cm/s . Tides with higher amplitudes did not produce higher flow velocities on any of the tides observed in this study (Figures 3.4 and 3.5). The flow field on the marsh surface was surprisingly consistent among tides (Figure 3.4).

Mean flow velocities observed on Phillips Creek marsh are significantly lower than mean velocities measured by Leonard and Luther (1995) ($5\text{-}10\text{ cm/s}$) and (Burke and Stoltzenbach 1983) (5 cm/s). Although the mean flow velocity is lower within the vegetation canopy than it would be at the same location if there was no vegetation, its order of magnitude is determined by regional scale forcing of the flow. In this case, regional scale implies the area around the entire length of Phillips Creek (Figure 1.2). Mean flow speed is controlled by water surface slope, which in return depends on the spatial gradient of the tidal wave, vegetation roughness of the marsh surface, and the landscape topography in the Phillips Creek area.

It is characteristic of the Phillips Creek area that the landscape slope is in the seaward direction; the marshes further landward are at a slightly higher elevation than the study site. As water level in the area increases, the wetted surface area of the marsh gradually increases, causing divergence of the flow. At the study site, flow velocities were estimated using marsh surface topography and water elevation change over a tidal cycle. The velocities estimated in this manner ($0.5\text{-}1.5\text{ cm/s}$) were in relatively good agreement with measured velocities (Figure 3.2). The marsh surface at the study site is fully inundated at the tidal elevations of interest in this study, but mean flow velocities may be affected by water spreading on to higher landscapes bordering the study site. Although the flow

velocities measured on Phillips Creek marsh were consistently low, spatial variability in forcing may produce greater spatial variability in mean flow velocity on a regional scale than implied by this data set.

Velocities measured at stations 1, 3 and 5 on the marsh surface (Figure 3.6), indicate higher velocities on the falling tide than on the rising tide. The seaward landscape slope may in part explain this slight asymmetry observed between velocities on the rising and falling tide. Water entering the marsh on the rising tide is flowing uphill relative to the landscape slope, and the water leaving the marsh is flowing downhill. In addition, resistance to the flow increases in the on marsh direction, an effect that would also act to decrease velocities of flow onto the marsh and increase flow velocities leaving the marsh.

3.8 Turbulence and sediment transport

Vegetation on the marsh surface modifies the hydrodynamical environment to one that favors sediment deposition. Measurements of turbulence structure within the canopy indicate that the turbulent energy of the flow decreases with distance from the tidal creek; the most dramatic decrease was observed at the vegetation boundary, in the transition between tidal creek and marsh (Figure 3.9). On the marsh surface, the greatest reduction in turbulent energy occurs across the levee. At station 3, 8 meters from the tidal creek, the turbulent structure is similar to the structure at station 4, 27 meters from the creek and station 5, 46 meters from the creek (Figure 3.9).

Frequency spectra of flow within the canopy suggest that turbulent energy within the canopy is reduced at all length scales, including the larger ones that transfer momentum within the flow. On the falling tide, increases in flow velocity are not followed by corresponding increases in turbulent energy at any length scale, indicating that the vegetation also prevents new turbulent eddies from being formed (Figures 3.9 and 3.8).

The temporal variation in turbulent energy was compared to temporal variation in suspended sediment concentration at station 1 to determine whether sediment concentrations decrease in response to decreased turbulence levels near high tide or if sediment settles independently of the turbulent energy level of the flow (Figure 3.16). This comparison shows that the decrease in sediment concentration occurs 30-45 minutes earlier, relative to high tide, than the decrease in turbulence level, leading to the conclusion that even the highest turbulence levels within the canopy are inade-

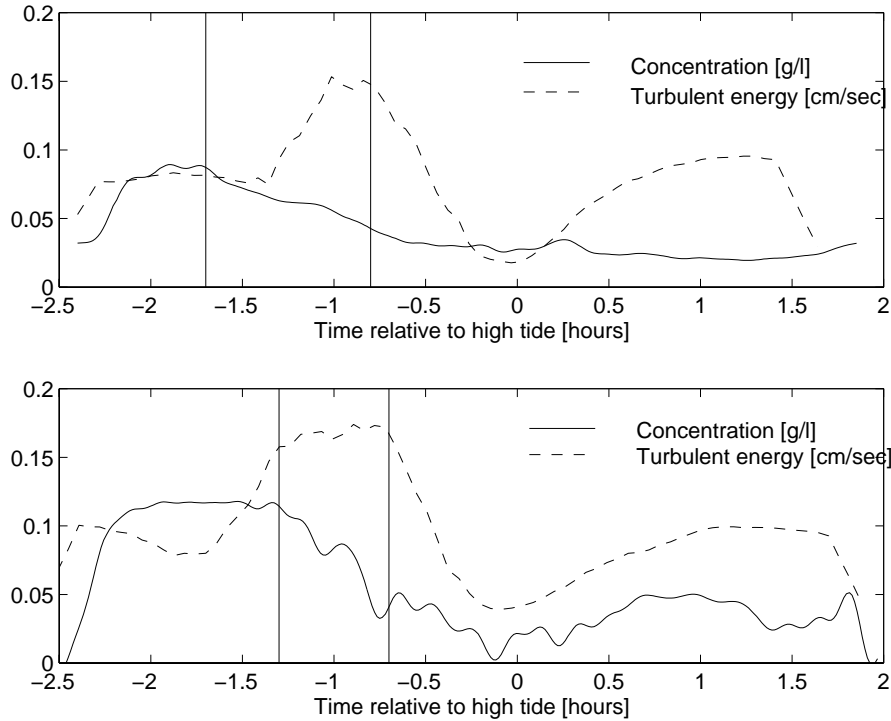


Figure 3.16: Comparison between temporal variation in concentration and turbulent energy for two different tides. The vertical lines indicate onset of decreasing sediment concentration and onset of decreasing turbulence levels. In the top panel, tidal amplitude was 110 cm, in the bottom panel tidal amplitude was 113 cm. Both sets of measurements were made at station 1.

quate to maintain the largest particles in suspension.

The effectiveness of turbulence in maintaining sediment in suspension can be evaluated from the Rouse number: $P_m = w_s/u_*$. Estimated values of u_* at station 1 (Figure 3.10) indicate that on the rising tide, the highest value of u_* is 0.03 cm/s. When the Rouse number, $P_m < 0.3$, the turbulence of the flow can maintain flocculated particles with diameters less than 50 μm in suspension, or individual particles with diameters less than 10 μm , in suspension (Table 3.6). In the interior, the flow can only maintain individual particles with diameters less than 6 μm in suspension. The lack of correlation between turbulent energy levels on the creek bank and decreased sediment concentration suggests that the particles moving in suspension are larger than 50 μm based on the Rouse number criterion. When the Rouse number, $P_m > 1$, particles cannot be maintained in suspension, and this criterion provides a lower size limit on particles settling out of suspension of 115 μm (Table 3.6). Complete particle size analysis are not available at this time. Our preliminary analysis, however,

Location	u_* [cm/s]	P_m	w_s [cm/s]	D_m (Stokes law, Eq. 2.7) μm	D_m (Flocs, Eq. 1.4) μm
Creek bank	0.03	0.3	0.009	10	50
Marsh interior	0.01	0.3	0.003	6	-
Creek bank	0.03	1	0.03	18	115

Table 3.6: Estimate of particle sizes maintained at the indicated Rouse number: $P_m = w_s/u_*$. When $P_m > 1$, sediment cannot be maintained in suspension, and when $P_m < 0.3$, sediment is maintained in suspension.

indicates that up to 75 % of the particles deposited on the marsh surface are from a flocculated source while 25 % are individual particles of 10-40 μm diameter (Figure 3.14). The lower size limit for flocculated particles is 100 μm (Sternberg et al. (in press)). This is larger than particle sizes suggested by the settling tube experiments, perhaps because flocs had been destroyed during sampling in the settling experiment (Figure 3.15).

Concentration levels simultaneously measured in the creek, at station 1 and at station 2, indicate that concentrations on the marsh surface near the creek bank are directly correlated with sediment concentrations in the creek, and that concentrations on the marsh surface decline in response to decreased concentration in the creek (Figure 3.17). This observation implies that processes in the tidal creek are controlling the amount of sediment settling on the marsh surface rather than processes on the marsh surface itself.

Sediment concentrations on the creek bank and levee are consistently higher on the rising tide than on the falling tide, indicating that deposition occurs on the rising tide. Sediment concentrations decrease significantly between station 1 and station 3, indicating deposition in vicinity of the tidal creek. The concentration measurements do not indicate resuspension of sediment from the marsh surface at any time including the falling tide when velocities and stresses on the marsh surface are greatest. The maximum boundary shear stress along the marsh transect was measured on the levee: $\tau_b = 0.001 \text{ dy/cm}^2$. In comparison, Widdows et al. (1998) determined critical erosion stresses ranging from 1.7 dy/cm^2 to 7 dy/cm^2 for estuarine mud in the U.K. The estimate of τ_b on the marsh surface is uncertain. The profile measurements shown in Figure 3.11 indicate that boundary shear stress may increase towards the bottom, in which case τ_b is under-estimated. The critical erosion stress for Phillips Creek marsh sediments could also be different from that of the U.K. estuarine mud, but it is difficult to measure. Comparing τ_b to the lowest value of critical erosion stress yields a 3 order of magnitude difference, and a critical erosion stress of this magnitude is not likely to be

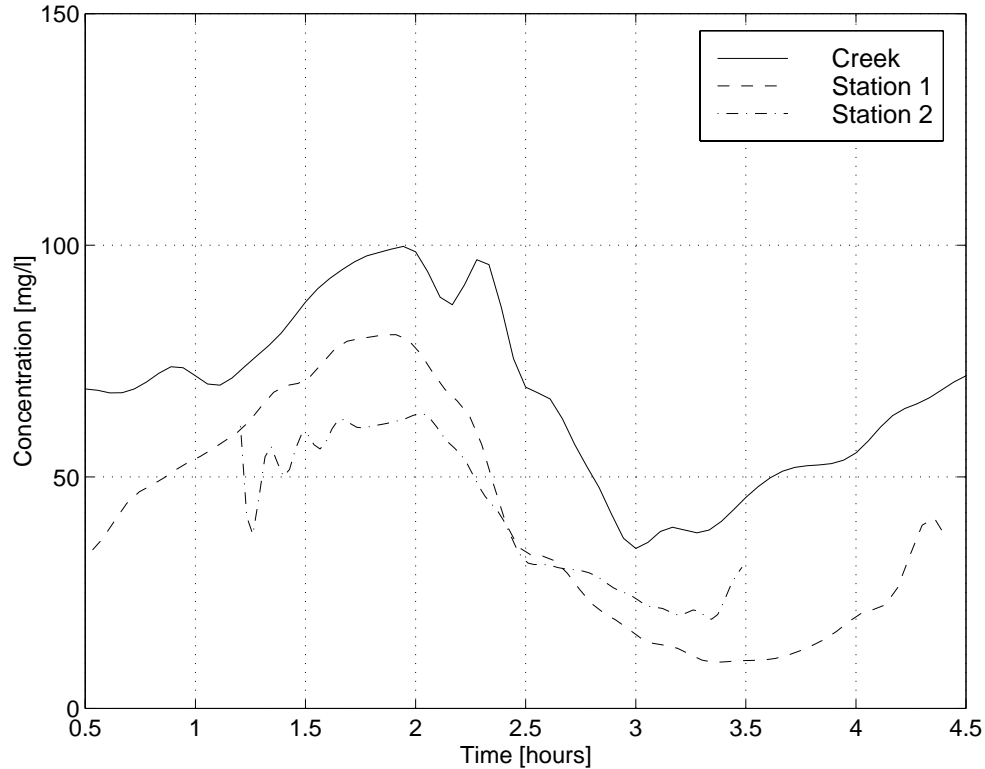


Figure 3.17: Simultaneous concentration measurements in the creek, at station 1 and at station 2.

exceeded during any of the flow conditions measured on Phillips Creek marsh.

Sediment concentrations on the creek bank (station 1) increase in response to increased tidal amplitude whereas concentrations in the marsh interior (station 5), do not (Figure 3.18). The difference between the response at these two stations, in conjunction with the general direction of flow on the marsh surface, implies that a portion of sediment brought onto the marsh at station 1, is not advected to station 5. This observation is in part due to the low mean flow velocities on the marsh surface. A particle moving horizontally at a mean flow velocity of 0.2 cm/s, travels 18 meters in 2.5 hours, and consequently will not reach station 5 (46 meters from the creek) during the time of rising tide; most of the sediment in suspension at station 1 will deposit in the vicinity of the creek bank. The large variability in sediment concentration at the creek bank as a function of tidal amplitude implies that sediment deposition also varies strongly with tidal amplitude. At station 5, the concentrations are likely to reflect background level of fine suspended particles with settling velocities that do not allow the particles to settle out of suspension over a tidal cycle.

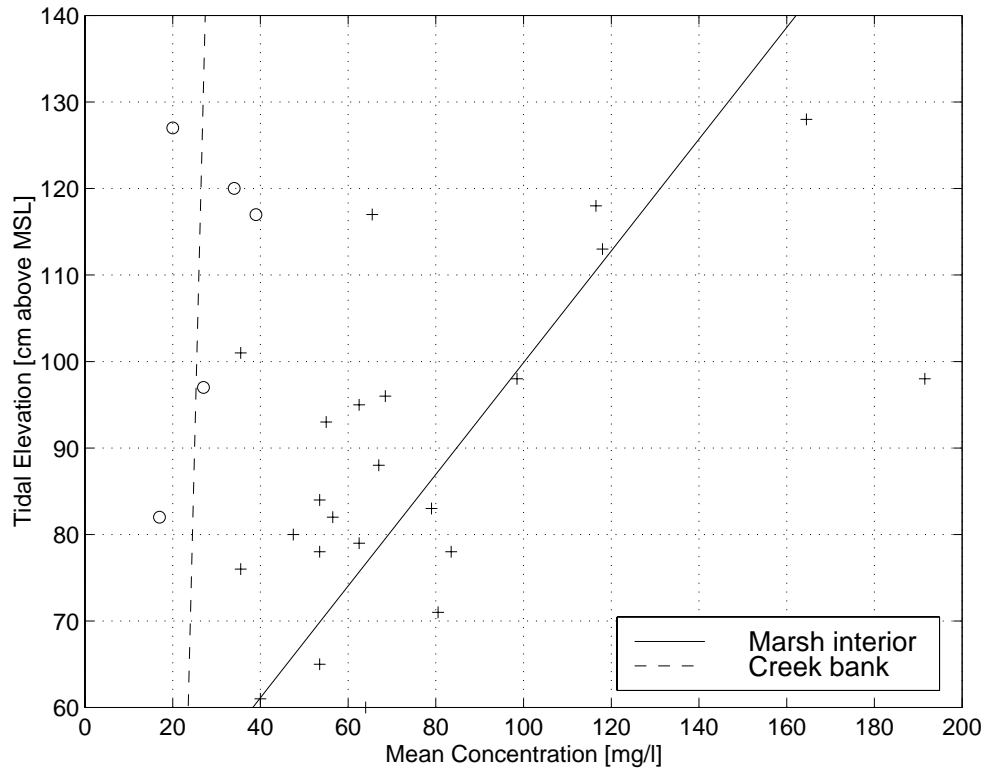


Figure 3.18: Concentration as a function of tidal amplitude on the creek bank and in the interior. On the creek bank, the regression line between measured concentrations and tidal elevation has an $r^2 = 0.48$. In the interior, there is no correlation between measured concentration and water level, $r^2 = 0.01$.

The processes acting on the marsh surface can be summarized as follows: the turbulent energy of the flow is insufficient to maintain the larger sediment in suspension on the marsh surface, regardless of tidal amplitude, and consequently sediment suspended in the tidal creek will settle out of suspension on the marsh surface (Figure 3.19). The low advection velocities promote deposition in the vicinity of the tidal creek and prevent large quantities of sediment from being advected to the marsh interior. The boundary shear stresses acting on the marsh surface during tidal flooding are of insufficient magnitude to suspend sediment already deposited on the marsh.

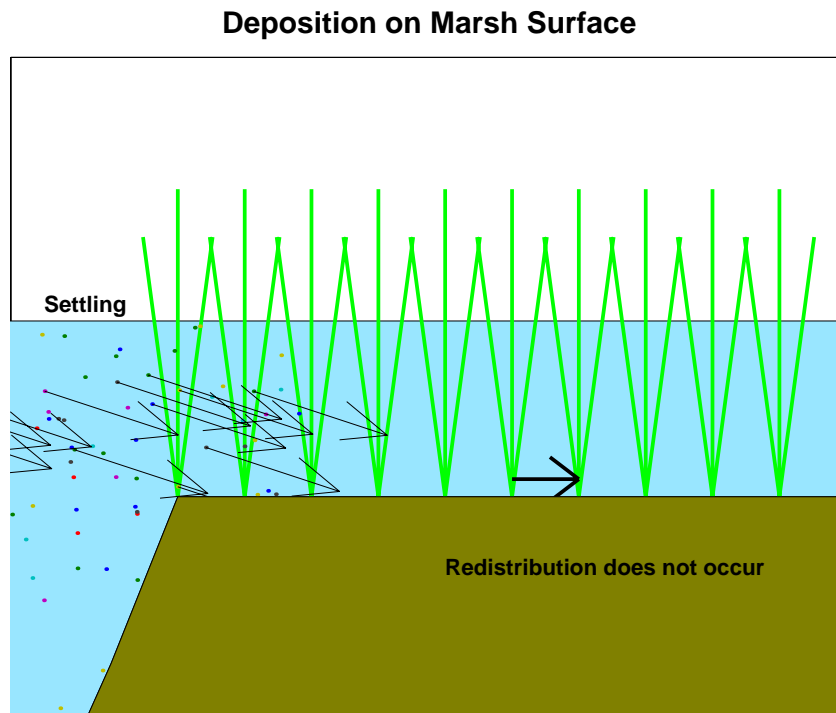


Figure 3.19: Sediment transport on the marsh surface. Sediment is advected on to the marsh surface from the tidal creek. The particles move horizontally with the flow and settle vertically. Redistribution of already deposited sediment does not occur.

Chapter 4

Sediment Deposition on a Marsh Surface

The measurements of flow, suspended sediment concentration and sediment accumulation on Phillips Creek marsh can be used to estimate sediment deposition rates using three different methods: direct measurements of deposition, deposition calculated from flux changes (derived from velocity and concentration measurements) between stations, and from calculations based on advection and settling of sediment introduced to the marsh surface.

4.1 Sediment deposition measured on sediment traps

Sediment mass accumulation on sediment traps installed on the marsh surface decreased with distance from Phillips Creek (Figure 4.1). The deposition measurements can be divided into those made during regular tidal flooding and those made during storms. Sediment deposition measured on individual tidal cycles (Figure 4.1, top panel) is representative of sediment deposited during regular tidal cycles. Sediment deposited in the two week period between June 17 and July 2, 1997 (12 tidal cycles) is also representative of sediment deposition during regular tidal flooding (Figure 4.1, middle panel). The deposition rates measured at station 2 are higher than deposition measured on individual tides; otherwise the rates are comparable.

Sediment deposition was measured during three different storms. A small northeaster on May 27 and 28, 1997 (2 tidal cycles), occurred in the sampling period between May 21 and June 3, 1997 (13 tidal cycles flooding the marsh). A large northeaster on June 2-June 8, 1997 (9 tidal cycles)

occurred in the sampling period between June 2 and June 17 (12 tidal cycles flooding the marsh) (Figure 4.1, middle panel). A very large northeaster occurred February 4 - February 9, 1998 (9 tidal cycles) (Figure 4.1, bottom panel). The storms consistently contribute more sediment to the marsh surface on the three creek bank stations (stations 1 - station 3). In particular, all three storm deposition measurements indicate larger quantities of sediment are deposited at station 3, 7 meters from the creek bank, suggesting that sediment is advected further into the interior on these storm tides.

Sediment deposition during the storm in February 1998 was measured on marker horizons. To convert the marker horizon measurement to mass deposited per unit area, the deposition thickness is divided by bulk density of the surface sediments (Kastler (1993)). Bulk density is not a well constrained parameter for newly deposited sediment and consequently it is difficult to directly compare this measurement with sediment deposited on sediment traps, but the rates seem comparable.

Deposition during the February, 1998 storm event, on the sediment traps during the two week periods of sampling, and during individual tidal cycles all indicate that more sediment deposits on the creek bank stations than in the interior, but that the quantity of sediment deposited on the creek bank is variable. These measurements suggest tidal deposition rates of $0.02 \text{ g/cm}^2/\text{tide}$ on the creek bank during storms and $0.004 \text{ g/cm}^2/\text{tide}$ during normal spring tides. At station 3, 7 meters from Phillips Creek, deposition rates are $0.008 \text{ g/cm}^2/\text{tide}$ during storms and $0.002 \text{ g/cm}^2/\text{tide}$ during normal spring tides. At station 4, 26 meters from the creek, no difference was observed between storm and spring tide deposition; the rate was $0.002 \text{ g/cm}^2/\text{tide}$.

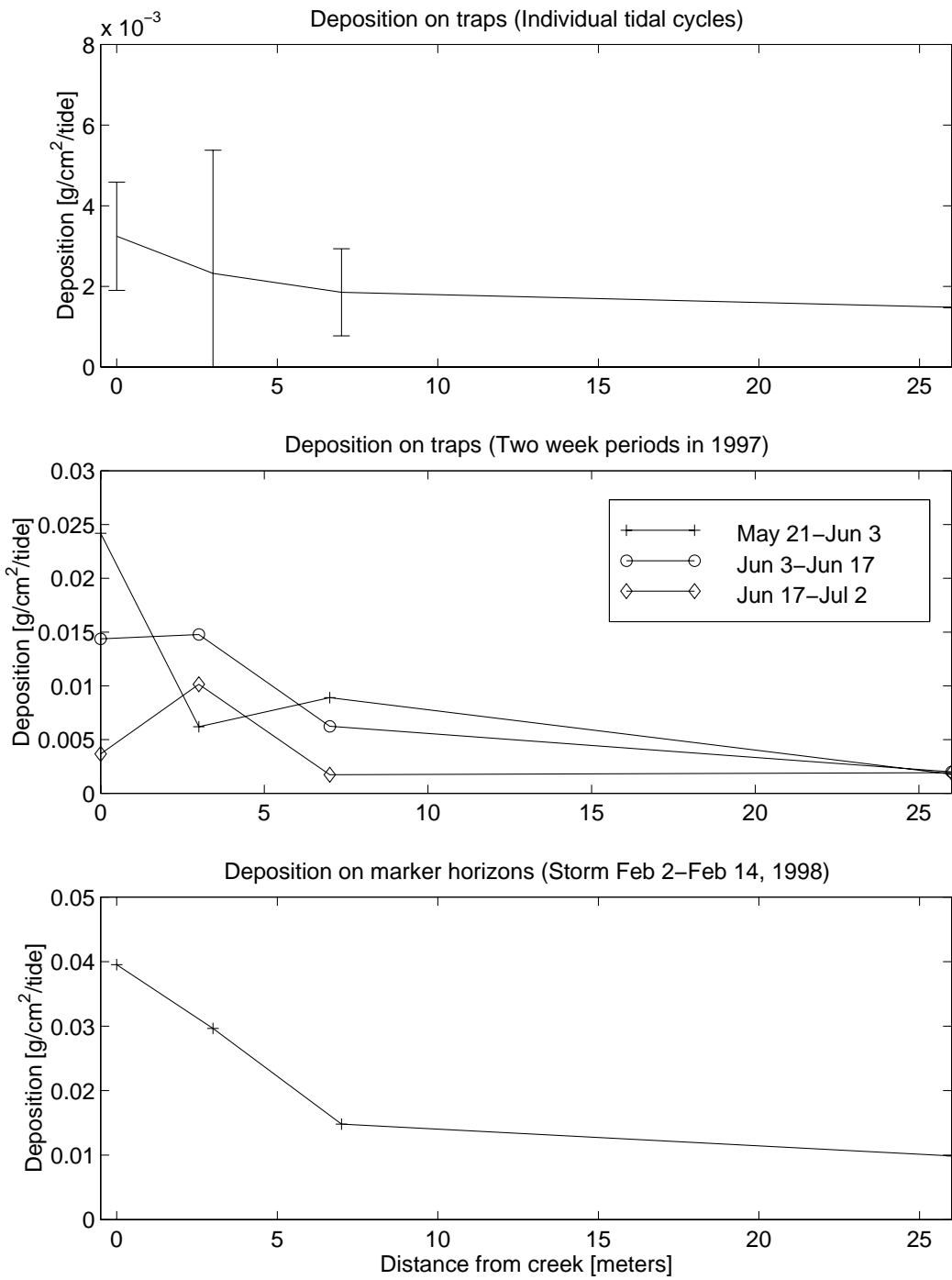


Figure 4.1: Sediment deposition on marsh surface. Sediment deposition as a function of distance from the tidal creek.

4.2 Sediment deposition calculated from measurements

Mean sediment deposition rates between station 1 and station 2 were calculated from changes in suspended sediment flux between the two creek bank stations on the rising part of the tide. Simultaneous concentration measurements at the two stations were combined with an estimate of velocity to calculate sediment flux at each of the two stations. The difference in flux between stations 1 and 2 is a measure of the amount of deposition (if flux is higher at station 1) that occurs. This calculation assumes flow direction is from station 1 to station 2.

Velocity measurements made at tidal amplitudes greater than 100 cm above MSL indicate that flow velocities were independent of tidal amplitude; the duration of marsh surface flooding increased, but flow velocities were not higher at higher tidal amplitudes. Therefore it was decided to estimate flow velocity on the marsh surface for tides for which only concentration measurements were made. The measurements also indicated that velocities were slightly higher at station 2 than at station 1. In addition, station 1 is flooded for a longer time because it is located at a lower elevation (50 cm above MSL) than station 2 (70 cm above MSL). Reasonable agreement between estimated and measured mean velocity at station 1 was found using the relationship:

$$v_{st1}(t) = -2v_{1,max} \sqrt{\sin \frac{\pi}{T}t} \quad (4.1)$$

where $v_{1,max}$ is the maximum velocity on the rising tide at station 1, t is time before high tide and T is duration of flooding at station 1. At station 2, a similar relationship was found:

$$v_{st2}(t) = -2v_{2,max} \sqrt{\sin \frac{\pi}{T}t} \quad (4.2)$$

where $v_{2,max}$ is the maximum velocity at station 2 and T is the duration of flooding at station 1. Velocity was scaled by duration of flooding at station 1 because at the onset of flooding, velocity at station 2 increased more rapidly than the shape of the sine curve allows. Further, depth at each station was estimated as a sine function:

$$d(t) = h \sin \frac{2\pi}{T}t \quad - \quad \text{station elevation} \quad (4.3)$$

where h is tidal amplitude, T is 12.5 hours, and t is time relative to high tide.

In contrast to the velocity measurements, the concentration measurements exhibited considerable variation on different tidal cycles. The same concentration was not always observed on different tides with similar tidal amplitude and concentration increased with increased tidal amplitudes. It was, however, found that on all tides where sediment concentrations were measured simultaneously at station 1 and station 2, that the concentration was always lower at station 2 (Tables 3.4 and 3.5), suggesting that sediment is deposited between these two stations. The relationships for depth and mean velocity are combined with measured mean concentrations, and integrated over the duration of the rising part of a tidal cycle to calculate flux at each of the two locations:

$$Q = \int_{dur} d(t)v(t)C(t)dt \quad (4.4)$$

Examples of time series used in Equation 4.4 are shown in Figure 4.2.

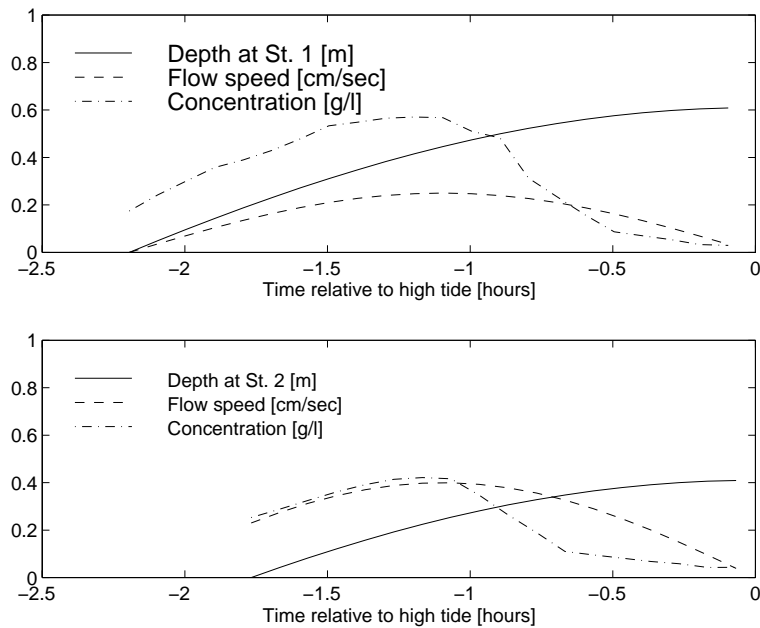


Figure 4.2: Example of time series used in flux calculation.

Flux was calculated at station 1 and station 2 for the 3, two-week time series of concentration measured at stations 1 and 2. Flux differences were used to determine mean deposition between the

two stations based on the erosion equation:

$$\frac{\partial \eta}{\partial t} = \frac{\partial Q}{\partial x} \quad (4.5)$$

where η is mass accumulation on the bed. Calculated deposition rates are listed in Table 4.1. The results are consistently lower than measured deposition rates, suggesting that the sediment traps consistently over-estimate deposition or that the flux measurements systematically under-estimate deposition. There is evidence of sediment traps decreasing trapping efficiency with time. For example, Kastler (1993) shows that traps of the type used in this study could on each of 5 consecutive days accumulate as much sediment as was sampled on a trap deployed for one month. In addition, Hutchkinson et al. (1995) consistently observed more sediment deposited on traps exchanged between each tidal cycle than on traps deployed for one week.

There are a number of uncertainties associated with the method chosen to calculate flux. Estimating water level on the marsh surface with a sine function produces a shorter inundation time than the actual tide. If the velocity at station 2 is too high or velocity at station 1 is too low the difference in flux between the two stations will be under-estimated. In addition it is assumed that the functions indicated in Equations 4.1 and 4.2 describe variation in mean flow velocity over the tidal cycle. The influence of the morphology of the plants on the flow structure may vary with time as water level increases. At water depth below 10 cm, the plants occupy a smaller portion of the cross-sectional area than at higher water levels, which may increase the flow speeds at these depths. Finally, it is assumed that sediment particles are well mixed in the water column; that there is no concentration difference between top and bottom of the flow. Turbulence levels decrease most at the transition between tidal creek and station 1, and it is likely that if a vertical concentration profile is established in response to decreased turbulence levels, it is stronger at station 2 than at station 1, in which case the flux at station 2 is over estimated. This effect may be related to tidal amplitude. In lower tides that carry large quantities of sediment, the vegetation protrudes through the surface of the flow producing a more efficient damping of turbulence than on flows above the vegetation canopy. The vegetation canopy is only fully inundated on the very highest tides (amplitude \geq 140 cm).

Although the magnitude of the calculated deposition is in question, it seems reasonable to compare the values calculated for different tides in a relative sense. Calculated sediment flux and depo-

sition have been correlated with tidal amplitude (Figure 4.3). The strongest correlation is observed between sediment flux at station 1 and tidal amplitude; deposition was not as strongly correlated with tidal amplitude. On the very highest tides, fluxes at station 1 and station 2 are both high, but there is little difference in flux between the two locations. On these very high tides sediment may be advected further away from the tidal creek than on other tides (Figure 4.3, bottom panel). The measured deposition at station 3, 7 meters from the creek, suggests that the storms proportionally contribute more sediment to this location. The correlation between tidal amplitude and sediment flux at station 1 (a measure of how much sediment is contributed to the marsh surface on a particular tide) is explored further in the next chapter.

Period	Calculated deposition <i>g/cm²/2weeks</i>	Measured deposition <i>g/cm²/2weeks</i>
May 21 - June 2	0.095	0.18
June 3 - June 17	0.089	0.19
June 17 - July 2	0.021	0.083

Table 4.1: Comparison of measured and calculated deposition for three sampling periods in May and June, 1997. Measured deposition is the average value of measured sediment deposition at station 1 and station 2.

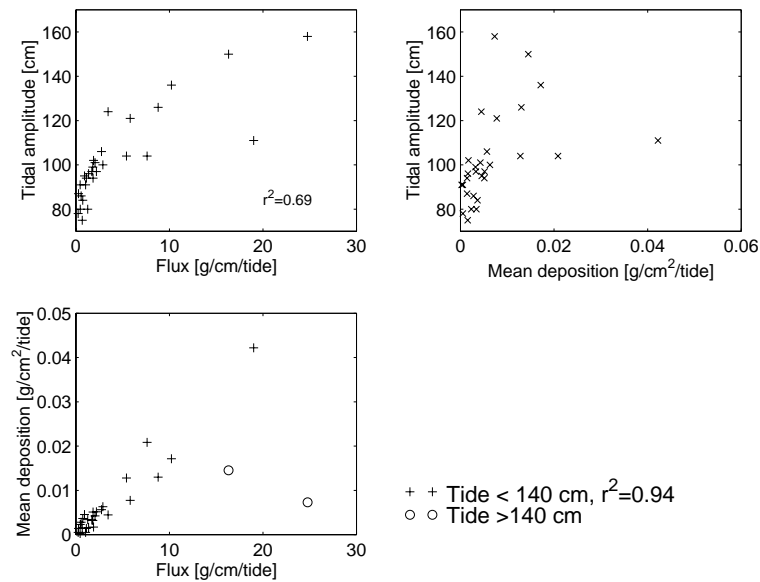


Figure 4.3: Correlations between tidal amplitude, mean deposition between station 1 and 2 and sediment flux calculated at station 1.

Station	Sediment mass [grams]	Stem mass [grams]	Number of stems	Sediment mass/ stem mass	Plant mass per stem [grams]	Sediment mass per stem [grams]
1	18.8	211.7	35	0.09	6.04	0.54
1	19.9	195.7	31	0.10	6.3	0.64
2	17.2	104.4	35	0.16	2.98	0.49
2	15.1	112.2	37	0.13	3.03	0.41
2	25.2	166.3	51	0.15	3.26	0.49
3	9.3	32.0	16	0.29	2.0	0.58
3	28.3	78.5	39	0.36	2.01	0.72
3	17.6	67.9	34	0.26	2.00	0.52
3	27.9	47.0	34	0.59	1.38	0.82
4	18.0	68.9	29	0.26	2.38	0.62
4	32.0	133.5	53	0.24	2.52	0.60
4	24.7	65.2	34	0.38	1.92	0.73
4	27.1	110.3	34	0.25	3.24	0.80
5	17.6	109.0	26	0.16	4.19	0.68
5	20.8	138.3	28	0.15	4.94	0.74
5	11.3	53.4	16	0.21	3.33	0.71

Table 4.2: Sediment accumulation on *Spartina Alterniflora*. Each line characterizes a 0.25 m² plot. Stem mass refers to dry mass of plants harvested from a plot.

4.3 Sediment accumulation on stems

To compare the amount of sediment accumulated on plants in a 0.25 m² plot at different sites, two parameters were determined: the ratio of total sediment mass to total plant mass, and the mean sediment mass accumulated per stem. Although larger plants have more leaves on which sediment can be trapped, sediment is primarily attached to the base of the plant and the bottom leaves; the top of the plants (especially the tall ones) are clean. It was therefore decided that the most consistent measure of sediment accumulation was mean sediment per stem.

The measurements were lumped into measurements made in the marsh interior (stations 3, 4 and 5) and measurements made on the creek bank (stations 1 and 2). In the interior, the average sediment accumulation per stem, $\mu = 0.67$ g/stem and on the bank, the average accumulation per stem, $\mu = 0.52$ g/stem.

To determine whether the measurements made at the creek bank were significantly different from the measurements made in the interior (Table 4.3) a t-test was used. The small sample size and an assumption that sediment accumulation on plant stems has a normal distribution, warranted using a two sample t-test (Devore (1991)). The null hypothesis tested, $\mu_{int} = \mu_{cb}$, was rejected at

Location:	Creek bank	Marsh interior
Mean:	0.52 g/stem	0.67 g/stem
Std:	0.084 g/stem	0.094 g/stem
number of samples:	5	11
S_p :	0.091	
$\Delta\mu$	0 g/stem	
t	3.056	
$t_{0.05,14}$	1.761	
Accept H_0 :	no	

Table 4.3: Comparison of mean sediment accumulation on stems. Stem accumulations have been divided into sediment accumulated on plants growing on the creek bank (station 1 and station 2), and sediment accumulated on plants growing in the interior (station 3, station 4 and station 5).

the confidence level of 0.05, i.e. the mean sediment accumulation on plant stems is significantly different between the creek bank and the interior. More sediment accumulates on stems in the interior than stems on the creek bank (Table 4.3).

The plants were harvested three months after being cleaned. This was a longer accumulation period than originally planned and to make a conservative estimate of the trapping efficiency of the vegetation, it was assumed that sediment on the stems represented accumulation over a 1.5 month period. This time period is likely to be representative because the Phillips Creek area received 56 millimeters of precipitation on August 1, 1996 (3 weeks after hurricane Bertha) which would have been enough precipitation to wash sediment off the stems. The plants were harvested on September 25, 1996. It is further assumed that the vegetation density of a particular location is represented by the highest number of stems counted (53 stems/plot in the interior and 51 stems/plot on the creek bank). In a 45 day period the marsh interior is flooded 85 times whereas the the creek bank is only flooded 35 times. The accumulation per tide in the interior is: $0.67 \cdot 53 / (2500 \cdot 85) = 0.00017 \text{ g/cm}^2/\text{tide}$, corresponding to 9 % of the accumulation measured by plates ($0.002 \text{ g/cm}^2/\text{tide}$) on the marsh surface in the same period. On the creek bank the accumulation is: $0.52 \cdot 51 / (2500 \cdot 35) = 0.00022 \text{ g/cm}^2/\text{tide}$, corresponding to 5 % of the sediment accumulated on the marsh surface ($0.004 \text{ g/cm}^2/\text{tide}$). This calculation indicates that the plants play a relatively larger role in determining the rate of deposition in the marsh interior than on the creek bank, and it is a conservative estimate of the importance of plant trapping. In comparison to these values, Stumpf (1983) determined that sediment retention by *Spartina alterniflora* could account for up to 50 % of the material lost from suspension in a Delaware marsh whereas French and Spencer (1993) found that plant retention could only account for 2-5 % of the total deposition

in the Hut Marsh. Leonard et al. (1995) found that retention by stems of *Juncus roemerianus* could account for 9% of the material deposited on the marsh surface of a west-central Florida marsh.

4.4 A model for sediment deposition

The primary processes thought to control sediment deposition on the marsh surface have been formulated mathematically to investigate whether these processes can account for the depositional patterns observed on the marsh surface.

The measurements of flow velocities and sediment turbidity on the marsh surface indicate that sediment deposition on the marsh surface is controlled by peak suspended sediment concentration during a tidal cycle, water depth, the settling rate of particles, and the flow velocity. Sediment concentration and water depth are a measure of the amount of sediment brought to the marsh surface, settling rates determine how quickly the particles settle out of suspension and the flow velocity determines how far a sediment particle has moved horizontally before it has settled to the marsh surface. It is assumed that all sediment is derived from an exterior source; no sediment is resuspended from the marsh surface. The concentration field along a transect on the marsh surface is described by:

$$\frac{\partial C}{\partial t} = \frac{\partial}{\partial z}(w_s C) - \frac{\partial}{\partial x}(u C) \quad (4.6)$$

where x is horizontal axis along the transect, z is the vertical axis, and u is mean flow velocity along the transect. It is assumed that the flow is non-diffusive; concentration change occurs as a consequence of advection and settling of particles.

The model chosen to describe sediment transport is a particle tracking model. Particles are introduced at the boundary of the marsh, in proportion to the measured sediment concentration and flow depth. Each particle is assigned a settling velocity, a random position above the boundary, and a horizontal velocity. At each time step, a particle moves horizontally in proportion to the flow velocity, and vertically in proportion to its settling velocity until it reaches the marsh surface. At each time step the horizontal and vertical particle positions, x_p and z_p , are described by (Anderson and Woessner (1992)):

$$\begin{aligned} x_p &= x_0 + u \Delta t \\ z_p &= z_0 + w_s \Delta t \end{aligned} \quad (4.7)$$

Sediment concentration, water depth and flow velocity are time-dependent variables. Flow velocity varies both as a function of time and as a function of location. In these calculations, for simplicity, flow velocity was assumed steady and uniform, 0.2 cm/s and flow depth increased with time. Calculations were only made for the rising part of the tide as observations indicated that deposition occurred during this time. Calculations were made for two different depositional events, a regular spring tide of amplitude 100 cm above MSL and a storm surge of amplitude 160 cm above MSL. For each event, calculations were made using two different grain size distributions; one that contained only particles of size 100 μm , and one that had 70 % of 50 μm particles and 10 % of 35, 20 and 10 μm particles.

For each calculation, the calculated temporal concentration variation at station 2 is compared to the measured one (Figures 4.4 and 4.5, panels 1 and 2), and deposition as a function of distance from the tidal creek is determined ((Figures 4.4 and 4.5, bottom panel).

The calculation that assumed only particles of 100 μm were moving in suspension does not explain deposition well for either of the two tidal events; particles settle within the first two meters of the marsh surface and calculated concentration at station 2 is much lower than the measured concentration (Figure 4.4). Deposition within such a narrow band leads to over-prediction of deposited amounts. Figure 4.1 shows measured deposition.

The distribution of particles used in the second calculation comprises particles that move further to the marsh interior than the 100 μm sediment with a small percentage (20 %) of smaller particles that do not settle out of suspension over a tidal cycle, consistent with presence of background level of suspended sediment of 20-30 mg/l. If the particle sizes are too small, they will not settle out of suspension in the duration of the rising tide. The particle size distribution used in this calculation shows better agreement for both events both with respect to deposition quantities and in comparison of measured and calculated concentration levels at station 2 (Figure 4.5). The deposition profile in this example, however, still favors more deposition in the vicinity of the bank than is observed (Figure 4.1) and than is suggested by the flux calculations (Figure 4.3). It was shown in the previous section, however, that particles smaller than 50 μm could be maintained in suspension by the turbulence of the flow, and it is likely that these particles do not settle readily to the bottom during the part of the rising tide when turbulence levels are high. Changing turbulence levels would in effect create a time varying settling rate. Particles in the 50 μm size class will settle quickly in response to decreased turbulence levels, and not be maintained in suspension on the falling tide. Settling rate

dependence on turbulence levels would tend to broaden the deposition zone because particles would be advected further away from the source before settling. Diffusional effects not included in this calculation would also tend to broaden the depositional zone.

The calculation for the high-amplitude tide indicates that the calculated concentration peak occurs closer to high tide than the measured peak does (Figure 4.5, 2nd. panel). Comparison of measured concentration at station 1 and station 2, indicates very similar timing and shape of the concentration peak, although concentrations are lower at station 2. The difference in timing between peak measured and calculated concentration might also be due to not including time-dependent velocity variations. The effect of reduced flow velocity at slack tide is to reduce the amount of material advected to the marsh interior.

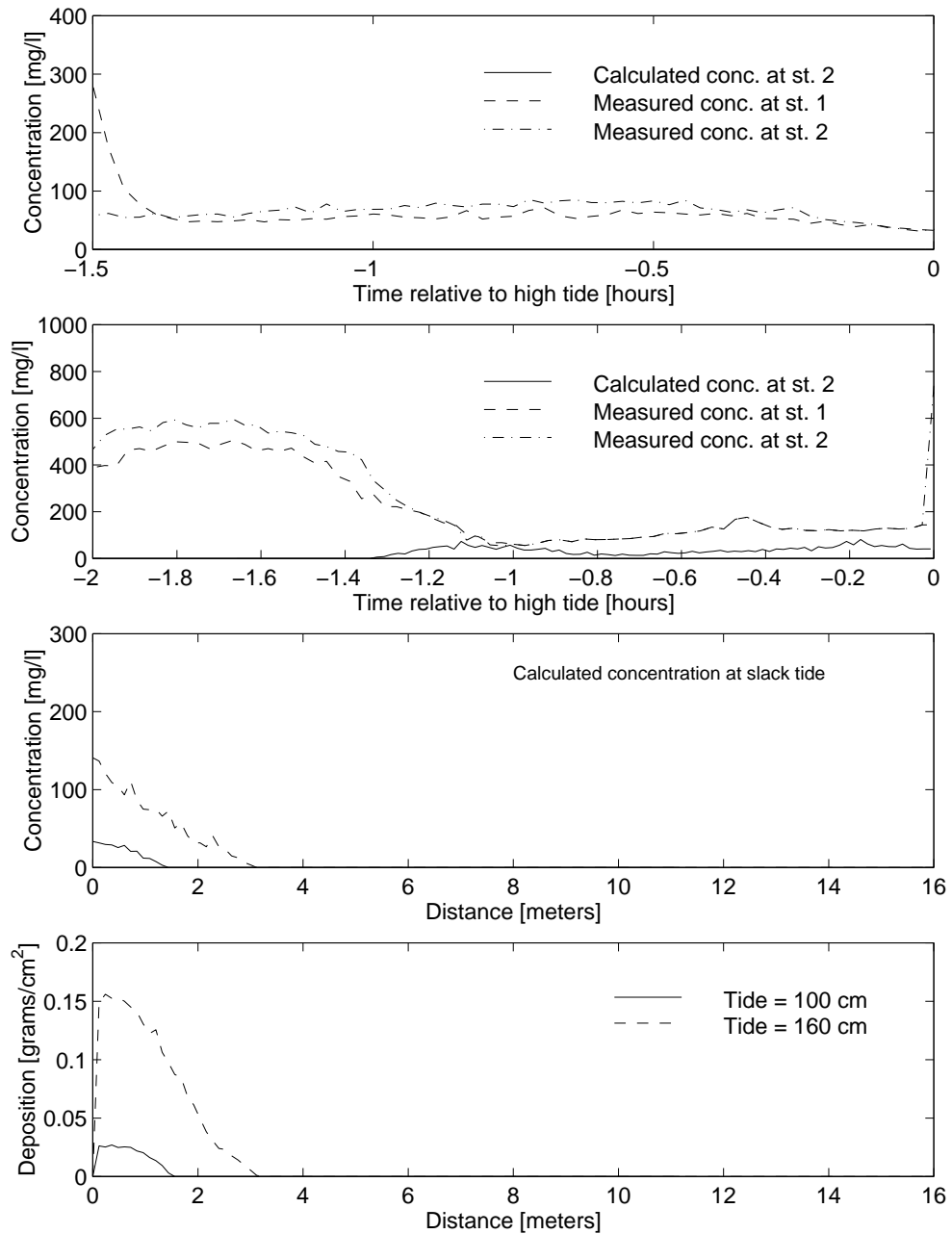


Figure 4.4: Calculated deposition on marsh surface during two different events, assuming all particles have $100 \mu\text{m}$ diameter. The top panel is an event measured during a tide with 100 cm amplitude. The second panel is an event measured during a tide with 160 cm amplitude. The two top panels show comparison between measured and calculated profiles, the third panel shows concentration at slack tide as a function of distance from tidal creek and the bottom panel shows deposition as a function of distance from creek.

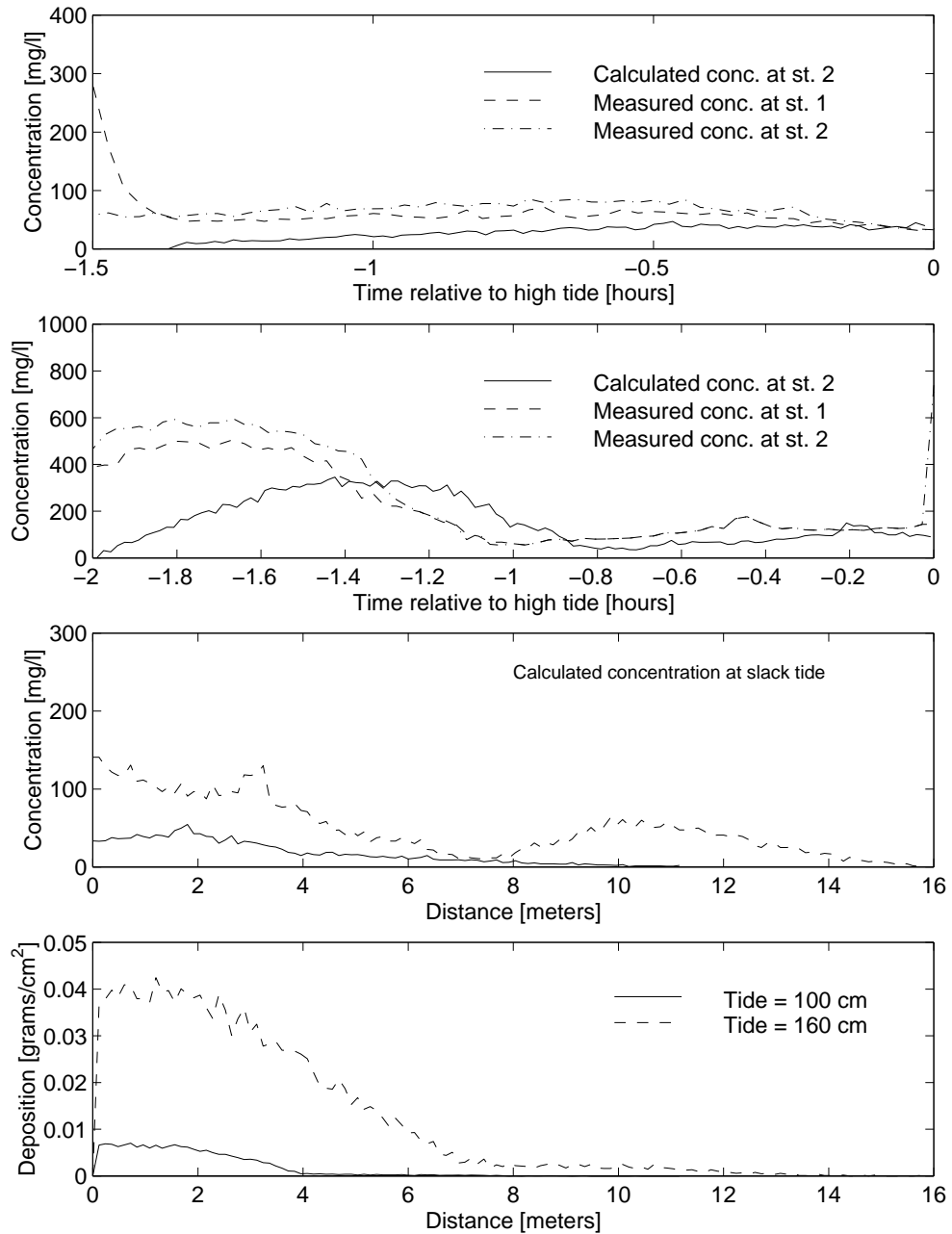


Figure 4.5: Calculated deposition on marsh surface during two different events assuming that 70 % of the particles are $50 \mu m$ in diameter and 10 % of 35 , 20 and $10 \mu m$ particles. The top panel is an event measured during a tide with 100 cm amplitude. The second panel is an event measured during a tide with 160 cm amplitude. The two top panels show comparison between measured and calculated profiles, the third panel shows concentration at slack tide as a function of distance from tidal creek and the bottom panel shows deposition as a function of distance from creek.

Chapter 5

Sediment Transport Events

5.1 Relationship between water level and meteorological forcing

In the open marine environment, sediment transport rates during storms, when waves and currents interact to enhance the bottom stress, is frequently an order of magnitude greater than sediment transport during non-wave conditions (Nittrouer and Wright (1994)). In contrast, Phillips Creek marsh is in a very sheltered location, and the primary effect of storms is to increase water level, and thus duration of marsh surface flooding, and to increase current velocities in the tidal creek.

In the previous chapter it was demonstrated that a relationship exists between maximum height of a particular tide and the amount of sediment transported onto the marsh surface. In this chapter it is shown that the transport primarily occurs during high water levels associated with storm surges produced during northeasterly winds. Due to this relationship, it is of interest to determine the climatic conditions that produce high water levels in Hog Island Bay, and thus on Phillips Creek marsh. This approach was motivated by interest in determining whether high water levels were produced by several different meteorological conditions or if only northeasters were able to generate storm surges in Hog Island Bay. The data that describe the meteorological conditions cover (at the time of this analysis) 7.5 years. Water level has been measured at Wachapreague for 15 years, and these measurements have been used to determine the distribution of tidal amplitudes. Due to the length of the record, the frequency of very high storm surges has been resolved.

5.2 Sediment Transport

Sediment concentrations were measured on 90 tidal cycles between May 12 and July 1, 1997. Of these tidal cycles, 37 had water levels high enough to flood the marsh surface. This time period included both spring tides and a very large storm that produced water levels up to 150 cm above mean sea level (Figure 5.1). Each of the 37 tidal cycles have been characterized by sediment concentration, maximum water level, mean wind speed and direction during the 12.5 hour period between two lows. Sediment concentration was characterized by the highest concentration measured on the rising tide in the tidal creek. The tidal creek measurements were chosen because the vertical elevation of this station was the lowest, and consequently measurements were available from the greatest range of conditions. The events were divided into two categories, events during onshore winds (from 15 - 205 degrees) and offshore winds. Winds from NNE are approximately parallel to the coast line, and these were considered in the onshore category because the response of water level to these winds is what one would expect from an onshore wind (water level increases).

To relate suspended sediment concentration to deposition on the marsh surface, the measured concentrations were converted to flux to the marsh surface using the method described in chapter 4. Sediment flux was correlated with each of the three parameters: maximum water level, mean wind speed, and mean direction during each of the 37 events (Figure 5.2). It is clear that the largest sediment flux to the marsh occurs during winds from the northeast with mean wind speeds greater than 10 m/s (Figure 5.2). These winds are also the winds that produce the largest storm surges along the Atlantic coast (Davis and Dolan (1993)). During offshore winds, there is also correlation between sediment flux to the marsh surface and increased water level, but the range is much smaller than during onshore winds. The sediment flux to the marsh surface during low amplitude tidal cycles (≤ 1 meter) is similar, regardless of wind speed or wind direction (Figure 5.2). All instances of tidal amplitudes ≥ 1.1 meters in this record are associated with northeast winds.

The strong relationship between water level and sediment concentration observed in May and June, 1997 led to a more extensive analysis of the climatic conditions that produce water levels above the astronomical tides to determine the relationship between high water level and northeasterly storms.

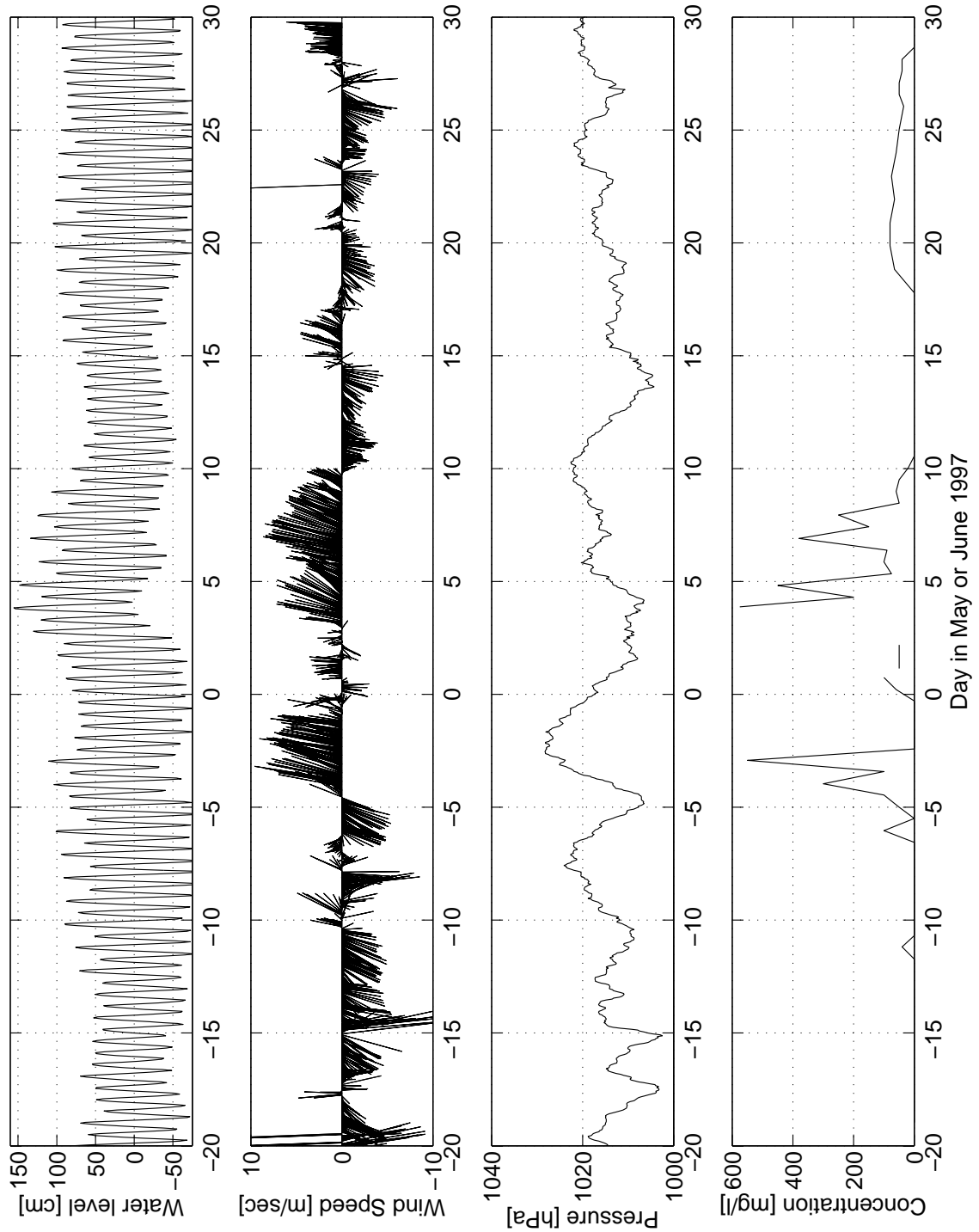


Figure 5.1: Water level at Wachapreague, sediment concentrations in Phillips Creek and wind and atmospheric pressure Measured at NDBC buoy 44014 during May and June, 1997. Days in May are negative.

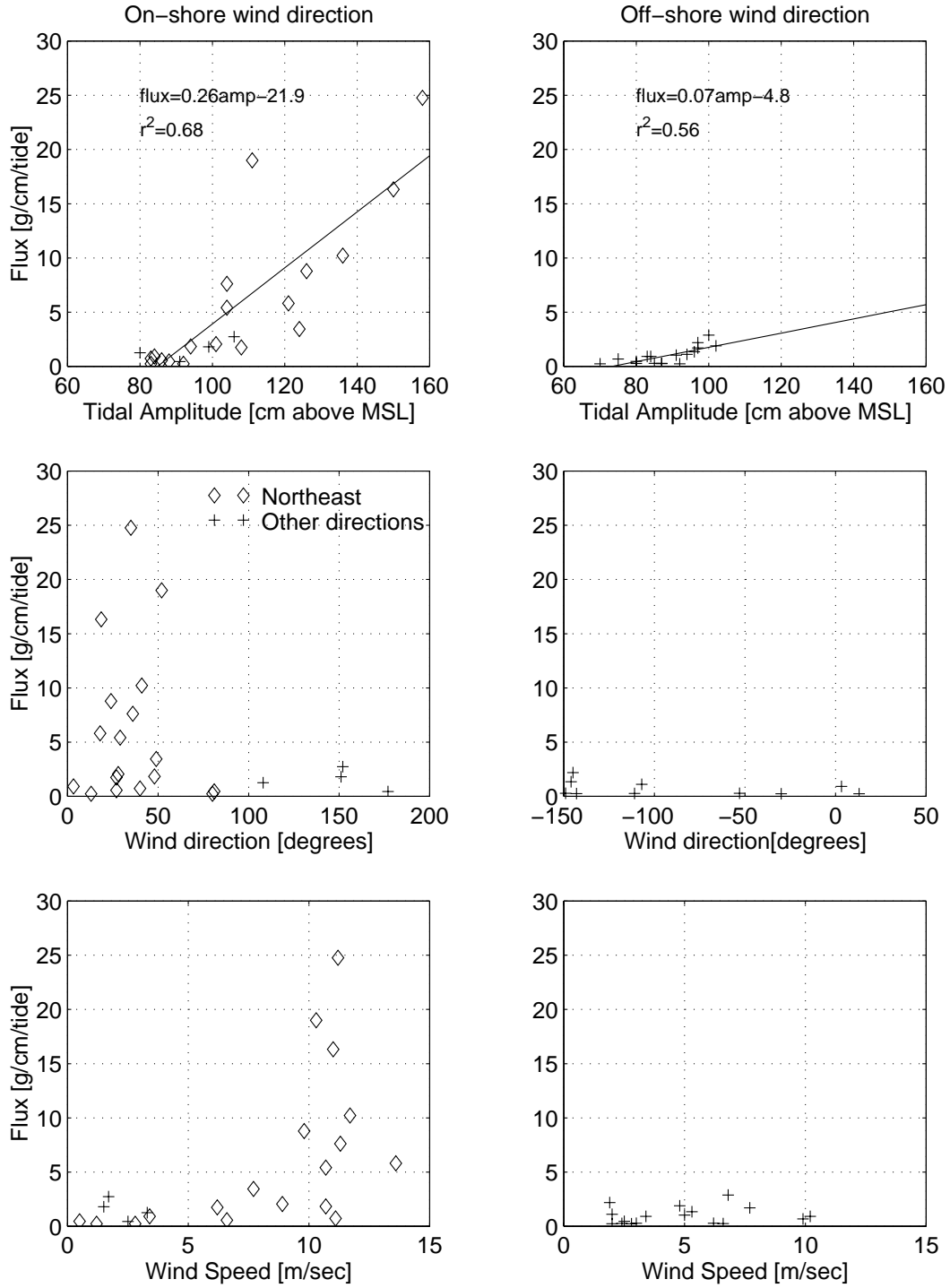


Figure 5.2: Correlation between sediment flux, tidal amplitude, wind direction and wind speed. The events have been divided into onshore and offshore wind events.

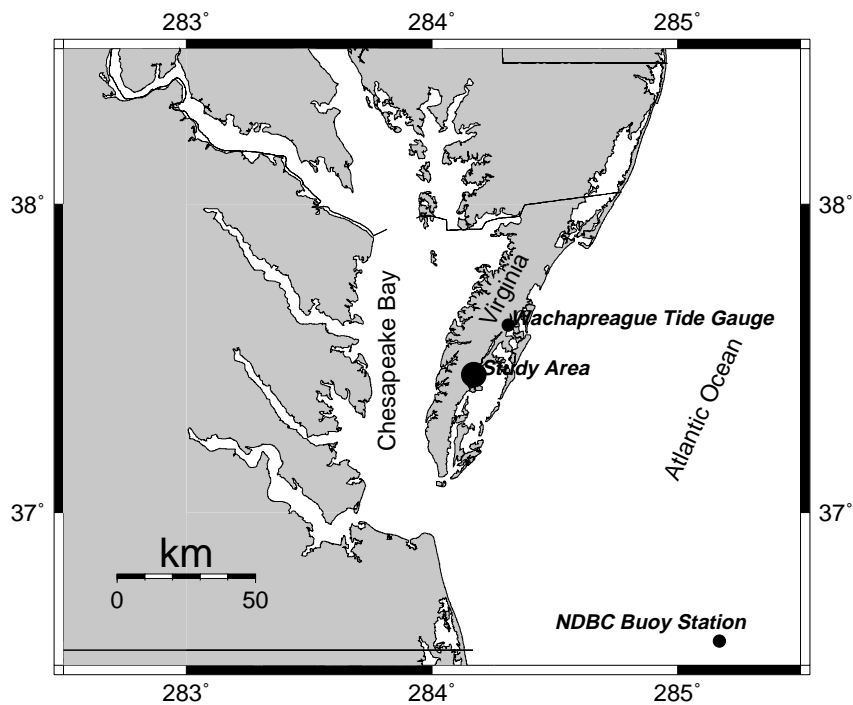


Figure 5.3: Location of Wachapreague tide gauge, NDBC buoy 44014 and Study site. The orientation of the Delmarva peninsula is NNE-SSW (it has an angle of 60 degrees with horizontal).

5.3 Correlation between water level and meteorological forcing

Water level in Hog Island Bay is affected by meteorological conditions as well as astronomical tides. The relationship between water level, wind speed, wind direction, storm duration and barometric pressure was investigated statistically to determine which of these parameters were necessary to predict water level. Water level measurements made at the Wachapreague tide gauge were used for this analysis because the Wachapreague record is longer and more complete than the Redbank record. Hourly values of wind and atmospheric pressure from NDBC buoy 44014 were used to describe the meteorological conditions in the area (Figure 5.3). The analysis covers the period between January 1990 and July 1997 when both stations were in operation.

Water level fluctuations in Hog Island Bay are primarily determined by astronomical tidal forcing although the astronomical predictions cannot account for the highest tides (Figure 5.4). For this

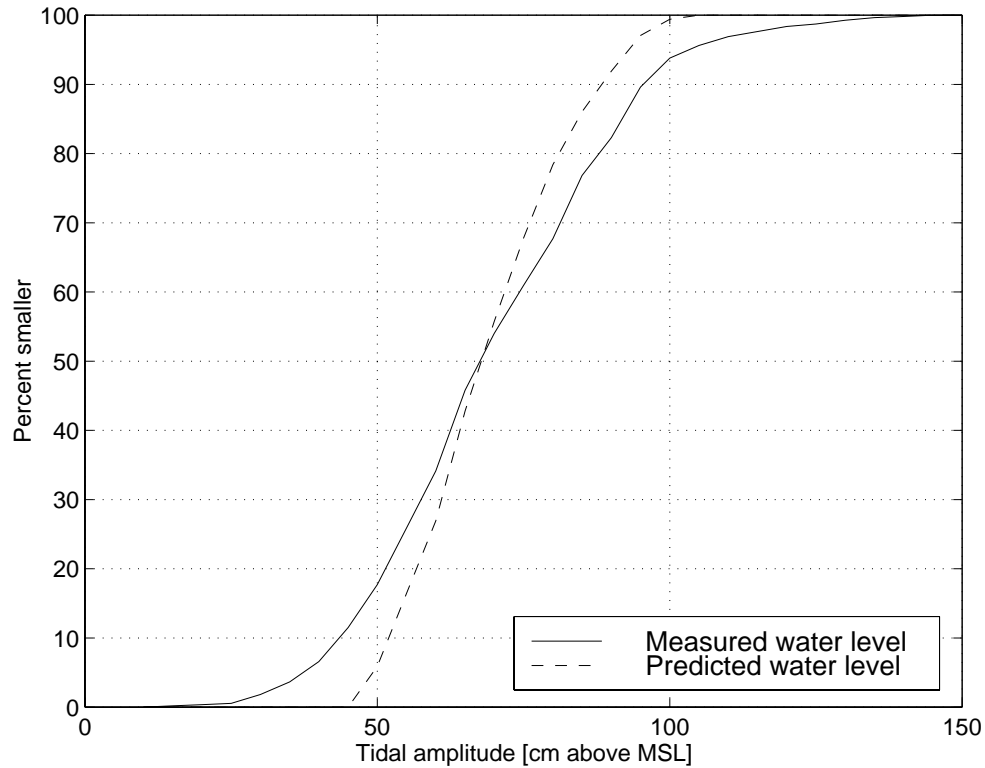


Figure 5.4: Distribution of measured and predicted tidal amplitudes. The distribution of measured amplitudes is broader than the distribution of predicted tides.

analysis, it was assumed that meteorological conditions were responsible for water level fluctuations in excess of the astronomical tides. Tidal variation was removed from the water level record by applying a low pass filter with a cut-off frequency of $1/30 \text{ hrs}^{-1}$ to the record. The lowest detectable tidal frequencies in a two year tidal record were related to the diurnal variation with a frequency of $1/25 \text{ hrs}^{-1}$, and variations at lower frequencies were assumed to be related to non-tidal effects and spring neap tidal cycles.

The inter-dependence between the wind vector, X , and water level response, Y , was determined as the cross-correlation $\rho_{xy}(k)$. The data sets X and Y are time series of equally spaced values with no missing values. The cross-correlation is a measure of the degree of relationship between two parameters at time lag k (Equation 5.1) (Diggle (1990)):

$$\rho_{xy}(k) = \frac{COV X_t, Y_{t-k}}{\sqrt{VAR(X)VAR(Y)}} \quad (5.1)$$

Here, the cross-correlation has been used to identify the lag between wind and water level response, and to identify the orientation of the wind vector coordinate system that produces the strongest correlation between wind speed and water level.

To obtain the strongest cross-correlation between water level and wind direction, the coordinate system was oriented with one axis parallel to the dominant wind direction, i.e. the wind direction that produces the strongest correlation with water level response. The strongest correlation between the wind vector and water level was found when the coordinate system was rotated 40 degrees, corresponding to an axis approximately parallel to the northeast wind direction and perpendicular to the coast line. This particular orientation was determined because the data segment used to calculate the cross-correlation was from a two month period in the winter. During the summer period, northeasterly winds occur less frequently, and water level response is more closely (negatively) correlated with southwesterly winds.

By rotating the coordinate system, the wind vector is divided into a subordinate and a dominant component (Figure 5.5). The subordinate axis is the axis approximately parallel with the coast line and the dominant axis is approximately perpendicular to the coast line. The time lag between water level and wind speed is approximately 15 hours (Figure 5.5); water level response is approximately 15 hours later than the wind forcing.

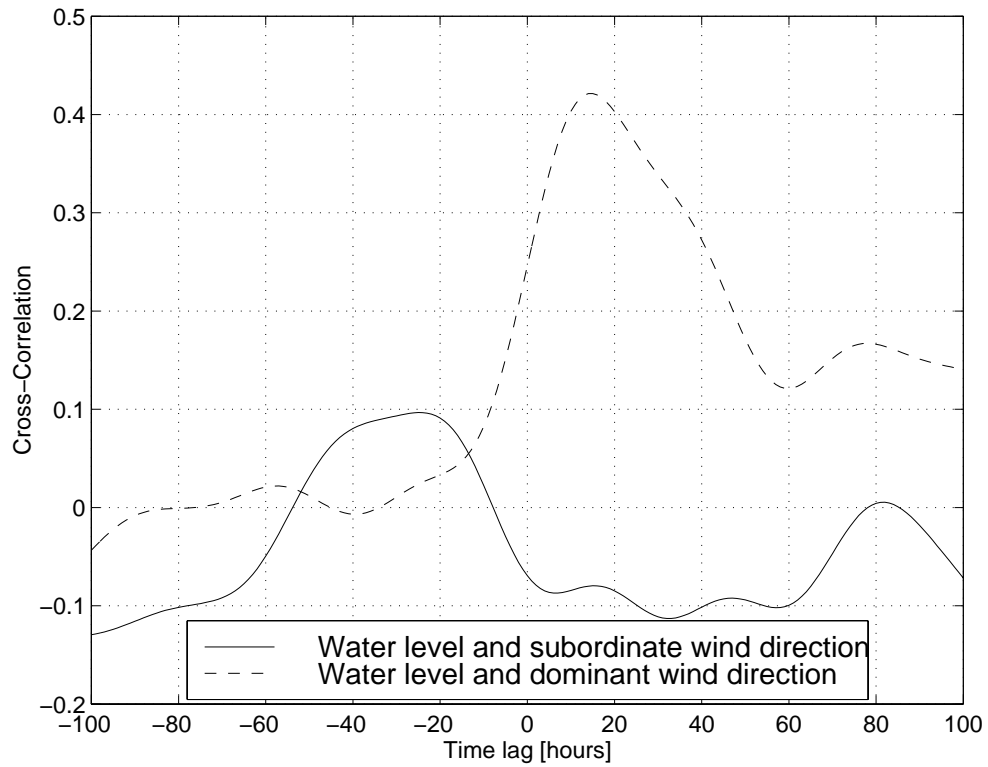


Figure 5.5: Cross correlation between residual water level and subordinate and dominant wind directions. The north/south/east/west coordinate system has been rotated 40 degrees in the direction north to east, to orient the new coordinate system with the dominant wind direction (northeast).

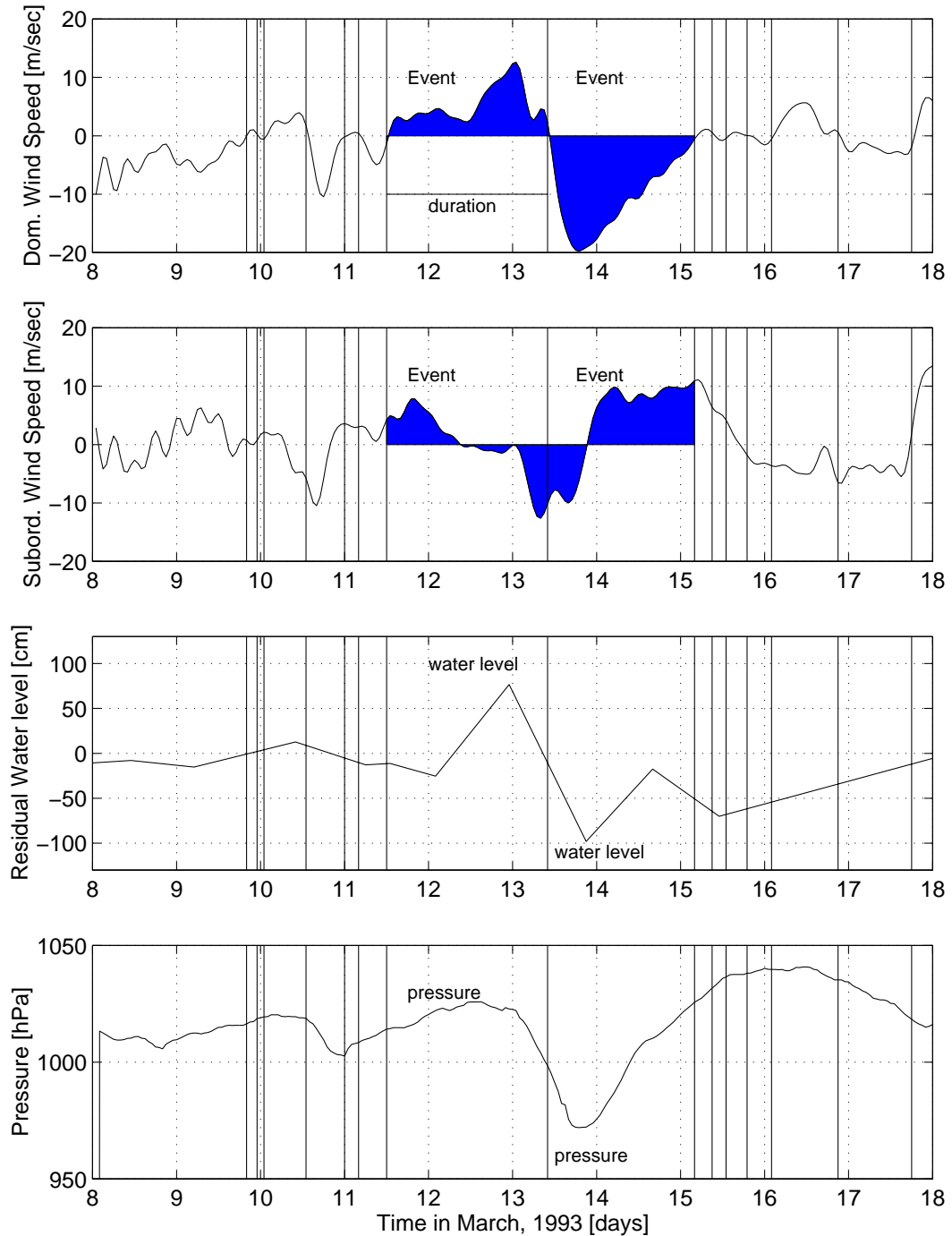


Figure 5.6: Selection of parameters associated with two events during a storm in March, 1993. The vertical lines indicate beginning and end times of events, but only the two highlighted events were selected for the statistical analysis. The first event is characteristic of an onshore wind event, and the second event is characteristic of an off shore wind event.

To determine the relationship between water level and meteorological conditions, high water level events have been selected from the tidal record, and correlated with meteorological conditions (Figure 5.6). A number of different approaches for characterizing the events were attempted, and the one presented here was found to provide the strongest correlations. The meteorological record was used to determine duration, wind speed, wind direction and pressure associated with each event, and the residual water level record was used to determine the maximum response to the wind forcing. Prior to the analysis, the high frequency variation in the wind record was removed by applying a low pass filter with a cut-off frequency of 6 hours and the water level record was adjusted to the 15 hour time lag found from the cross-correlation analysis. To ensure that water level was responding to the particular wind event considered, only peaks and troughs of water level were matched with the wind events. Both the water level and the meteorological data records contain periods of missing data. The smaller gaps (less than 5 hours) were closed by interpolating the time series through the missing values using a cubic spline.

Selection of events was divided into three steps. The first step was to divide the time series of dominant wind direction into 2438 events. A new event was selected each time the dominant wind direction changed from NE to SW or SW to NE (wind velocity component passed through zero)(Figure 5.6, top panel). The second step was to match wind events with water level peaks or troughs during the event. If no peak or trough occurred during a wind event, the event was discarded. Only events of strong water level response were of interest and it was required that the difference between adjacent peaks and troughs exceed 30 cm (Figure 5.6, third panel). If the difference was less, the event was also discarded. The third step was to pick the largest pressure deviation from the mean (Figure 5.6, bottom panel). The final requirement for event selection was that there could be no missing values in any of the three (wind, pressure and water level) records during an event. This method of selecting events, reduced the original 2438 events to 157.

Each of the 157 events were characterized by maximum residual water level, event duration, mean wind speed, mean wind direction, and largest pressure deviation from the mean. The contribution of each wind component was determined by adding all hourly values throughout an event. The mean wind angle is determined by the relative proportion of these two vectors. The mean wind speed is calculated by adding the two vectors and dividing by the event duration. Finally, the events were divided into two categories; those with offshore wind directions and those with onshore wind directions (Figure 5.7). The relationship between water level and the four parameters: wind speed,

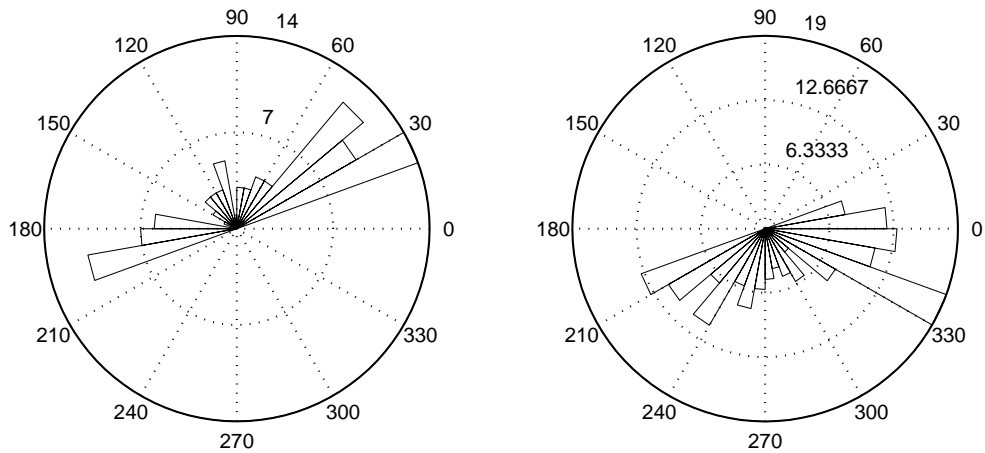


Figure 5.7: Distribution of wind directions during events. Left panel shows distribution of onshore winds, right panel shows distribution of offshore winds. North is at 0 degrees, east is at 90 degrees, south is at 180 degrees and west is at 270 degrees.

wind direction, event duration and pressure within each category was determined using multiple regression analysis for each of the two categories. The null hypothesis tested in the analysis was whether no relationship existed between the dependent variable (residual water level), and the selected parameters thought to affect residual water level (Devore (1991)). The alternative hypothesis was that at least one of the selected parameters describes a significant linear relationship between it and the dependent variable.

$$\text{The null hypothesis: } H_0 : \beta_1 = \beta_2 = \dots = \beta_k = 0$$

$$\text{Alternative hypothesis: } H_a : \text{at least one } \beta_i \neq 0 (i = 1, \dots, k) \quad (5.2)$$

$$\text{Rejection region: } \text{p-value} \leq \alpha \Rightarrow \text{reject } H_0 \text{ at level } \alpha$$

The hypothesis is tested by fitting a linear model to a selected set of parameters (Equation 5.3):

$$Y = \beta_1 X_1 + \beta_2 X_2 + \beta_3 X_3 + \beta_4 X_4 + \epsilon \quad (5.3)$$

In this analysis, the dependent variable, Y , is always chosen to be residual water level. The four parameters $X_1 - X_4$ are wind speed, event duration, pressure and wind direction within each category.

Coefficient	onshore	offshore
Mean Wind Speed	0.2439	0.0412
Duration	0.3198	-0.0500
Pressure	-0.4213	-0.3559
Direction	0.1592	0.3079
r^2	0.5901	0.2660
p	0	0.0000
SSE	37.3	113.8
f	31.3	13.6
F ($\alpha=0.01$)	3.32	3.32
Number of events	92	156
Rejection of H_0 (99 % confidence)	yes	yes

Table 5.1: Regression coefficients and test statistics for events selected using zero up-crossings of water level to define each event. The dependent variable used was residual water level. Independent variables were mean wind speed, duration pressure and wind direction..

5.3.1 Results

The results of the multiple regression analysis are listed in Table 5.1. The standardized regression coefficients ($\beta_1 - \beta_4$) are comparable with larger coefficients indicating a more strongly linear relationship. The null hypothesis (Equation 5.2) was tested at a 99% confidence level (Table 5.1) and it was rejected for both onshore and offshore events indicating that least one of the parameters (wind speed, event duration, atmospheric pressure or wind direction) acts to alter water level from the pure astronomical tidal level. During both onshore winds and offshore winds, the strongest correlation is obtained between residual water level and atmospheric pressure and the significance of the relationship between these two parameters is also seen in Figure 5.9. The overall correlation was stronger for the onshore events ($r^2=0.59$) than for the off-shore events ($r^2=0.27$).

Not all of the correlation coefficients are important. The linear model (Equation 5.3) was reduced to only include the parameters with the largest correlation coefficients. In the case of onshore winds, the model was reduced to include coefficients for wind speed, duration and pressure (Table 5.2). The linear model would be equally sound statistically if it were reduced to only include pressure and duration but because it seems intuitive that greater wind speeds contribute to producing higher water levels and seems related to sediment concentration in the tidal creek, this parameter was kept in the model. In the case of offshore winds the model was reduced to include only pressure and direction (Table 5.2). The sum of squares error (SSE) is used to compare the reduced model to the full model, by determining the reduction in unexplained variation between the two models

(f). When $f < F$, the reduced model provides as good a fit as the full model. In the two reduced models, the overall correlation was again stronger for the onshore events ($r^2=0.56$) than for the off-shore events ($r^2=0.26$); but in both cases the reduced model was sufficient.

Coefficient	onshore	offshore
Mean Wind Speed	0.2298	-
Duration	0.3316	-
Pressure	-0.4426	-0.3717
Direction	-	0.3115
r^2	0.5654	0.2627
p	0.0000	0.0000
SSE	39.55	114.3
f	5.24	0.3
F ($\alpha=0.01$)	7	4.61
Number of events	92	156
Rejection of H_0 (99 % confidence)	yes	yes

Table 5.2: Regression coefficients and test statistics for events selected using zero up-crossings of water level to define each event (reduced model). The dependent variable used was residual water level. Independent variables were mean wind speed, duration and pressure in the case of onshore wind events. In the case of offshore wind events, the independent variables were mean wind speed and pressure.

The greater degree of correlation between residual water level and each of the regression parameters for onshore events reflect that these events produce a more consistent water level response than the offshore events do. During onshore winds, water level increases with decreased pressure and water level increases with increased wind speed and event duration (Figures 5.8 and 5.9). Most of the lowest residual water levels are associated with high atmospheric pressure, weak wind speeds and events of short duration.

The goal of this analysis was to determine whether a straight-forward relationship exists between water level and climate conditions in Hog Island Bay. It was found that the influence of pressure on water level is strong, and it is not possible to conclude that high residual water levels are produced by a particular combination of wind direction, wind speed or storm duration. The largest residual water levels occur when the wind direction is between NW and E (-30 to 90 degrees), and atmospheric pressure is less than 1010 hPa. These low pressure events are frequently associated with strong wind speeds (mean event wind speed greater than 7 m/s). During N to NW winds, the low pressure is offshore from the Delmarva Peninsula, and during strong NW winds, the low pressure center is close to the coast and produces elevated water levels. During N to NE winds, the wind direction is

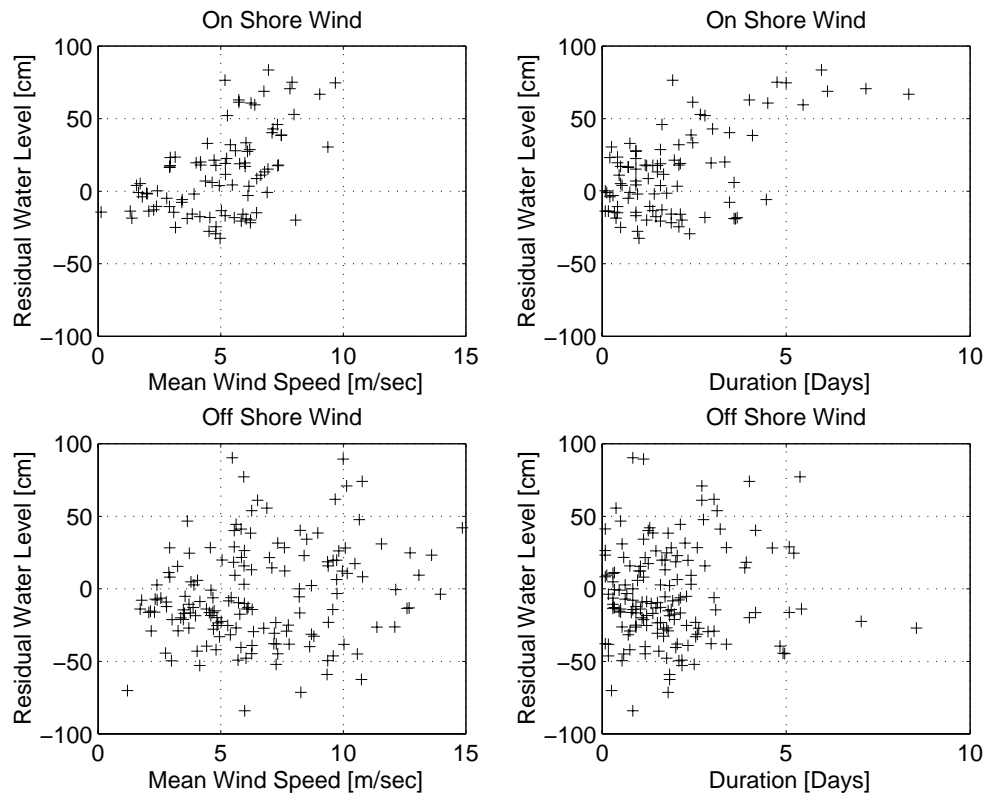


Figure 5.8: Left panels show correlation between residual water level and wind speed during on-shore and off-shore wind direction. Right panels show correlation between residual water level and event duration during on-shore and off-shore wind events.

onshore, and wind shear on the water surface forces water against the coast, causing elevated water levels.

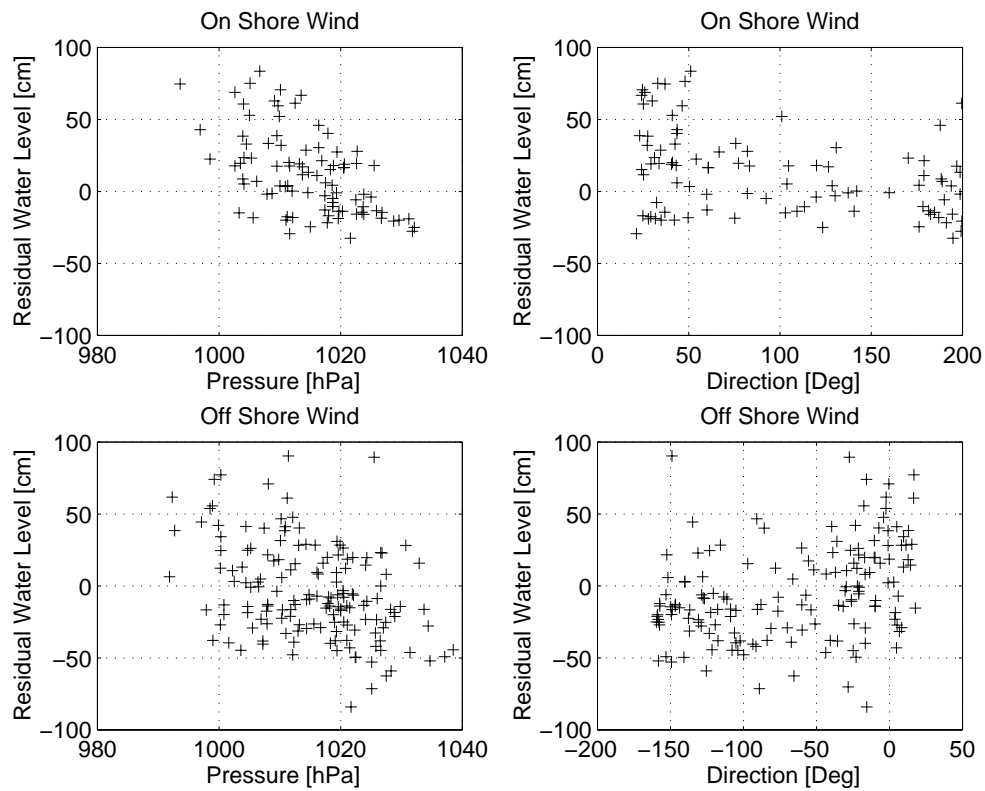


Figure 5.9: Left panels show correlation between residual water level and pressure during on-shore and off-shore wind direction. Right panels show correlation between residual water level and event direction during on-shore and off-shore wind events. Directions are oriented such that north is 0 degrees, east is 90 degrees, south is 180 or -180 degrees, and west is -90 degrees.

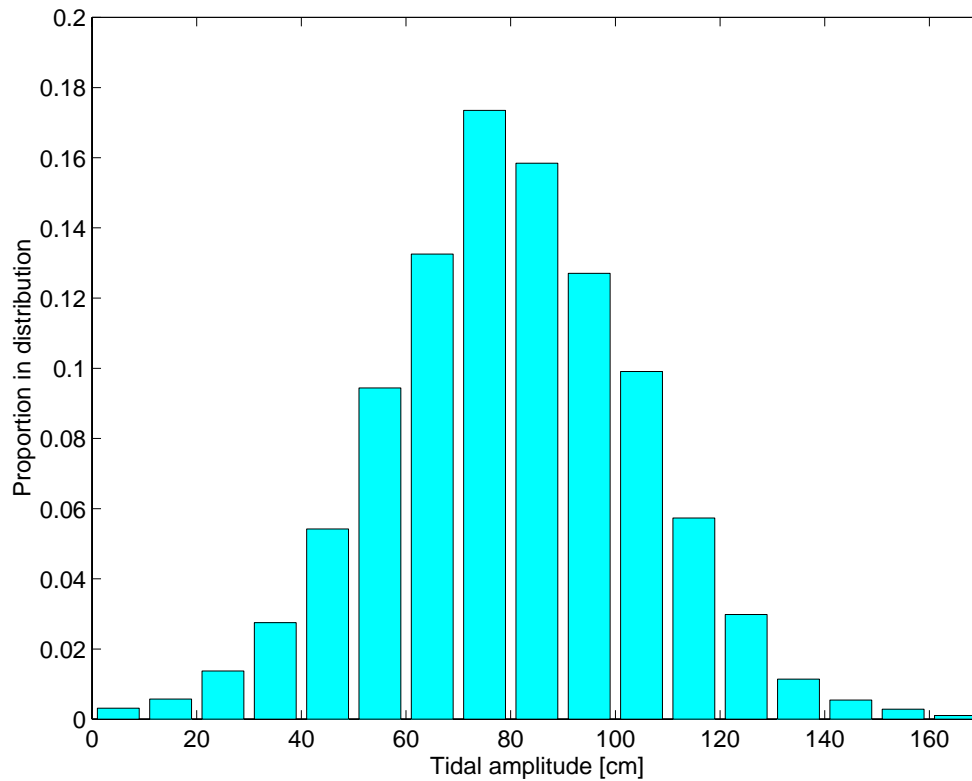


Figure 5.10: Distribution of tidal peaks at Redbank in the period between 1990 - 1997.

5.4 Frequency of sediment transport events

To determine the frequency of depositional events, each tidal cycle measured at Wachapreague was characterized in terms of a tidal amplitude, mean wind speed and mean wind direction. The tidal amplitudes were converted to tidal elevations at the Redbank tide gauge using the relationship indicated in Figure 2.4. Water level and wind speed was measured simultaneously between January 1, 1990 and July 1, 1997.

Water level at Redbank (based on measurements made at Wachapreague) were compiled into a histogram (Figure 5.10). The record covers 7.5 years, providing reasonable resolution of the high-end tail of the distribution, although higher tides occur than the highest tides measured in this time period (up to 220 cm above MSL). These extreme tides are, however, infrequent.

Sediment deposition occurs on the marsh levee during tidal amplitudes that exceed 75 cm above MSL, and as tidal amplitude increases, more sediment is deposited on a particular tide. During northeasterly storms, sediment flux to the marsh surface is increased relative to sediment flux on

other tides (Figure 5.2). The relative proportion of northeasters within each water level category was determined (Figure 5.11).

The tidal cycles were divided into those that occur during northeasters with mean wind speeds that exceed 6 m/s, and those that occur during weak northeasterly or non-northeasterly winds. The proportion of tides during strong northeasterly wind events increases slightly with increased tidal amplitude, but only at the highest tidal amplitudes were the strong northeasterly winds associated with all occurrences. In the previous section, it was shown that atmospheric pressure contributes strongly to water level elevation in Hog Island Bay, and this calculation indicates only 11 % of high water events are associated with northeasters (Figure 5.11).

Using the relationship between sediment flux to the marsh surface and tidal amplitude derived in Figure 5.2 combined with the relative frequency of each type of event (Figure 5.11), the mean annual flux to the marsh surface is calculated (Table 5.3). This calculation indicates that the mean annual sediment flux to the marsh surface is 813 g/cm/year. It is assumed that all of this sediment is deposited on the levee, in a layer of even thickness which provides a mean annual deposition rate of 1.02 g/cm²/year. The width of levee is approximately 800 cm. In reality, more sediment will be deposited in vicinity of the creek; deposition will not occur uniformly across the levee. This approach indicates that sediment deposition during northeasterly winds accounts for 27 % of calculated sediment deposition on the marsh surface.

	Flux [g/cm/year]	Mean deposition [g/cm ² /year]	Proportion %
y Northeasters (11 % of tidal cycles)	217	0.27	27
Non-northeasters (89 % of tidal cycles)	596	0.75	73
Annual	813	1.02	100

Table 5.3: Calculated annual sediment flux to the marsh surface and mean annual deposition rate. The mean annual deposition rate is obtained by assuming that all sediment that is brought to the marsh surface brought to the marsh surface is deposited on the levee in an even layer; the sediment flux is divided by the width of the levee (800 cm).

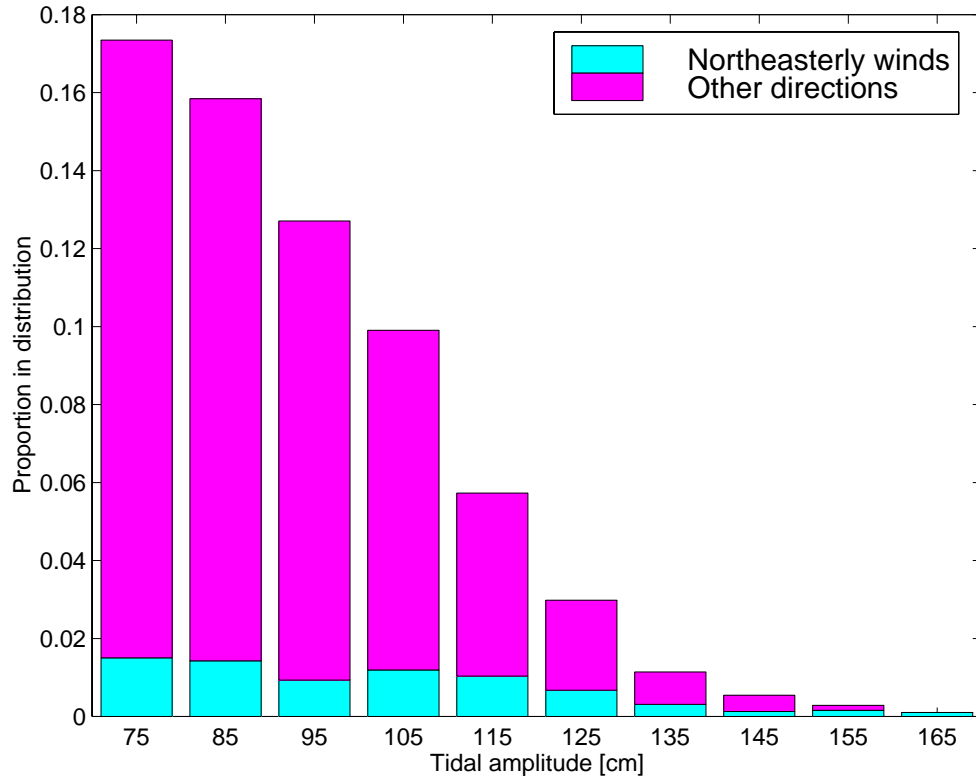


Figure 5.11: Relative proportion of northeasterly winds on tides with amplitudes sufficiently high to fully inundate the marsh surface. Tidal amplitude is at Redbank.

Chapter 6

Conclusions

6.1 Annual deposition rates on the marsh surface

Sediment deposition rates on Phillips Creek marsh have been measured on sediment traps and calculated from suspended sediment flux measurements. These measurements based on short term (day-weeks) measurements can be extrapolated to annual values and compared to long term deposition rates determined using ^{210}Pb dating. In the marsh interior, ^{210}Pb dating indicates a long term deposition rate of 2 mm/year (Kastler (1993)). This deposition rate includes long term accumulation of mineral and organic matter and compaction of the marsh surface sediments. On the creek bank, bioturbation rates are too high for accurate ^{210}Pb dating. To compare the long term ^{210}Pb deposition rate to short term mass accumulation measurements on sediment plates, long term deposition has been multiplied by the bulk density of the marsh sediments (0.84 g/cm^3 for loosely consolidated surface sediment, from Kastler (1993)) to obtain mass accumulation per unit area per year. To obtain annual deposition from the trap measurements made in this study, it was estimated that out of 350 tidal cycles in a year, sediment was deposited in non-storm quantities ($0.004 \text{ g/cm}^2/\text{tide}$) on 40 % of the tidal cycles and in storm quantities ($0.02 \text{ g/cm}^2/\text{tide}$) on 10 % of the tidal cycles on the creek bank, reflecting the percentage of northeasters. On the remaining 50 % of the tides no sediment was deposited. In the interior, sediment was deposited on 100 % of the tidal cycles at a rate of $0.002 \text{ g/cm}^2/\text{tide}$.

Good agreement was observed between annual sediment deposition measured on traps and

Method	Interior [g/cm ² /year]	Creek Bank [g/cm ² /year]
²¹⁰ Pb	0.17	-
Traps, this study	0.7	1.26
Traps, (Kastler 1993)	0.63	3.5
Flux, this study	-	1.02

Table 6.1: Annual deposition rates measured in Phillips Creek marsh

annual sediment deposition estimated from sediment flux to the marsh surface (Table 6.1). The flux based calculation of sediment deposition suggests that $0.27 \text{ g/cm}^2/\text{year}$ is deposited during northeasterly storms and $0.75 \text{ g/cm}^2/\text{year}$ is deposited during non storm conditions. Both on the creek bank and in the marsh interior, the short term deposition measurements indicate more sediment deposited on the marsh surface than the long term measurement suggests. In this study, only depositional processes were accounted for, and the long term measurement also includes erosion of the marsh surface. Erosion of the marsh surface has been observed during intense rain events, when these occur when the marsh surface is exposed at low tide. No attempts have been made to quantify this process.

6.2 Summary of results

The measurements made in this study of flow, sediment transport conditions and sediment characteristics on Phillips Creek marsh indicate that the primary mechanism of deposition on the marsh surface is settling of particles that are in a flocculated form. Model calculations of deposition as a function of advection velocity and direct settling has lead us to hypothesize that settling rate of the particles changes with time, in response to decreased turbulence level as slack tide is approached. Vegetation strongly modifies the turbulence of the flow, which is an important contribution to creating an environment where sediment can settle out of suspension. Sediment intercepted by plants is only a minor contribution (5-9 %) of the sediment brought to the marsh surface. Interception by plants is a more important contribution in the marsh interior than on the creek bank.

A direct relationship exists between concentration levels in the tidal creek, concentration levels on the creek bank, and sediment deposition. The higher the concentration in the tidal creek the greater the sediment flux to the marsh surface. The low advection velocities and relatively higher settling velocities of flocculated particles promote deposition within the nearest 10 meters of the

tidal creek. Sediment concentrations are strongly correlated with tidal amplitude; the highest concentrations are observed on tidal cycles with high tidal amplitude.

The measurements indicated that sediment was advected to the marsh surface on the rising tide and that shear stresses within the vegetation canopy were insufficient to resuspend sediments after initial deposition. Consequently all sediment deposited on the marsh surface is derived from an exterior source.

Most sediment is deposited within 10 meters of the tidal creek, and this pattern in deposition is reflected by the development of a levee at the edge of the marsh. The average annual deposition rate is $1.26 \text{ g/cm}^2/\text{year}$ on the creek bank and $0.7 \text{ g/cm}^2/\text{year}$ in the interior. Consequently sediment deposition on the marsh surface is not strongly affected by flow circulation in the marsh interior. Advection velocities were not found to vary with tidal amplitudes for the conditions measured (tidal amplitudes ranging 80-130 cm above MSL).

Flux was calculated at the two creek bank stations for a number of different tides where sediment concentration was measured simultaneously at those two locations. These calculations indicate that sediment deposits between station 1 and station 2 on all tides and that tides of very high amplitude contribute more sediment to the marsh surface and advect sediment further away from the tidal creek.

The results of this study indicate that sediment flux to the marsh surface is greatly increased during northeasterly storms. These storms tend to be associated with the largest storm surges in the Phillips Creek area. Calculations describing the relative contribution to deposition of sediment advected onto the marsh during regular tides and during storms on an annual basis suggest that 27 % of the sediment deposited on the marsh is deposited during storms that occur on 10 % of the tides that flood the marsh surface.

Bibliography

- Allen, J. (1990). Salt-marsh growth and stratification: A numerical model with special reference to the Severn Estuary, southwest Britain. *Marine Geology* 95, 77–96.
- Anderson, M. and W. Woessner (1992). *Applied Groundwater Modeling*. Academic Press.
- Bauman, R., J. J.W. Day, and C. Miller (1984). Mississippi deltaic wetland survival: sedimentation versus coastal subsidence. *Science* 224(6), 1093–1095.
- Bayliss-Smith, T., R. Healey, R. Lailey, T. Spencer, and D. Stoddart (1979). Tidal flows in salt marsh creeks. *Estuarine and Coastal Marine Science* 9, 235–255.
- Bowden, K. (1983). *Physical Oceanography of Coastal Waters*. Ellis Horwood Limited.
- Burke, R. and K. Stoltzenbach (1983). Free surface flow through salt marsh grass. MIT Sea Grant College Program, Massachusetts Institute of Technology.
- Cahoon, D., J. Lynch, and A. Powell (1996). Marsh vertical accretion in a Southern California estuary, U.S.A. *Estuarine, Coastal and Shelf Science* 43, 19–32.
- Cahoon, D. and D. Reed (1995). Relationships among marsh surface topography, hydroperiod and soil accretion in a deteriorating Louisiana salt marsh. *Journal of Coastal Research* 11(2), 357–369.
- Cahoon, D., D. Reed, and J. J.W. Day (1995). Estimating shallow subsidence in microtidal salt marshes of the southeastern United States: Kaye and Barghoorn revisited. *Marine Geology* 128, 1–9.
- Davis, R. and R. Dolan (1993). Nor'easters. *American Scientist* 81, 428–439.
- DeLaune, R., J. Nyman, and W. Patrick (1994). Peat collapse, ponding and wetland loss in a rapidly submerging coastal marsh. *Journal of Coastal research* 10(4), 1021–1030.

- DeLaune, R., J. W.H. Patrick, and R. Buresh (1978). Sedimentation determined by ^{137}Cs dating in a rapidly accreting salt marsh. *Nature* 275(12), 532–533.
- Devore, J. (1991). *Probability and Statistics for Engineering and the Sciences*. Brooks/Cole publishing Company.
- Diggle, P. (1990). *Time Series, A Biostatistical Introduction*. Oxford Science Publications.
- Dyer, K., J. Cornelisse, M. Dearnaley, M. Fennessy, S. Jones, J. Kappenberg, I. McCave, M. Pejrup, W. Puls, W. V. Leussen, and K. Wolfstein (1996). A comparison of *in situ* techniques for estuarine floc settling velocity measurements. *Netherlands Journal of Sea Research* 36(1/2), 15–29.
- Eisma, D., P. Bernard, G. Cadee, V. Ittekkot, J. Kalf, R. Laane, J. Martin, W. Mook, A. van Put, and T. Schumacher (1991). Suspended-matter particle size in some West-european estuaries; part i: particle size distribution. *Netherlands Journal of Sea Research* 28(3), 193–214.
- Fennessy, M., K. Dyer, and D. Huntley (1994). INSSEV: an instrument to measure the size and settling velocity of flocs *in situ*. *Marine Geology* 117, 107–117.
- Fonseca, M. (1996). The role of seagrasses in nearshore sedimentary processes: a review. In K. Nordstrom and C. Roman (Eds.), *Estuarine Shores: Environment and Human Alterations*, pp. 261–286. John Wiley and Sons Ltd.
- Franco, A. (1988). *Tides: fundamentals, analysis and prediction*. Fundação Centro-Tecnológico de Hidráulica.
- French, J., N. Clifford, and T. Spencer (1993). High frequency flow and suspended sediment measurements in a tidal wetland channel. In N. Clifford, J. French, and J. Hardisty (Eds.), *Turbulence: Perspectives on Flow and Sediment Transport*, pp. 251–277. John Wiley & Sons Ltd.
- French, J. and T. Spencer (1993). Dynamics of sedimentation in a tide-dominated backbarrier salt marsh, Norfolk, U.K. *Marine Geology* 110, 315–331.
- French, J., T. Spencer, A. Murray, and N. Arnold (1995). Geostatistical analysis of sediment deposition in two small tidal wetlands, Norfolk, U.K. *Journal of Coastal Research* 11(2), 308–321.
- French, J. and D. Stoddart (1992). Hydrodynamics of salt marsh tidal creek systems: implications

- for marsh morphological development and material exchange. *Earth Surface Processes and Landforms* 17, 235–252.
- Harrison, E. and A. Bloom (1977). Sedimentation rates on tidal marshes in Connecticut. *Journal of Sedimentary Petrology* 47(4), 1484–1490.
- Healey, R., K. Pye, D. Stoddart, and T. Bayliss-Smith (1981). Velocity variations in salt marsh creeks, Norfolk, England. *Estuarine, Coastal and Shelf Science* 13, 535–545.
- Hill, P., C. Sherwood, R. Sternberg, and A. Nowell (1994). *In Situ* measurements of particle settling velocity on the northern California continental shelf. *Continental Shelf Research* 14(10/11), 1123–1137.
- Holdahl, S. and N. Morrison (1974). Using precise relevelings and mareograph data. *Tectonophysics* 23, 373–390.
- Hu, G., M. Johnson, and R. Krone (1996). Hydraulic and sediment models for design of restoration of a former tidal marshland. In *Estuarine and coastal modeling, proceedings of the 4th international conference*, San Diego, California, pp. 215–228.
- Hutchinson, S., F. Sklar, and C. Roberts (1995). Short term sediment dynamics in a Southeastern U.S.A. *spartina* marsh. *Journal of coastal Research* 11(2), 370–380.
- Kadlec, R. (1990). Overland flow in wetlands: vegetation resistance. *Journal of Hydraulic Engineering* 116(5), 691–706.
- Kastler, J. (1993). Sedimentation and landscape evolution of Virginia salt marshes. Master's thesis, University of Virginia.
- Kastler, J. and P. Wiberg (1996). Sedimentation and boundary changes of Virginia salt marshes. *Estuarine, Coastal and Shelf Science* 42, 683–700.
- Katul, G. and J. Albertson (in press). An investigation of higher order closure models for a forested canopy. *Boundary Layer Meteorology*.
- Kearney, M., J. Stevenson, and L. Ward (1994). Spatial and temporal changes in marsh vertical accretion rates at Monie Bay: implications for sea level rise. *Journal of Coastal Research* 10(4), 1010–1020.
- Kearney, M. and L. Ward (1986). Accretion rates in brackish marshes of a Chesapeake Bay estuarine tributary. *Geo Marine Letters* 6, 41–49.

- Knott, J., W. Nuttle, and H. Hemond (1987). Hydrologic parameters of salt marsh peat. *Hydrological Processes* 1, 211–220.
- Kraeuter, J. (1976). Biodeposition by salt-marsh invertebrates. *Marine Biology* 35, 215–233.
- Kranck, K., E. Petticrew, T. Milligan, and I. Droppo (1993). *In situ* particle size distributions from flocculation of suspended sediment. In A. Mehta (Ed.), *Nearshore and estuarine cohesive sediment transport*, pp. 60–74. American Geophysical Union.
- Kranck, K., P. Smith, and T. Milligan (1996). Grain-size characteristics of fine grained unflocculated sediments I: 'one-round' distributions. *Sedimentology* 43, 589–596.
- Krumbein, W. and F. Pettijohn (1938). *Manual of Sedimentary petrography*. D. Appleton-Century Company.
- Leonard, L., A. Hine, and M. Luther (1995). Surficial sediment transport and deposition processes in a *juncus roemerianus* marsh, West-central Florida. *Journal of coastal Research* 11(2), 322–336.
- Leonard, L., A. Hine, M. Luther, R. Stumph, and E. Wright (1995). Sediment transport processes in a West-central Florida open marine marsh tidal creek; the role of tides and extra-tropical storms. *Estuarine, Coastal and Shelf Science* 41, 225–248.
- Leonard, L. and M. Luther (1995). Flow hydrodynamics in tidal marsh canopies. *Limnology and Oceanography* 40(8), 1474–1484.
- Letzsch, W. and R. Frey (1980). Deposition in a holocene salt marsh, Sapelo Island, Georgia. *Journal of Sedimentary petrology* 50(2), 529–542.
- Mehta, A. (1988). Laboratory studies on cohesive sediment deposition and erosion. In J. Dronkers and W. van Leussen (Eds.), *Physical processes in estuaries*, pp. 427–445. Springer Verlag.
- Milligan, T. and K. Kranck (1991). Electroresistance particle size analyzers. In J. Syvitski (Ed.), *Principles, methods, and application of particle size analysis*, pp. 109–118. Cambridge University Press.
- Milligan, T. and D. Loring (1997). The effect of size distributions of bottom sediment in coastal inlets: implications for contaminant transport. *Water, Air and Soil Pollution* 99, 33–42.

- Nerem, R., T. van Dam, and M. Schenewerk (1998). Chesapeake Bay subsidence monitored as wetland loss continues. *EOS* 79(12), 156–157.
- Nittrouer, C. and L. Wright (1994). Transport of particles across continental shelves. *Reviews of Geophysics* 32(2), 85–113.
- Odd, N. (1988). Mathematical modelling of mud transport in estuaries. In J. Dronkers and W. van Leussen (Eds.), *Physical processes in estuaries*, pp. 503–531. Springer Verlag.
- Oenema, O. and R. DeLaune (1988). Accretion rates in salt marshes in the Eastern Scheldt, South-west Netherlands. *Estuarine, Coastal and Shelf Science* 26, 379–394.
- Oertel, G., J. Kraft, M. Kearney, and H. Woo (1992). A rational theory for barrier-lagoon development. In *Quaternary Coasts of the United States: Marine and Lacustrine Systems*, Volume 48 of *SEPM Special Publication*, pp. 77–87. SEPM (Society for Sedimentary Geology).
- Pejrup, M. (1991). The influence of flocculation on cohesive sediment transport in a microtidal estuary. In D. Smith, G. Reinson, B. Zaitlin, and R. Rahmani (Eds.), *Clastic Tidal Sedimentology*, pp. 283–289. Canadian Society of Petroleum Engineers.
- Peltier, W. and X. Jiang (1996). Mantle viscosity from the simultaneous inversion of multiple data sets pertaining to post-glacial rebound. *Geophysical Research Letters* 101, 503–506.
- Postma, H. (1967). Sediment transport and sedimentation in the estuarine environment. In G. Lauff (Ed.), *Estuaries*, Volume 83, pp. 158–179. American Association for the Advancement of Science.
- Raupach, M. and R. Shaw (1982). Averaging procedures for flow within vegetation canopies. *Boundary Layer Meteorology* 22, 79–90.
- Reed, D. (1988). Sediment dynamics and deposition in a retreating coastal salt marsh. *Estuarine, Coastal and Shelf Science* 26, 67–79.
- Robinson, S. (1994). Clay mineralogy and sediment texture of environments in a barrier island-lagoon system. Master's thesis, University of Virginia.
- Sharma, P., L. Gardener, W. Moore, and M. Bollinger (1987). Sedimentation and bioturbation in a salt marsh as revealed by ^{210}pb , ^{137}cs , ^7be studies. *Limnology and Oceanography* 32(2), 313–326.

- Sternberg, R., I. Berhane, and A. Ogston (in press). Measurement of size and settling velocity of suspended aggregates on the Norther California continental shelf. *Marine Geology*.
- Stevenson, J. and M. Kearney (1996). Shoreline dynamics on the windward and leeward shores of a large temperate estuary. In K. Nordstrom and C. Roman (Eds.), *Estuarine Shores: Environment and Human Alterations*, pp. 233–259. John Wiley and Sons Ltd.
- Stevenson, J., M. Kearney, and E. Pendleton (1985). Sedimentation and erosion in a Chesapeake Bay brackish marsh system. *Marine Geology* 67, 213–235.
- Stevenson, J., L. Ward, and M. Kearney (1988). Sediment transport and trapping in marsh system: implications of tidal flux studies. *Marine Geology* 80, 37–59.
- Stull, R. (1988). *An Introduction to Boundary Layer Meteorology*. Kluwer Academic Publishers.
- Stumpf, R. (1983). The process of sedimentation on the surface of a salt marsh. *Estuarine, Coastal and Shelf Science* 17, 495–408.
- Tennekes, H. and J. Lumley (1972). *A First course in turbulence*. The MIT Press.
- Tsujimoto, T., T. Kitamura, and T. Okada (1991). Turbulent structure of flow over rigid vegetation covered bed in open channels. In *KHL Progressive Report*, pp. 1–14. Hydraulics laboratory, Kanazawa University.
- Tsujimoto, T. and Y. Shimizu (1994). Flow and suspended sediment in a compound channel with vegetation. In *Proc. 1st international symposium on habitat hydraulics*, Trent, Norway, pp. 357–370.
- van Leussen, W. and J. Cornelisse (1993). The role of large aggregates in estuarine fine-grained sediment dynamics. In A. Mehta (Ed.), *Nearshore and estuarine cohesive sediment transport*, pp. 75–91. American Geophysical Union.
- Wang, F., T. Lu, and W. Sikora (1993). Intertidal marsh suspended sediment transport processes, Terrebonne Bay, Louisiana, USA. *Journal of Coastal Research* 9(1), 209–220.
- Wiberg, P., D. Drake, and D. Cacchione (1994). Sediment resuspension and bed armoring during high bottom stress events on the northern California inner continental shelf: measurements and predictions. *Continental Shelf Research* 14(10/11), 1191–1219.
- Widdows, J., M. Brinsley, N. Bowley, and C. Barret (1998). A benthic annular flume for *in situ* measurement of suspension feeding/biodeposition rates and erosion potential of intertidal

cohesive sediments. *Estuarine, Coastal and Shelf Science* 46, 27–38.

Woolnough, S., J. Allen, and W. Wood (1995). An exploratory numerical model of sediment deposition over tidal salt marshes. *Estuarine, Coastal and Shelf Science* 41, 515–543.